# ENANTIOSELECTIVE CATALYSIS INSIDE RESORCIN[4]ARENE HEXAMER AND ITS DERIVATIVES

**Inauguraldissertation**

zur Erlangung der Würde eines Doktors der Philosophie

vorgelegt der

Philosophisch-Naturwissenschaftlichen Fakultät

der Universität Basel

von

**Daria Sokolova**

2022

Genehmigt von der Philosophisch-Naturwissenschaftlichen Fakultät

auf Antrag von

Prof. Dr. Konrad Tiefenbacher, Prof. Dr. Florian Seebeck und Prof. Dr. Agnieszka Szumna.

Basel, den 14.12.2021

Prof. Dr. Marcel Mayor

(Dekan)

Die vorliegende Arbeit wurde von November 2017 bis December 2021 an der Universität Basel unter Leitung von Prof. Dr. Konrad Tiefenbacher angefertigt. Teile dieser Arbeit wurden veröffentlicht oder zur Veröffentlichung eingereicht:

**D. Sokolova**, K. Tiefenbacher*, Chiral hexameric resorcin[4]arene capsule derivatives enable enantioselective tail-to-head terpene cyclizations, *manuscript submitted*

**D. Sokolova**, K. Tiefenbacher*, Optimized iminium-catalysed 1,4-reductions inside the resorcinarene capsule: achieving >90% *ee* with proline as catalyst, *RSC Adv.* **2021**, *11*, 24607–24612

Just keep swimming.

Just keep swimming.

Just keep swimming, swimming, swimming.

What do we do?

We swim, swim.

*“Finding Nemo”*

*To my grandparents*

*Valerii and Liudmila*

# ACKNOWLEDGMENTS

First and foremost, I would like to thank *Prof. Dr. Konrad Tiefenbacher* for accepting me as a PhD student and giving me the opportunity to work on such a fascinating research topic. I really appreciate your support and assistance over these four years. You always inspired and motivated me, especially during difficult times. I am very thankful that I had a chance to improve myself both professionally and personally.

I would sincerely like to thank *Prof. Dr. Florian Seebeck* for agreeing to become a co-referee for this dissertation and *Prof. Dr. Agniezska Szumna* for accepting to be the external expert.

Moreover, I want to acknowledge my colleagues from the TIEFENBACHER group for the great working atmosphere and the unforgettable time we spent together. Thank you, *Fabian Huck*, for meeting me at the main entrance on my first day, showing me around, and helping to set up the working place in the lab. *Qi Zhang*, *Thomas Bräuer*, *Jesper Köster*, *Michael Heilmann*, *Severin Merget* and *Fabian Bissegger*, thank you for a warm welcome in the group. *Leonidas-Dimitrios Syntrivanis* and *Jonathan Pfeuffer-Rooschüz*, thank you for being such nice labmates, it was always a pleasure to work right next to you. I would also like to acknowledge *Dario Schmid* for our fruitful tennis discussions, especially the ones we did in German. Thank you, *Melina Knezevic*, for the amazing time we had at the conference in Cagliari. I will never forget this adventure. Special thanks go to *Suren Nemat*. Thank you for our conversations, your contribution to the research, and for proofreading this thesis. Thank you for being not only a great colleague but also a good friend. I also want to acknowledge all the other group members *Ivana Nemethova*, *Tian-Ren Li*, *Mattias Zenka*, *Giacomo Persiani*, and *Iris Martyn,* for the time we had together and for being a part of my life. Thank all of you guys for your support in the lab and beyond!

The research would not have been possible without the entire staff of the Chemistry Department. I would like to acknowledge the SPARR group for letting me perform ozonolysis and some analytical measurements in their lab. I also want to thank *Prof. Dr. Daniel Häussinger* for the support concerning NMR experiments, *Dr. Michael Pfeffer* for performing HRMS measurements, and *Dr. Alessandro Prescimone* for the X-Ray analysis. I am also grateful to the whole Werkstatt team and *Jonas Zurflüh* for solving problems with instruments and lab equipment and to the IT support, especially *Dr. Bernhard Jung,* for figuring out all the technical issues. I would like to thank *Isa Worni* for your help with administrative questions and your kind words.

Over the last four years, I have met so many amazing people from the chemistry department who also became my friends. Many thanks go to *Ivan Urosev*, *Alessandro Castrogiovanni*, *Zlatko Jončev*, *Snizhana Zaitseva,* and *Oleksandr Vyhivskyi*. I am also incredibly grateful to *Oleks* for his professional help and for proofreading this thesis.

The whole SEEBECK group deserves to be mentioned for always being friendly and welcoming. Thank you guys for inviting me to your cozy parties and celebrations! It was always great to feel like a part of your group. I especially thank *Dzmitry Miarzlou, Egor Nalivaiko*, and *Davey Lim* for being very supportive friends and colleagues. A special thank deserves *Mariia Beliaeva*, who is my friend, neighbor, and colleague. Thank you for sharing all the good and bad days with me and for being such a great person and friend.

I would not have been where I am now without my best friend and partner, *Boris*. Thank you for your unconditional love and support. Thank you just for being with me. You are my soulmate.

Last but not least I want to thank my family. Thank you, mom and dad, for believing in me. Thank you, grandma and grandpa, for always being on my side. Thank you, my little bro, for being my inspiration. I love you all!

# DEUTSCHE ZUSAMMENFASSUNG

Molekulare Kapseln können als Enzymanaloga dienen, die die katalytische Umwandlung von Substraten innerhalb des umschlossenen Hohlraums ermöglichen. Der supramolekulare Wirt **XII** organisiert sich selbst über Wasserstoffbrückenbindungen aus sechs Resorcin[4]aren-Bausteinen **9b** und hat ein Innenvolumen von 1400 $Å^3$. Aufgrund seiner hochdynamischen Natur kann **XII** Gastmoleküle reversibel einschließen und eine Vielzahl von Reaktionen ermöglichen.

Einige der Reaktionen mit kationischen Intermediaten erfordern HCl als Cokatalysator, um in der hexameren Kapsel **XII** ablaufen zu können. Die Wirkung des Säureadditivs wurde jedoch nie für die kapselinduzierte Iminium-cokatalysierte 1,4-Reduktion von α,β-ungesättigten Aldehyden untersucht. Im Rahmen dieser Arbeit wurde der Einfluss von HCl und weiteren Additiven auf die Reaktion untersucht und die allgemeinen Reaktionsbedingungen überarbeitet. Von besonderem Interesse ist der positive Effekt von Alkoholadditiven, der sich für diese Umwandlung im Inneren von **XII** als vorteilhaft erwiesen hat. Die optimierten Reaktionsbedingungen ermöglichten Enantioselektivitäten von bis zu 92% *ee*.

Darüber hinaus untersuchten wir die Möglichkeit des direkten Chiralitätstransfers in enantiomerenreinen, molekularen Kapseln, die eine ähnlichen Aufbau wie Kapsel **XII** aufweisen. Dabei wurden zwei unterschiedliche Wege zur Einführung von Chiralität in den Resorcin[4]aren Baustein wurden untersucht. Alle so erhaltenen chiralen Derivate waren in der Lage sich in Lösung zu hexameren, supramolekularen Containern zusammenzusetzen. Diese potentiell katalytisch aktiven Systeme wurden im weiteren in der Zyklisierung von Terpenen getestet. In dieser Arbeit berichten wir über die ersten Beispiele optisch aktiver hexamerer Resorcin[4]aren-basierter Kapseln und deren Fähigkeit, asymmetrische tail-to-head Zyklisierung von Terpenen mit bis zu 62% *ee* zu katalysieren.

# ENGLISH ABSTRACT

Molecular capsules can serve as enzyme mimetics enabling catalytic conversion of substrates inside the enclosed cavity. Supramolecular host **XII** self-assembles *via* hydrogen bonds from six resorcin[4]arene building blocks **9b**, and has an internal volume of 1400 $Å^3$. Due to its highly dynamic nature, **XII** can reversibly encapsulate guest molecules and facilitate numerous reactions.

Some of the reactions involving cationic intermediates require HCl as a co-catalyst to occur inside hexameric capsule **XII**. However, the effect of the acid additive has never been investigated for capsule-induced iminium-co-catalyzed 1,4-reduction of α,β-unsaturated aldehydes. In the course of this work, we examined the influence of HCl and other additives on the reaction and revised the reaction conditions. Of particular interest is the positive effect observed for alcohol additive, which proved to be beneficial for this transformation inside **XII**. The optimized reaction conditions allowed to reach enantioselectivity of up to 92% *ee*.

Additionally, we investigated the possibility of the direct chirality transfer inside similar to **XII** molecular capsules. Two different ways of introducing chirality on the resorcin[4]arene were explored. All of the obtained derivatives proved to self-assemble in solution into hexameric capsules. These potentially catalytically active systems were further tested in terpene-cyclization reactions. In this work, we report the first examples of optically active hexameric resorcin[4]arene-based capsules and their ability to asymmetrically catalyze tail-to-head terpene cyclization reactions delivering up to 62% *ee*.

# TABLE OF CONTENTS

# 1. INTRODUCTION

People have always been striving to be able to imitate and sometimes even surpass nature. This desire has led to countless discoveries, without which our life today would be impossible. Even in the present, we still draw inspiration from nature and apply it in fields such as mechanical engineering, architecture, robotics, and medicine, to name a few. When it comes to chemistry, mimicking natural processes is still a main driving force for major developments improving our everyday lives. One of the most challenging tasks remaining in chemistry to this day is to find a way to efficiently synthesize naturally occurring molecules in the laboratory setting. Chemists often need dozens of linear steps to reach a target molecule, unlike nature, which does it extraordinarily elegantly from simple starting materials utilizing enzymatic pathways.

Enzymes are specific and highly efficient biocatalysts that are able to catalyze reactions under ambient conditions in aqueous media.[1] Most enzymes are proteins with unique amino acids sequences that allow for the formation of a three-dimensional structure with hydrophobic cores surrounded by hydrophilic shells.[2] An active site that can specifically bind a given substrate and efficiently catalyze a certain reaction is buried in the hydrophobic core, while hydrophilic shells provide solubility in the aqueous environment. Such a complex structure is used by nature to provide highly specific and efficient catalysts for essential chemical transformations in living systems. Despite current advances in biocatalytic applications,[3,4] there are several drawbacks (e.g., temperature sensitivity, solubility in organic solvents, etc.) that limit the use of enzymes in organic synthesis. Therefore, there is a growing interest in creating organic enzyme-like structures as efficient catalysts to overcome these limitations. Supramolecular chemistry represents a powerful tool for designing such systems.[5–7]

Supramolecular chemistry is a relatively new field that combines chemistry, biology, and physics.[8] Nobel Laureate JEAN-MARIE LEHN defined supramolecular chemistry as "chemistry beyond the molecule". It often takes inspiration from nature and focuses on the assembly of simple building blocks *via* intermolecular interactions to build highly complex chemical systems.[9] Unlike traditional chemistry, which concentrates on the covalent bond, supramolecular chemistry is based on the weaker and reversible non-covalent interactions between molecules, such as hydrogen bonding, hydrophobic interactions, π–π, and COULOMB interactions.[10]

In 1987 the Nobel Prize in Chemistry was awarded to PEDERSEN, CRAM, and LEHN for the development of new functional molecules capable of a guest binding.[11–13] PEDERSEN published

the very first examples of crown ethers **1**, which can selectively bind alkali metal ions,[14] and LEHN and CRAM expanded this study to three-dimensional derivatives of crown ether – cryptands[15] **2** and spherands[16] **3** – which showed improved selectivity and higher binding constants (Fig. 1). These results are considered as milestones of supramolecular chemistry, however, their remarkably specific properties, such as high binding affinities and exceptional size selectively, resulted in limited substrate scope and restricted catalytic application of such molecules.[17,18]

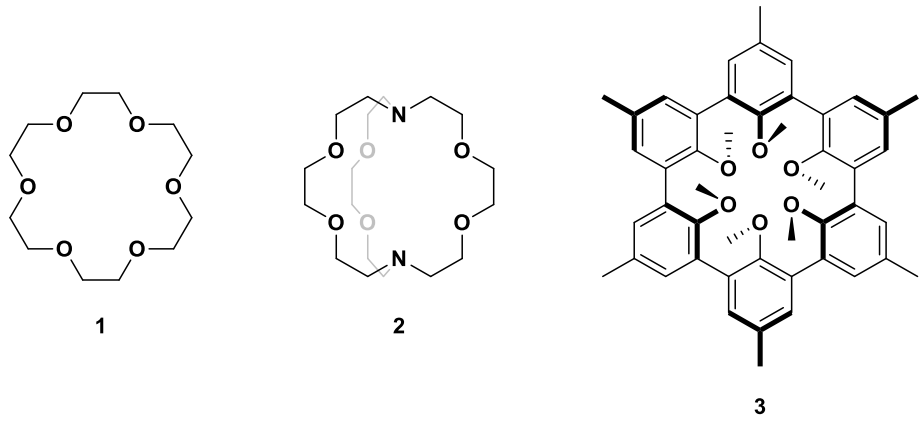


**Figure 1.** Crown ether **1** by PEDERSEN, cryptand **2** by LEHN, and spherand **3** by CRAM.

Naturally occurring cyclic oligosaccharides – cyclodextrins – represent a type of enzyme mimetics applied since the early stage of supramolecular chemistry development (Fig. 2). These compounds are water-soluble and can bind small molecules inside a hydrophobic pocket, which can also be used for drug delivery.[19] BRESLOW et al. have demonstrated that α-cyclodextrin (**4**) accelerates the regioselective chlorination of anisole.[20] Other examples of macrocycles used in catalysis include the porphyrin-based compound **5**, which catalyzed an intermolecular acyl transfer reaction,[21] and cyclophanes (e.g., compound **6**, Fig. 2) utilized as catalysts in the oxidation of aromatic aldehydes.[22] Another class of supramolecular host structures is cucurbiturils, which can be accessed *via* condensation of glyoxal, formaldehyde, and urea (e.g., **7**, Fig. 2).[23] The size of a macrocycle comprised of glycoluril units, which are linked by methylene fragments, can vary depending on the reaction conditions. Cucurbiturils' property to bind cationic guest molecules was used in cucurbit[6]uril-assisted 1,3-dipolar cycloaddition between azides and alkynes, each carrying an ammonium group for enhanced binding within the cucurbituril cavity, to generate 1,2,3-triazoles.[24] Further reactions accelerated in a biomimetic fashion by exploiting these supramolecular structures have been reported.[23]

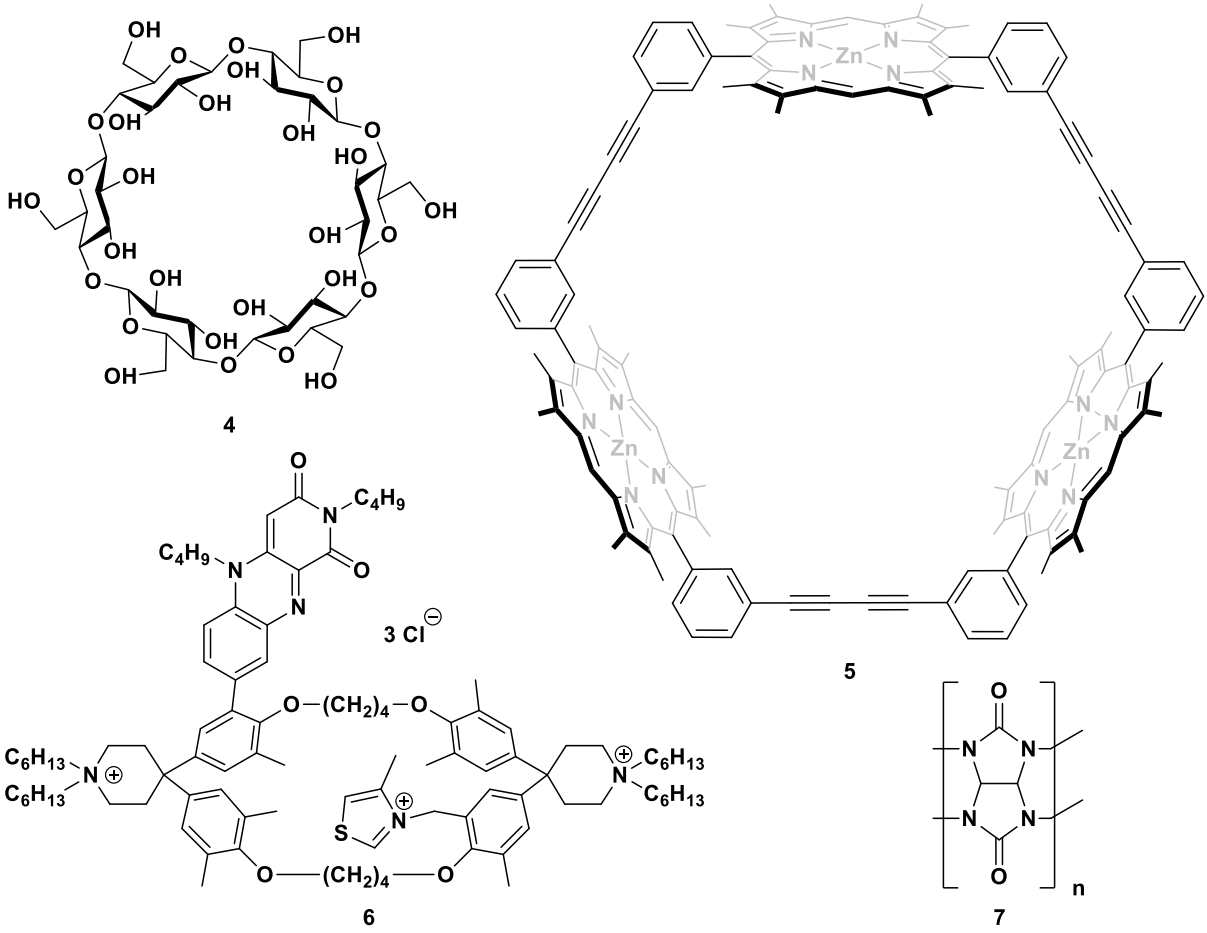


**Figure 2**. Different types of macrocycles utilized in enzyme mimetic catalysis: α-cyclodextrin (**4**), porphyrin-based structure **5**, cyclophane **6**, cucurbituril **7**.

Bowl-shaped macrocycles based on phenol and its derivatives represent a diverse class of supramolecular structures. They often serve as building blocks for supramolecular containers. Synthetic availability, together with the notable capability to act as receptors for different guests, depending on the structural properties, makes calixarenes **8**, resorcinarenes **9**, and pyrogallolarenes **10** interesting for supramolecular chemistry (Fig. 3).[25,26] Acid-catalyzed condensation of the phenolic units – resorcinol and pyrogallol – with the corresponding aldehydes yields quite selectively the resorcin[4]- or pyrogallol[4]arenes (**9** and **10**), respectively, nevertheless larger macrocycles also can be obtained.[27–29] Base-catalyzed condensation of 4-*tert*-butylphenol with formaldehyde, depending on the chosen conditions, leads to the formation of calixarenes of different sizes.[30] These bowl-shaped molecules can be easily modified on the upper and/or lower rims to customize their properties for specific applications.[31,32] A few other new macrocycles (e.g., catecholarene **11**,[33] pillararene **12**,[34] xanthenearene **13**[35]) have been reported in past years, which indicates interest in such covalently linked structures for future application in the field of supramolecular chemistry, despite the existing limitations of their size and properties.

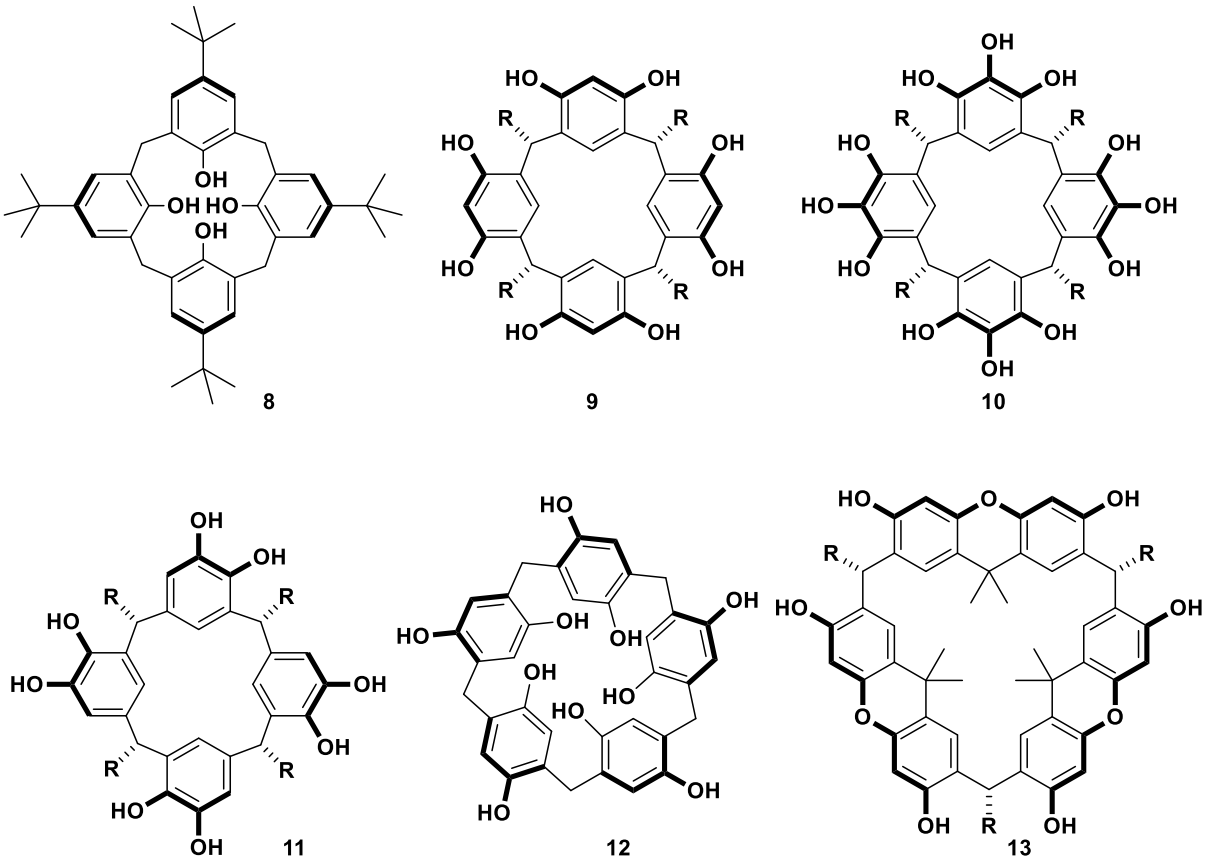


**Figure 3**. Bowl-shaped macrocycles: calix[4]arene **8**, resorcin[4]arene **9**, pyrogallol[4]arene **10**, catechol[4]arene **11**, pillar[5]arene **12**, xanthene[3]arene **13**.

Interest in the synthesis and study of supramolecular structures has greatly increased over the last decades. The main reasons for this can be attributed mainly to (1) advances in synthetic organic chemistry, which allow synthesis and modification of a wider range of building blocks for the construction of more sophisticated and efficient supramolecular receptors, (2) advanced computer modeling tools as well as improved methods of analysis, such as NMR spectroscopy, X-ray crystallography, mass spectrometry, and (3) generally enhanced fundamental understanding of supramolecular chemistry. The possibility to vary receptor cavity sizes, their geometries and their chemical environment has resulted in the creation of diversified supramolecular containers of different nature with unique properties.

## 1.1. Supramolecular Containers

The largest and best-studied class of supramolecular containers are metal-ligand assemblies. A wide range of multidentate ligands with rigid backbones and metal ions with fixed coordination geometries allows a controlled and highly modular construction of different assemblies. The FUJITA group first published a $Pd_6L_4$ coordination capsule **Ia** that forms *via* spontaneous self-assembly from dimethylethylenediamine end-capped $Pd^{II}$ ions and 1,3,5-tris(4-pyridyl)triazine in a 6:4 ratio in aqueous solutions (Scheme 1).[36] The inner compartment is comprised of a cavity with a volume of roughly 500 Å$^3$ and has been shown to take up various organic compounds in aqueous solutions.[37,38] Cage **Ia** has been successfully used for acceleration of DIELS-ALDER reaction for aromatic substrates due to supportive π-stacking interactions.[39] A Pt-based derivative of **Ia** was recently used for a biomimetic base mediated amide cleavage reaction, adjusting the reactivity of the amide by inducing mechanical strain, thereby imitating the enzyme-based activation mechanism.[40]

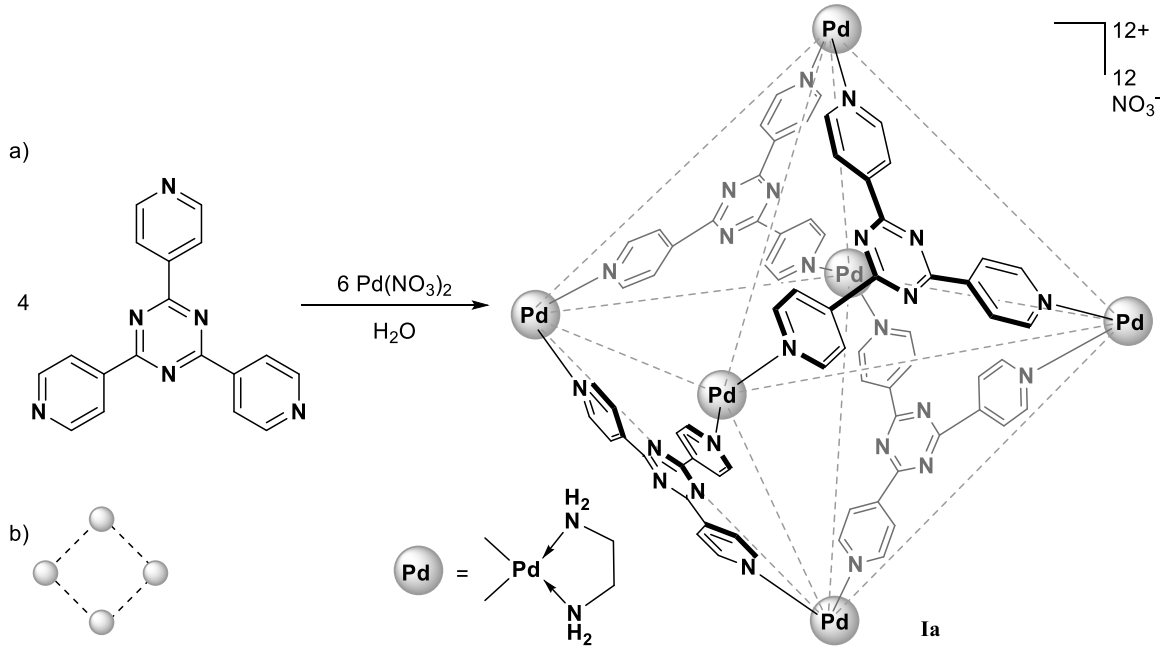


**Scheme 1**. a) Self-assembly of the FUJITA $Pd_6L_4$ cage **Ia**. b) Schematic 2D-representation of capsule **Ia**.

Another example of the metal coordination-based cage was reported by the NITSCHKE group.[41] Tetrahedral structure **II** self-assembles from $Fe^{II}$ ions and imine ligands, which form *in situ* from 4,4′-diaminobiphenyl-2,2′-disulfonic acid (**14**) and 2-formylpyridine (**15**) (Scheme 2). The inner volume of the obtained host reaches 141 Å$^3$, which makes it suited for encapsulation of small neutral organic molecules (e.g., cyclohexane) by virtue of hydrophobicity in an aqueous solution. Due to the small cavity size, which reduces the number of suitable guest molecules, the application of cage **II** in catalysis is somewhat limited.

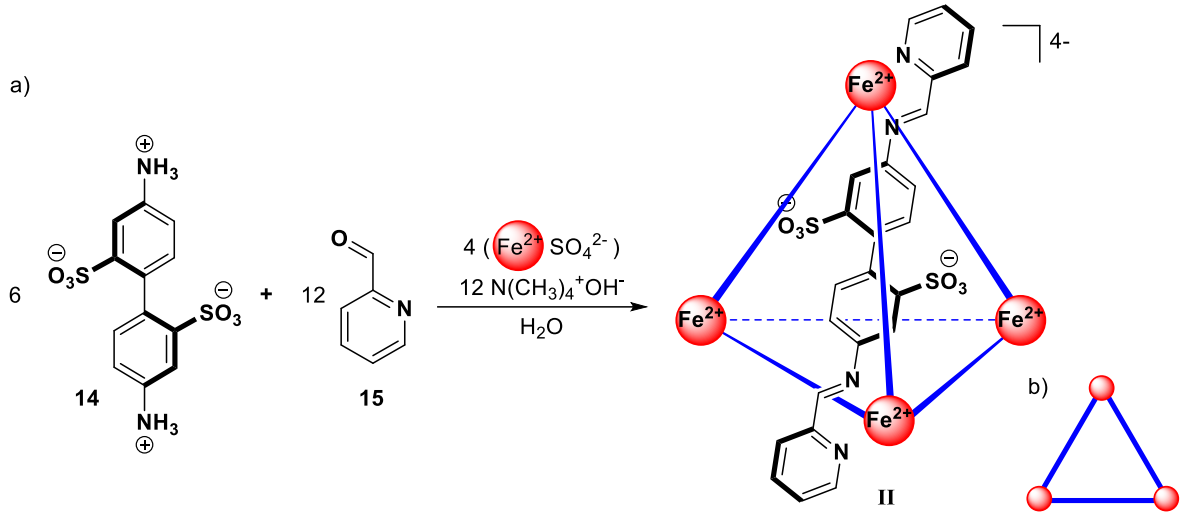


**Scheme 2.** a) Self-assembly of cage **II** reported by NITSCHKE. b) Schematic 2D-representation of cage **II**.

The group of REEK, inspired by natural metalloenzymes, made use of both metal-ligand coordination and cation-dipole interactions to design a new supramolecular host with a defined nanoenvironment. By using porphyrins, they were able to construct a second coordination sphere and encapsulate a transition metal catalyst.[42] The applied ligand-template synthetic strategy leads to the formation of a self-assembled host consisting of three $Zn^{II}$ tetraphenylporphyrins **16** selectively bound to pyridyl phosphine ligand **17** capable of binding a catalytically active [RhH(CO)$_3$] complex to form a supramolecular catalyst **IIIa** (Scheme 3). The obtained catalyst can selectively catalyze the hydroformylation reaction of alkenes.[43] This selectivity, which only applies to terminal alkenes, is not achievable with traditional homogeneous transition metal catalysts.

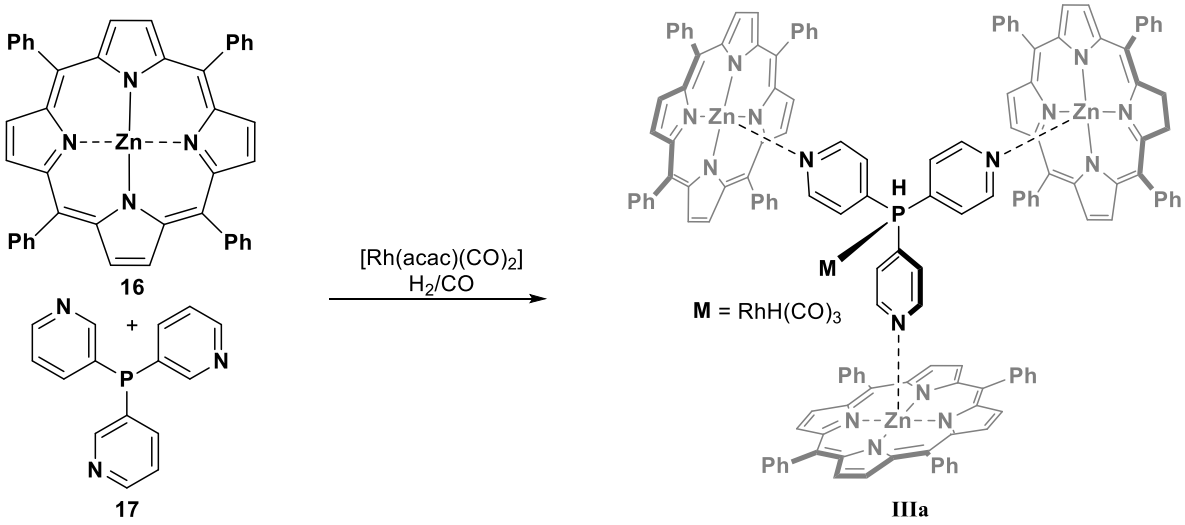


**Scheme 3.** Synthesis of supramolecular Rh-based catalyst **III** from Zn-porphyrin **16** and phosphine **17**.

Supramolecular structures can also be assembled based on the hydrophobic effect.[44] GIBB reported the dimeric structure **IV** (Scheme 4) based on the resorcinarene derived cavitand **18**,

which is easily accessible on a large scale. Due to the available carboxylic acid moieties, compound **18** is well soluble in water (pH = 10), where it exists in a monomeric form.[45] Once a suitable guest is added as a template (e.g., butane), **18** self-assembles into a dimer, which was also tested in photochemical reactions and showed some changes in product selectivity when compared to the reaction in solution.[46]

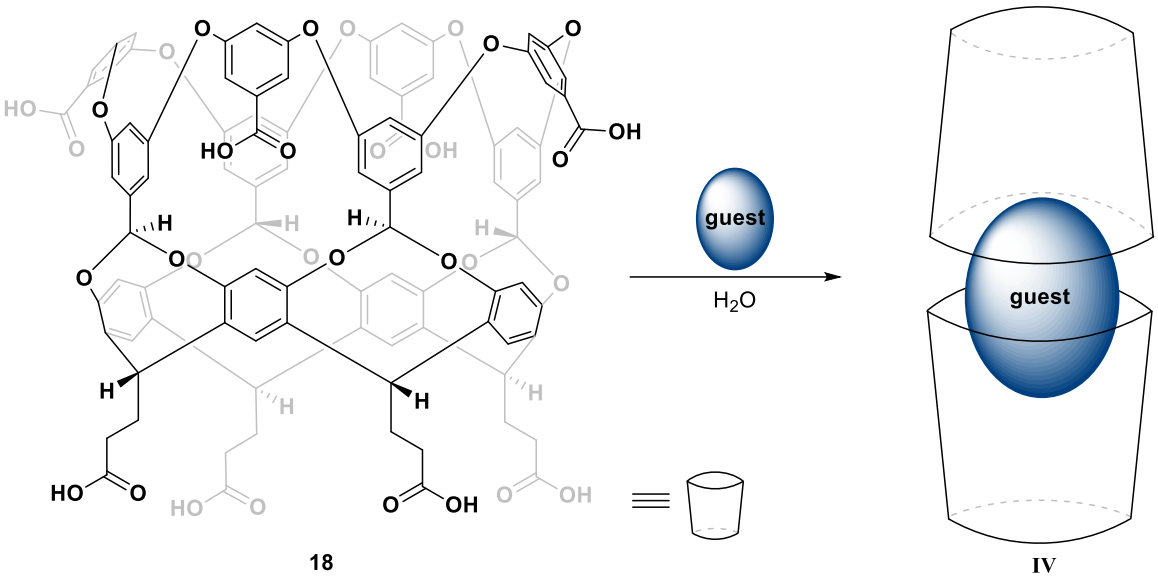


**Scheme 4**. Guest-templated self-assembly of dimer **IV** from resorcinarene building block **18**.

Another remarkable example of hydrophobic effect-based self-assembled structures was reported by the YOSHIZAWA group.[47] The described nature-inspired micellar capsules **V** are constructed from curved polyaromatic frameworks **19** composed of two trimethylammonium groups linked to two anthracene units (Scheme 5a).[48] **V** showed the ability to encapsulate different hydrophobic aromatic guests such as fluorescent dyes, fullerenes, and nanographene due to hydrophobic effect and π–π-stacking.[49] Incorporation of the perfluorinated derivative of manganese tetraphenylporphyrin complex **20** (Scheme 5b) allowed the formation of a 1:1 host-guest complex utilized to efficiently catalyze the epoxidation of 3-chlorostyrene **21** in the presence of iodosylbenzene (PhIO) as an oxidant forming the corresponding epoxide **22** (Scheme 5c).[50,51]

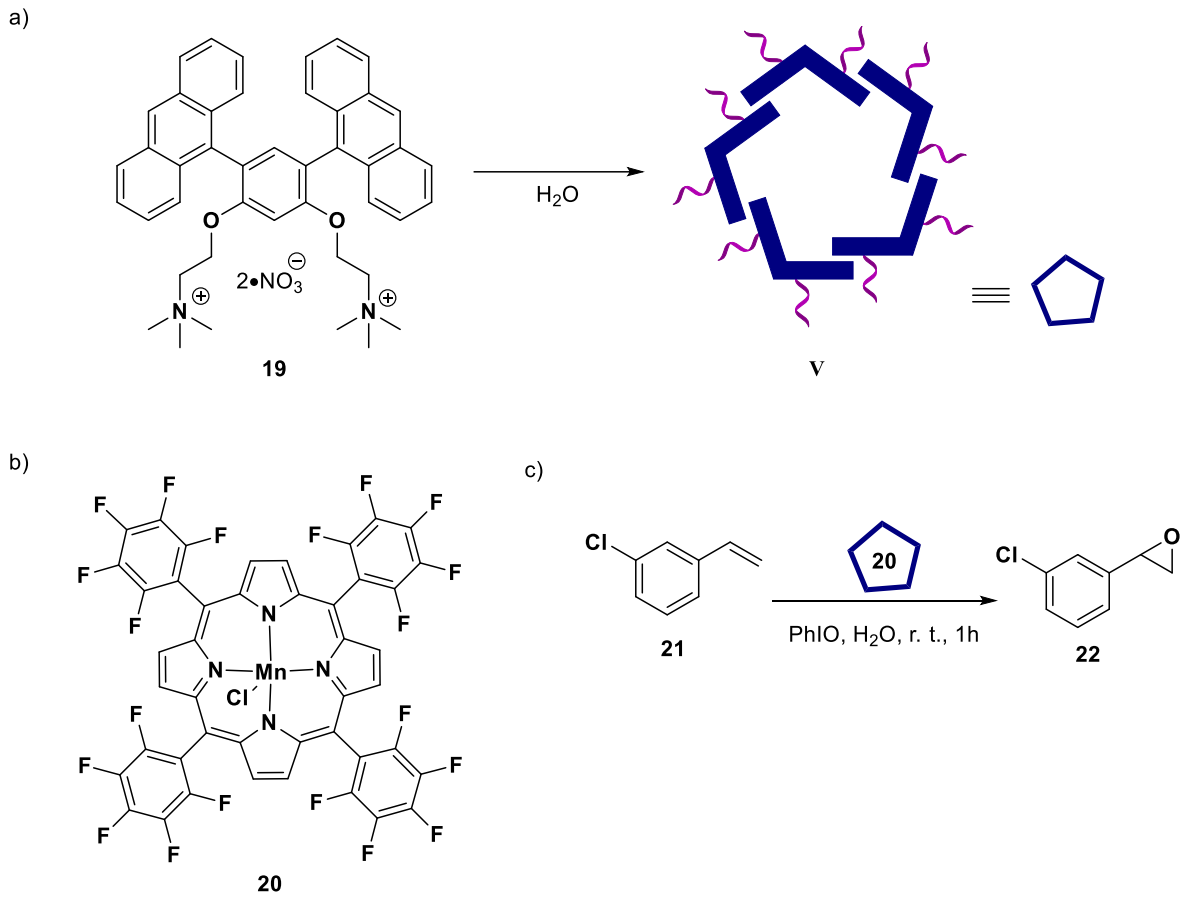


**Scheme 5**. a) Self-assembly of nature-inspired micellar capsule **V**. b) Manganese complex **20**. c) Catalytic epoxidation using complex **20** encapsulated by **V**.

Halogen bonding represents another possibility for designing molecular assemblies. Using this approach, the group of DIEDERICH, inspired by earlier work from PILATI,[52] reported a dimeric self-assembly **VI** formed from two resorcinarene-based subunits **23** and **24**, which are complementary to each other (Scheme 6a).[53] The obtained structure **VI** is suitable for encapsulation of small guests (e.g., 1,4-dioxane). Later, the group has also confirmed the formation of similar dimers in the solid state, in solution, and in the gas phase.[54]

Another interesting example of halogen bonding-based molecular assemblies was presented by the group of RISSANEN.[55] Using the building block **25** linked by $Ag^+$-ions, they were able to replace metal ions with $I^+$ by simple reaction with molecular iodine to form a multimeric structure **VII** (Scheme 6b).[56] Chalcogen bonding is currently also being explored regarding its application to construct supramolecular structures.[57–59]

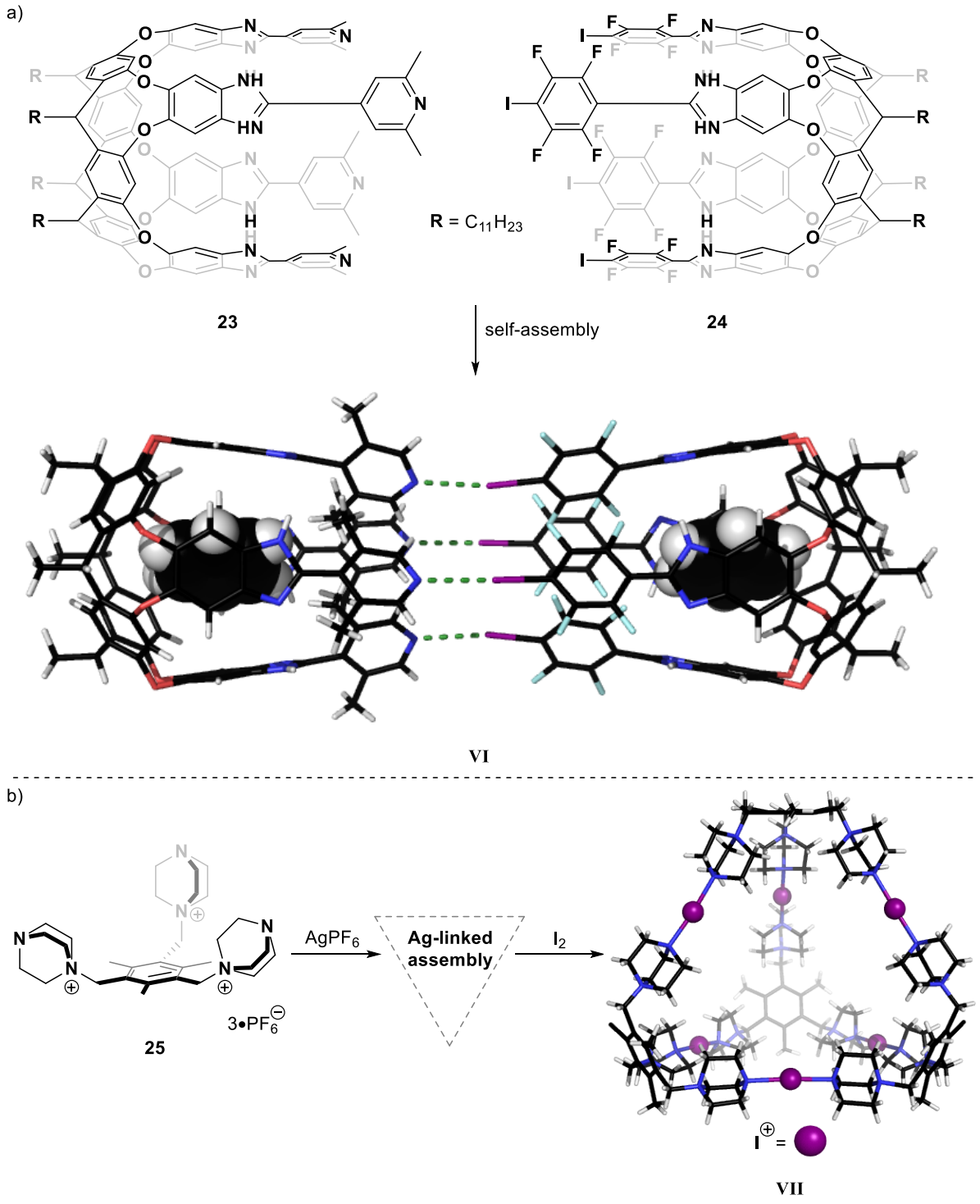


**Scheme 6**. a) Formation of the halogen-bonded dimer **VI** (with two encapsulated benzene molecules) from building blocks **23** and **24**. Feet (R) and additional solvent molecules were omitted for clarity. b) Silver-templated self-assembly of tetramer **VII**. Solvent molecules and counterions were omitted for clarity.

There is a number of reports about catalytically active enzyme-like systems relying on hydrogen bonds.[60–64] Construction of self-assemblies based on hydrogen bonding allows the formation of large multimeric structures due to the highly dynamic nature of hydrogen bonds. However, it is also important to choose the right geometry of building blocks, which need to be preorganized and possess a certain degree of curvature to be capable of the formation of the

desired assembly. A distinctive feature of such supramolecular structures is the need to partially or fully disrupt the hydrogen bonding network to allow guest exchange, which occurs *via* the portal mechanism.[65]

An early example of a hydrogen bond-based molecular capsule was published by REBEK, who reported a softball-like structure **VIII** with a volume of 320 Å$^3$, which assembles in apolar solvents from two glycoluril-containing fragments connected together by a bicyclo[2.2.2]octadiene-based linker **26** (Scheme 7a).[66] The obtained supramolecular host is capable of reversible guest encapsulation, which occurs *via* hydrogen bonding to the capsule walls or alternatively by VAN DER WAALS interactions in the case of hydrophobic guests (e.g., adamantane). Capsule **VIII** was also found to catalyze the DIELS-ALDER reaction between compound **27** and *p*-benzoquinone (**28**) (Scheme 7b). The reaction leads to the formation of molecule **29** and is accelerated by a factor of 10 compared to the bulk solution.[67] The same group has also reported a dimeric capsule **IX** formed from resorcinarene building block **30** (Scheme 7c), which was used to catalyze 1,3-dipolar cycloaddition reaction between phenyl azide and phenylacetylene.[68]

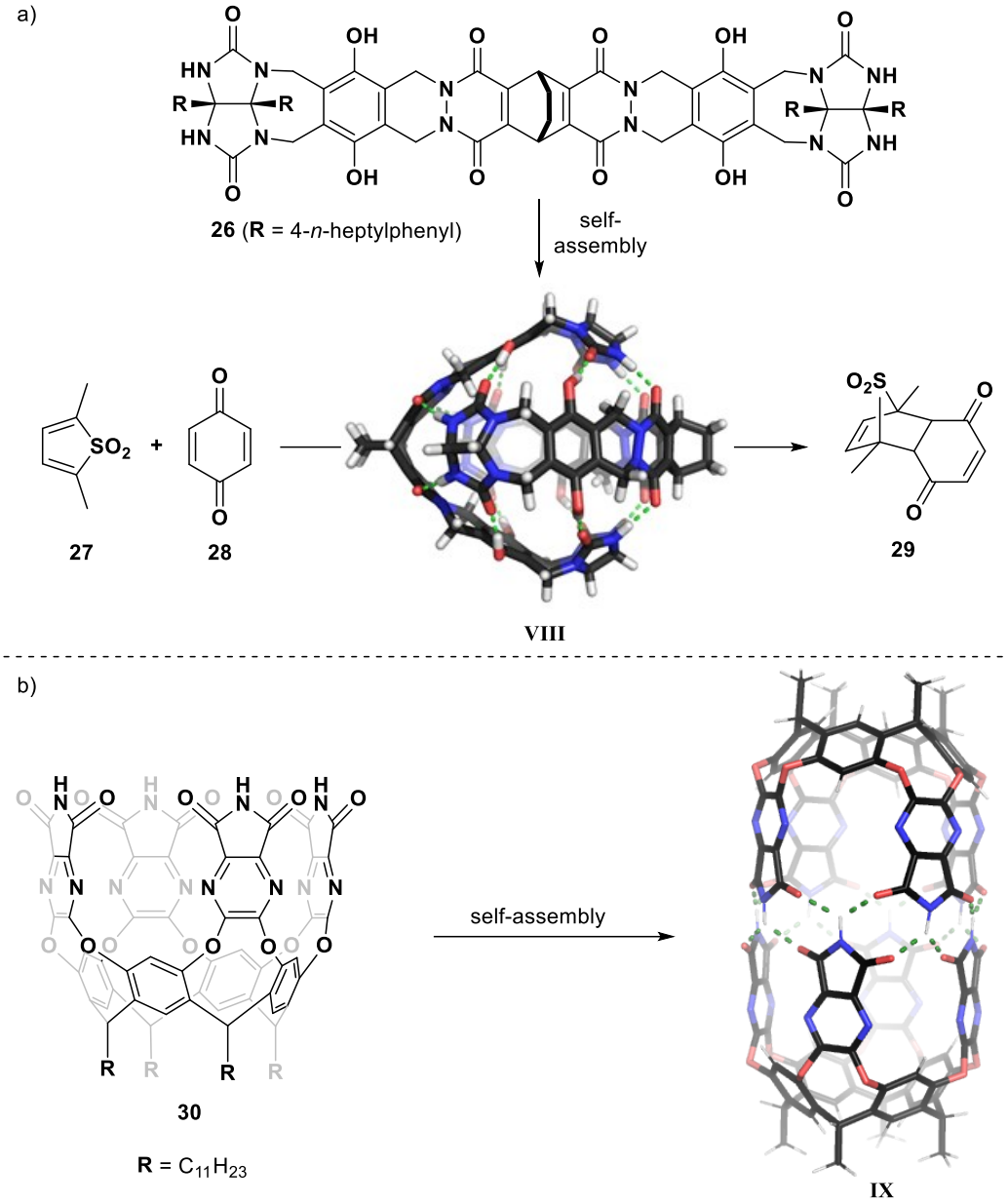


**Scheme 7**. a) Self-assembly of softball-capsule **VIII** and DIELS-ALDER reaction catalyzed inside **VI** forming product **29**. b) Self-assembly of resorcinarene-based dimer **IX** from **30**.

Furthermore, REBEK described **X**, which is a water-soluble analog of **IX**.[69] Dimerization of macrocycle **31** in the presence of hydrophobic guest molecules (e. g., stilbene **32**) leads to the formation of container **X** (Scheme 8a). Hydrogen bonding, in this case, is strong enough to tolerate competing solvents such as DMSO or water, as long as the assembly is templated by a suitable guest. SZUMNA group observed the same templating effect of $C_{60}$ to assemble dimer **XI**, obtained from modified resorcinarenes **33** with amino acid moieties on the upper rim (Scheme 8b).[70]

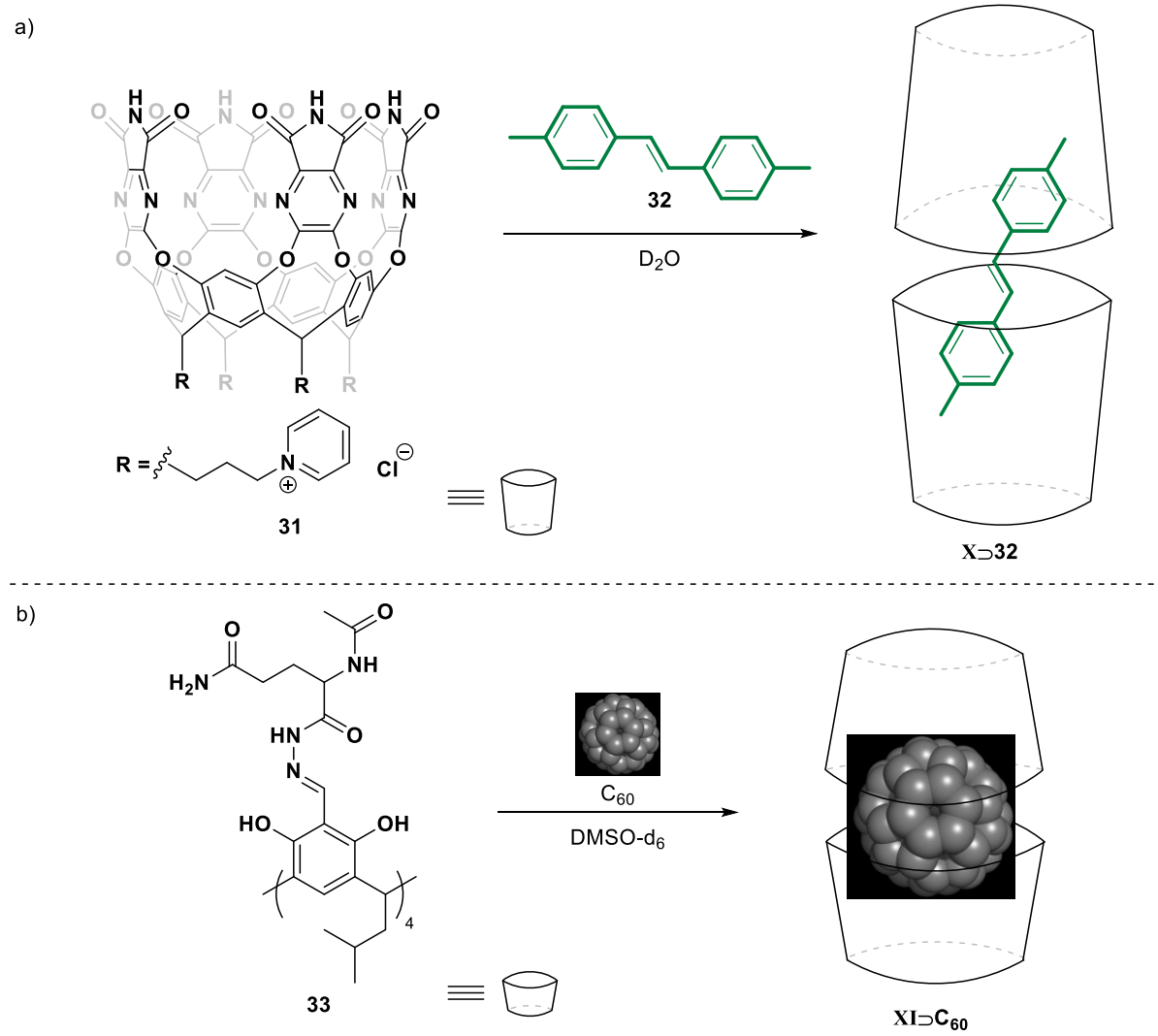


**Scheme 8**. a) Self-assembly of **X** in water with stilbene **32** as a template. Feet were omitted for clarity. b) Self-assembly of dimer **XI** from resorcinarene derivative **33** in DMSO in the presence of $C_{60}$.

The first hexameric assembly based on the C-methyl resorcinarene macrocycle **9a** was reported in 1997 by ATWOOD and MACGILLIVRAY for the solid state.[71] The resorcinarene capsule **XII** with a cavity volume of 1400 Å$^3$ self-assembles from six building blocks **9** and eight water molecules *via* sixty hydrogen bonds (Scheme 9a). Even though the building blocks are achiral, they are slightly tilted, making the assembly chiral. Later, MATTAY and co-workers reported a crystal structure of a closely-related hexameric capsule self-assembled from macrocycle **10** (Scheme 9b).[72] Interestingly, this assembly is held by seventy-two hydrogen bonds, and water is not required. REBEK and COHEN proved the presence of such hexameric structures in solution when lipophilic derivatives of resorcinarene and pyrogallolarene with longer alkyl "feet" (depicted as R in Scheme 9) are dissolved in apolar organic solvents.[73–75] Synthetic availability of the building blocks together with the enzyme mimetic properties of the formed hexamers makes these self-assemblies exceptionally interesting for the ongoing research in supramolecular chemistry.

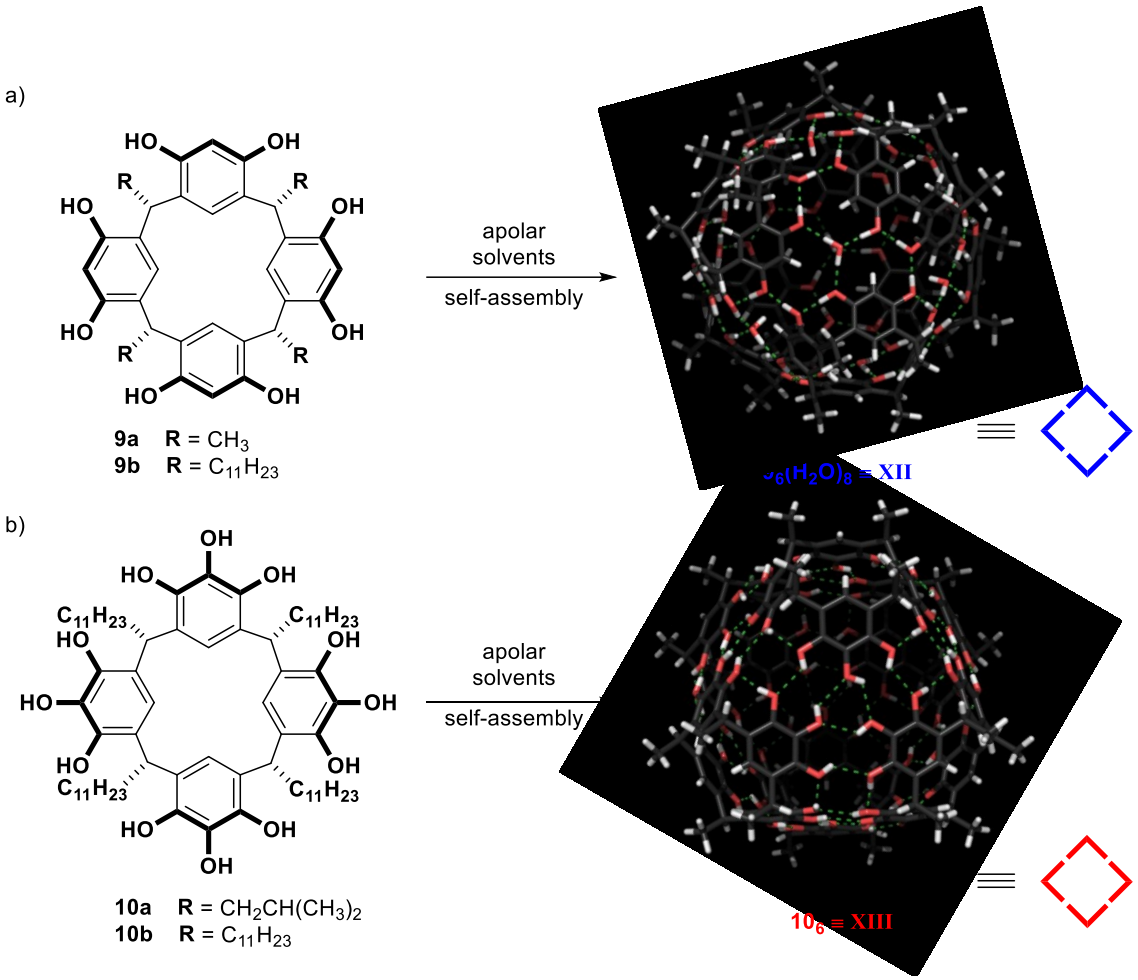


**Scheme 9**. a) Self-assembly of the resorcinarene hexamer **XII** in apolar solvents. b) Self-assembly of the pyrogallolarene hexamer **XIII** in apolar solvents. Feet (R) were omitted for clarity.

Guest encapsulation properties of both hosts **XII** and **XIII** were investigated using $^{1}$H-NMR spectroscopy. Hexamer **XII** was shown to encapsulate tetraalkyl ammonium salts and tetraalkyl phosphine salts in $CDCl_3$ due to supportive cation-π-interactions.[76] Using the DOSY-NMR spectroscopy, COHEN and co-workers showed that the hexamers **XII** and **XIII** self-assemble in apolar solvents even when suitable guest molecules are not presented.[75] The stability of **XII** and **XIII** in relation to polar media was also investigated using DOSY-NMR. Titration with competitive solvents such as methanol and DMSO showed an increase of the diffusion coefficient, which indicates the disassembly of the hexameric structure. Despite the similar nature of capsules **XII** and **XIII**, they behave differently when it comes to their guest uptake properties. For example, self-assembly **XII** can encapsulate neutral amines,[77] ammonium salts,[76] alcohols,[78] carboxylic acids and sugars,[79] metal complexes,[80] and radical species.[81] In contrast, host **XIII**, which is able to bind neutral amines,[77] is not capable of encapsulation of ammonium salts in $CDCl_3$, which was recently explained by the TIEFENBACHER group.[82] The authors demonstrated that due to stabilization *via* strong cation-π interactions, capsule **XIII**

can well encapsulate cationic species. Anions, which cannot be stabilized inside **XIII**, mostly remain outside of the cavity. Capsule **XII**, in contrast, stabilizes the entire ion pair avoiding the charge separation. Later, COHEN and co-workers reported that the presence of benzene as a solvent allows partial encapsulation of ammonium salts by capsule **XIII**.[83]

SCARSO, REEK, and co-workers reported the first successful utilization of the resorcinarene capsule **XII** in catalysis.[84] Capsule **XII** readily encapsulates cationic gold complexes with *N*-heterocyclic carbene (NHC) ligands. The encapsulation of the metal catalyst strongly influences the outcome of the catalysis and leads to a change in product distribution. The presence of hexamer **XII** in reaction with substrate **34** provides some of the *anti*-MARKOVNIKOV product **37** and dihydronaphtalene (**36**) in contrast to free catalyst reaction in solution, which gives mainly the MARKOVNIKOV product **35** (Scheme 10). Such an outcome is explained as a direct influence of the confined space of the cavity.

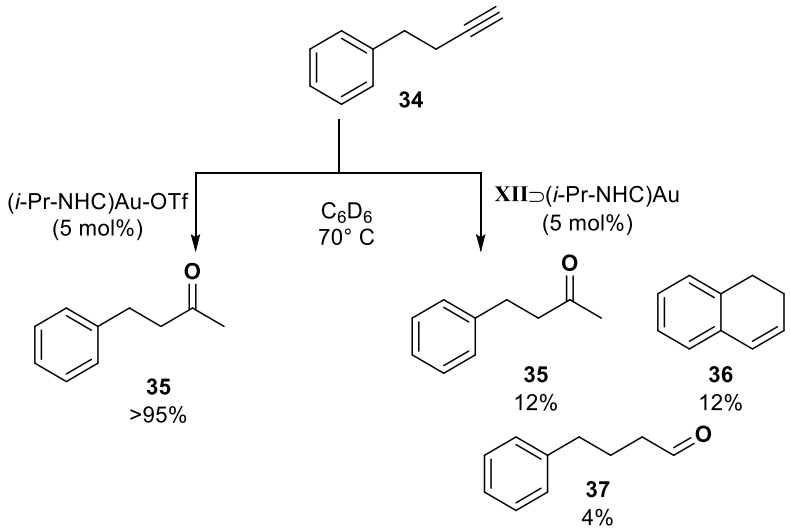


**Scheme 10**. Cyclization products of Au-catalyzed alkyne hydration reactions in the absence and presence of capsule **XII**.

In 2013, SCARSO and STRUKUL reported that hexamer **XII** efficiently catalyzes the hydrolysis of isonitriles *via* protonation of the substrate and subsequent attack of a water molecule leading to formylamides.[85] The TIEFENBACHER group further expanded the scope of reactions utilizing **XII** as a catalyst. For instance, hydrolysis of acetals to corresponding aldehydes occurs in capsule **XII**, which acts as a BRØNSTED acid (confirmed by NMR studies, $pK_a$ of 5–6) with a good substrate size-selectivity.[86] Later studies by the group indicated the need of HCl as an additive to act as a co-catalyst for acetal hydrolysis and some other reactions inside capsule **XII**.[87] Due to the ability of **XII** to encapsulate and stabilize positively charged species, it was utilized for a number of acid-catalyzed reactions such as intramolecular hydroalkoxylation,[88] a cyclodehydration-rearrangement cascade,[89] the hydration of alkynes with $HBF_4$,[90] and the isomerization of epoxides.[91] TIEFENBACHER and co-workers reported

the first case of a tail-to-head (THT) terpene cyclization utilizing the resorcinarene capsule **XII**, which is likely possible due to its ability to stabilize cationic intermediates and prevent premature quenching.[92,93] This reaction is of particular interest for this work, therefore it will be discussed further in detail in chapter 1.3.1.

Larger resorcinarene-based supramolecular structures can also be built utilizing dynamic covalent chemistry (DCC). This approach allows constructing assemblies by employing reversible reactions such as imine formation, disulfide formation, boronic ester formation, metathesis reactions, and others. Building blocks with corresponding functionalities, which are supposed to be complementary to each other (e.g., carbonyl and amine), are mixed together and allowed to equilibrate to form a thermodynamic product.

In 1991 QUAN and CRAM reported the first supramolecular capsule, based on two tetraaldehyde resorcinarene units (**38** with different "feet") merged together by imine condensation with 1,3-diaminobenzene.[94] The obtained assembly could encapsulate different guests (e.g., menthol, camphor, ferrocene) upon heating. Later the WARMUTH group expanded this approach and reported the formation of similar structures based on resorcinarene **38** and different diamine linkers (e.g., **XIV**, Scheme 11).[95]

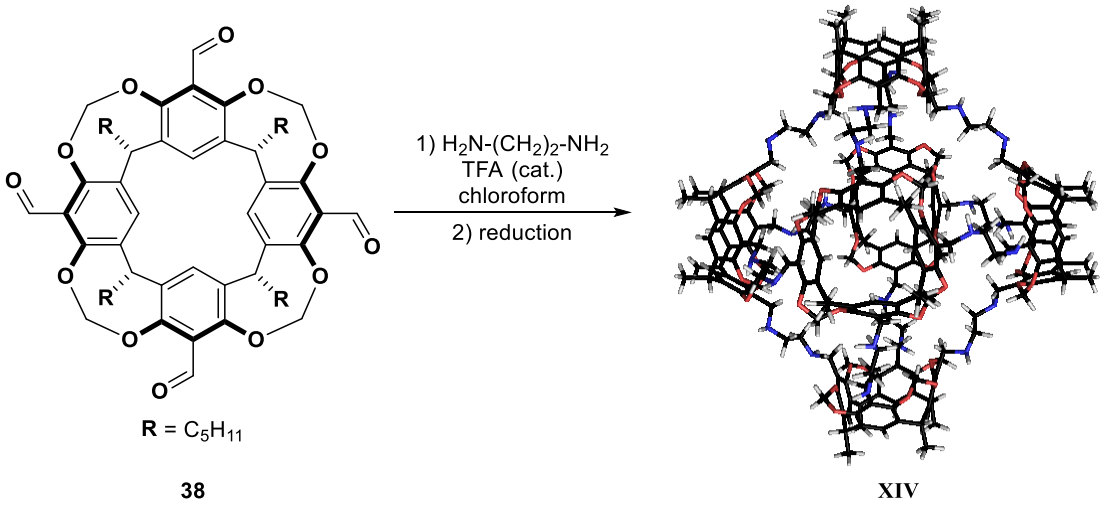


**Scheme 11**. Supramolecular assembly **XIV** synthesized from **38** using imine formation followed by reduction. Feet (R) were omitted for clarity.

Exceptionally large cavities (with internal volumes of up to 13 000 Å$^3$)[96] have been reported emphasizing the potential of this approach to synthesize large organic cages. So far, DCC-based assemblies were not utilized in catalysis, but their high surface area together with the defined pore size allows their use as porous materials for gas sorption,[97,98] gravimetric sensoring,[99] molecular sieving,[100] as a stationary phase in gas chromatography.[101,102]

## 1.2. Selected Examples of Optically Active Molecular Containers and Enantioselective Reactions Inside Supramolecular Hosts

Some of the previously described achiral supramolecular structures can also be accessed in an optically active form, which can be beneficial for enantioselective catalysis. For example, the substitution of ethylenediamine with an optically active amine allows obtaining an optically active Pd-based cage **Ib.** Supramolecular host **Ib** was used to stereo- and regioselectively catalyze [2+2] olefin cross-photoaddition.[103] Suspending 3-methylfluoranthene (**39**) and N-cyclohexylmaleimide (**40**) in a $D_2O$ solution containing cage **Ib** led to the formation of host-guest complex cage **Ib**⊃(**39**·**40**), which was irradiated for 30 minutes at room temperature to give the final product **41** with up to 50 % *ee* (Scheme 12). It is particularly important that the confined cavity of cage **Ib** not only allowed generally inert (under such conditions) fluoranthene to react in the photochemical pericyclic process but also provided high regioselectivity of the reaction since only the $C_4$=$C_5$ bond was involved in the transformation.

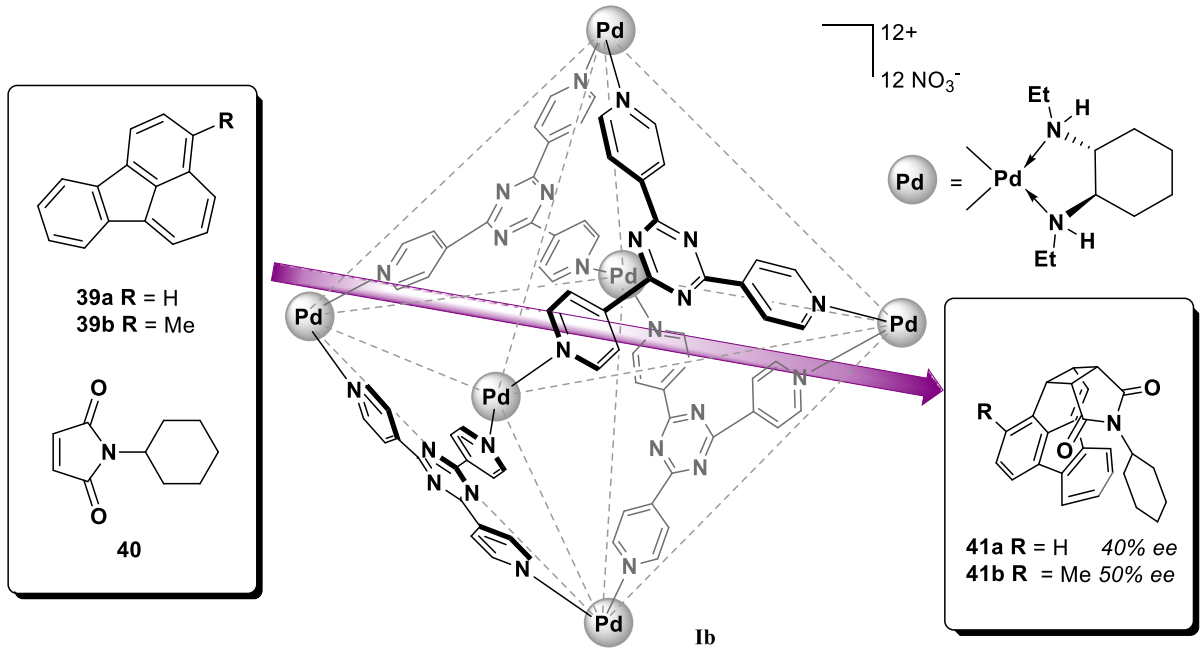


**Scheme 12**. Regio- and enantioselective [2+2] photoaddition reaction of **39** with maleimide (**40**) catalyzed by Pd-cage **Ib**.

The coordination cage **II** reported by NITSCHKE and co-workers was utilized for a one-pot relay reaction involving a multicatalytic system which includes cage **II**, methylene blue (**42**), and L-proline.[104] The transformation starts from the hetero-DIELS-ALDER reaction between furan **43** and singlet oxygen generated from the methylene blue (**42**), forming intermediate endoperoxide **44** (Scheme 13). At the same time, cage **II** self-assembles in solution and transforms endoperoxide **44** into more stable fumaraldehydic acid **45**, which then undergoes L-proline-catalyzed 1,4-addition with nitromethane to form butanolide **46** (30% isolated yield).

The reaction occurred enantioselectively, delivering 68% *ee* in the product compared to 40% *ee* for the reaction catalyzed only by L-proline. Further control experiments illustrated the importance of cage **II** for the stabilization of the active intermediate and its transformation to fumaraldehydic acid. The racemic cage **II** can also be accessed in an optically active fashion if enantiopure ligands are applied. Such substitution also leads to the formation of a larger cavity with an approximate internal volume of 418 Å$^3$.[105]

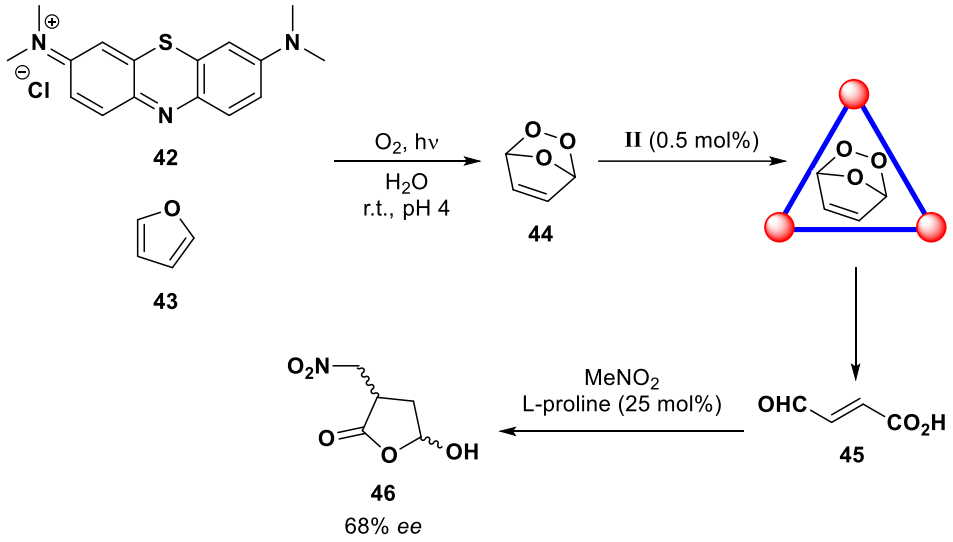


**Scheme 13**. Catalytic relay consisting of methylene blue (**42**), cage **II**, and L-proline transforming furan (**43**) to butanolide **46**.

Using a similar approach, the second generation of the REEK catalyst **IIIb** based on bis-(Zn-salphen) phosphoramidite ligands was obtained and used for the enantioselective hydroformylation of internal alkenes (Scheme 14).[106] The self-assembly of phosphoramidite **47** and bis-(Zn-salphen) **48** acts as a bidentate ligand for Rh$^I$, thus forming a confined catalytic active site of catalyst **IIIb** (Scheme 14a). Although the obtained chiral supramolecular catalyst could only provide a maximal conversion of 20%, it proved to be highly regio- and enantioselective towards aldehyde **51**, providing the following regio- and stereoselectivity: **50**/**51** = 30/70, 86% *ee* for (*R*)-**51** using *cis*-**49** as starting material; **50**/**51** = 40/60, 72% *ee* for (*R*)-**51** using *trans*-**49** (Scheme 14b). Thus, the developed chiral supramolecular catalyst demonstrated the ability to transfer chirality onto achiral substrates.

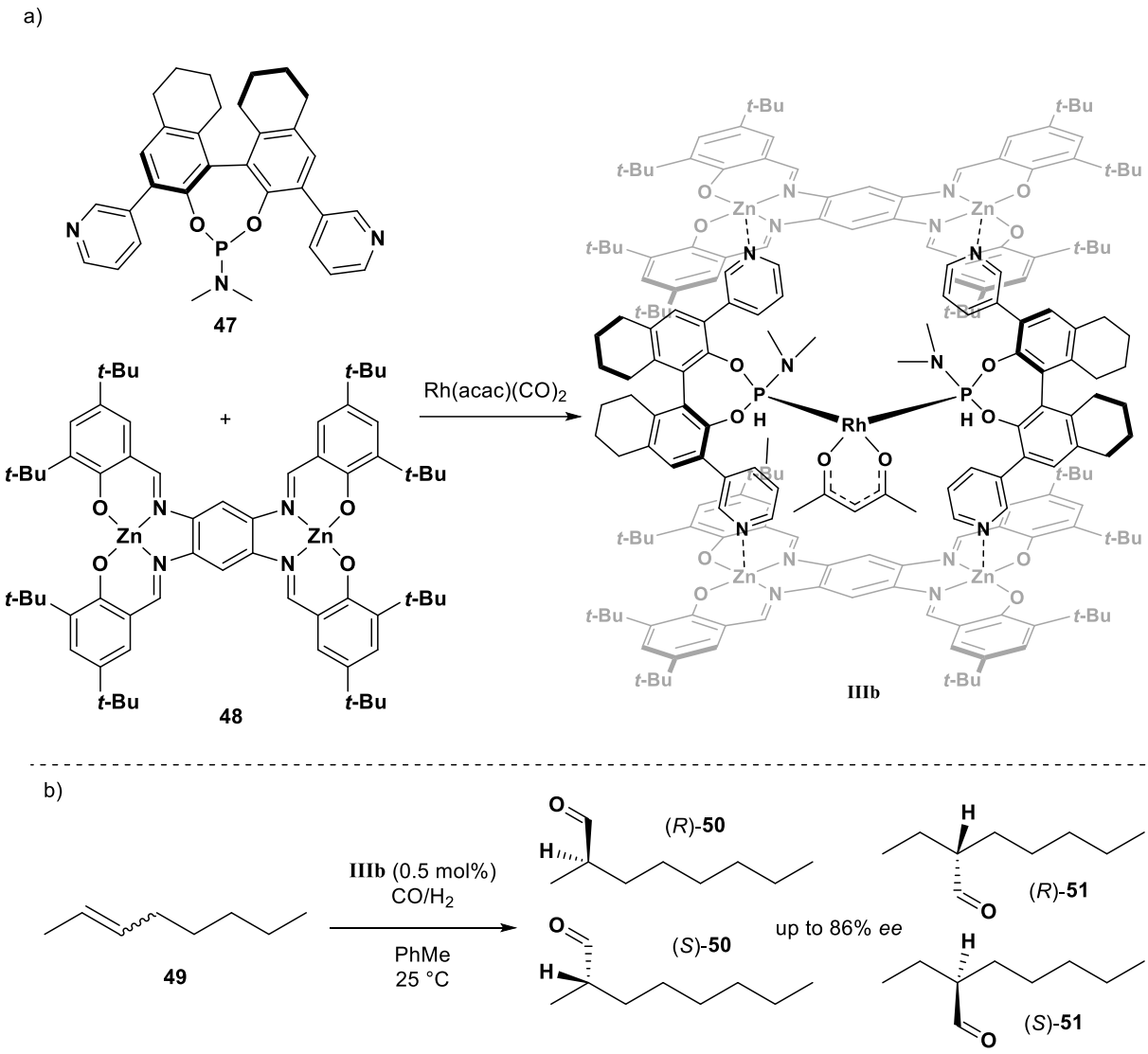


**Scheme 14**. a) Formation of chiral supramolecular catalyst **IIIb** reported by REEK. b) Hydroformylation of internal alkene **118** catalyzed by supramolecular Rh-complex **IIIb,** leading predominantly to the formation of the (*R*)-**120**.

CUI and co-workers recently reported a chiral octahedral coordination cage **XV**, which was constructed from twelve units of enantiopure Mn(salen)-derived dicarboxylic acids (**52**) as linear linkers and six $Zn_4$-*p*-*tert*-butylsulfonylcalix[4]arene building-blocks (**53**) as tetravalent four-connected vertices (Scheme 15).[107] The large hydrophobic cavity (V = 3944 $Å^3$) of the porous cage is decorated with catalytically active metallosalen moieties so it can catalyze the oxidative kinetic resolution (OKR) of racemic secondary alcohols with up to 97% *ee* and $k_{rel}$ = 35. Metallosalen monomer **52** was only half as efficient as cage **XV** in terms of the obtained $k_{rel}$ values, providing lower enantiomeric excess and similar conversions in comparison to cage **XV**. Fluorescent titration studies demonstrated the formation of the host-guest complex from the alcohol and cage **XV**, which confirms that OKR is most likely associated with alcohol being encapsulated due to a suitable pore shape and size of the host.

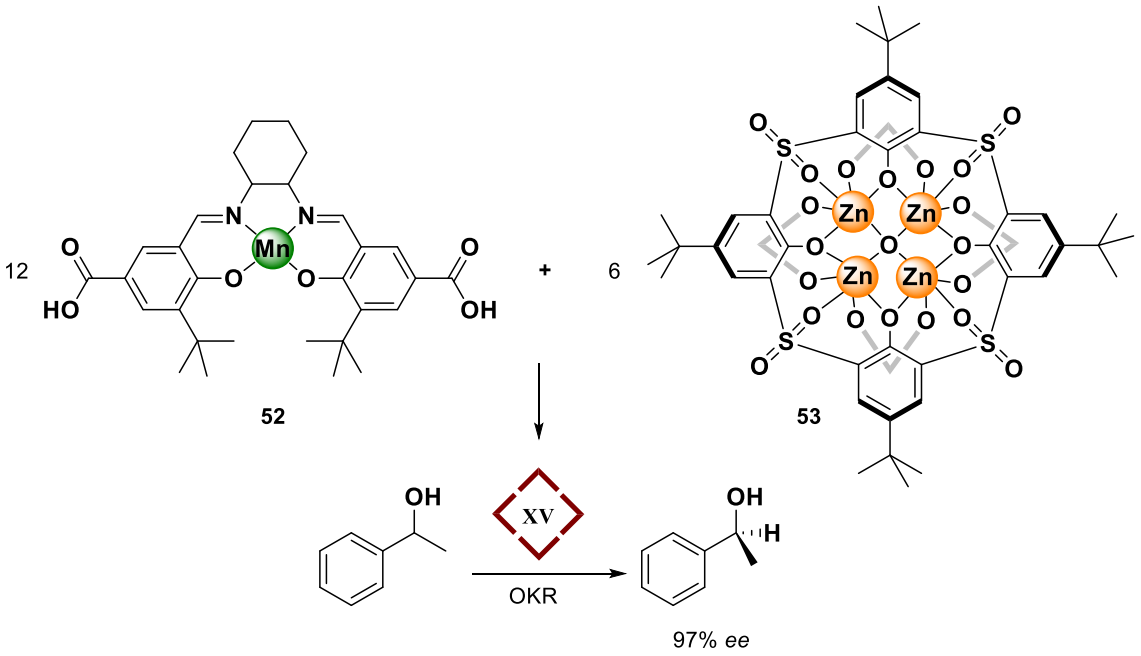


**Scheme 15**. Assembly of capsule **XV** from subunits **52** and **53** and a scheme of oxidative kinetic resolution (OKR) catalyzed by **XV**.

Of particular interest is the water-soluble metal-based cage **XVI,** first reported by RAYMOND in 1998 (Scheme 16a and b). The tetrahedral host **XVIa** assembles from $Ga^{III}$ ions and ditopic catecholate-containing ligands in a 4:6 stoichiometry.[108] The negative charge of the host allows encapsulation of cationic guests due to preferred Coulomb interactions. Entropy-driven encapsulation of neutral organic molecules occurs through the exclusion of solvent molecules from the cavity upon encapsulation.[109] Interestingly, structure **XVIa** is chiral even though it consists of only achiral building blocks. Strong mechanical coupling of the ligands helps to transfer the configuration of one gallium center to the other three, which leads to the exclusive formation of diastereomerically pure ΔΔΔΔ- and ΛΛΛΛ-capsules. Later it was shown that the addition of chiral guest molecules leads to a chiral resolution of the racemic capsule.[110]

Another approach leading to more defined capsules is the use of chiral ligands dictating which enantiomer is formed (capsule **XVIb**).[111] Numerous examples have been reported using the cages **XVIa** and **XVIb** for chiral discrimination of guest molecules and as a supramolecular catalyst in reactions involving cationic intermediates and transition states.[112] RAYMOND and BERGMAN reported the accelerated cationic 3-aza-COPE rearrangement inside the tetrahedral supramolecular host **XVIa** (Scheme 16c).[113,114] The cationic substrates **54** are well stabilized inside the cavity due to cation-π interactions.[109] The reaction involves a [3,3]-sigmatropic rearrangement *via* a chair-like transition state; the formed iminium ion is subsequently hydrolyzed to the final aldehyde **55**. Detailed investigation of iminium hydrolysis indicated two possible mechanisms, both taking place outside of the cavity. The tight iminium cavity ion pair

can either be attacked by water or dissociate in the presence of alkyl ammonium ions with the following hydrolysis of the iminium in solution. Inhibition experiments with an excess of the strongly binding competitive guest proved that the reaction is accelerated inside the cavity. The chiral derivative **XVIb** was successfully utilized in this reaction delivering enantioselectivity of up to 78% *ee* depending on the size and shape of the substrate and the temperature of the reaction.[112]

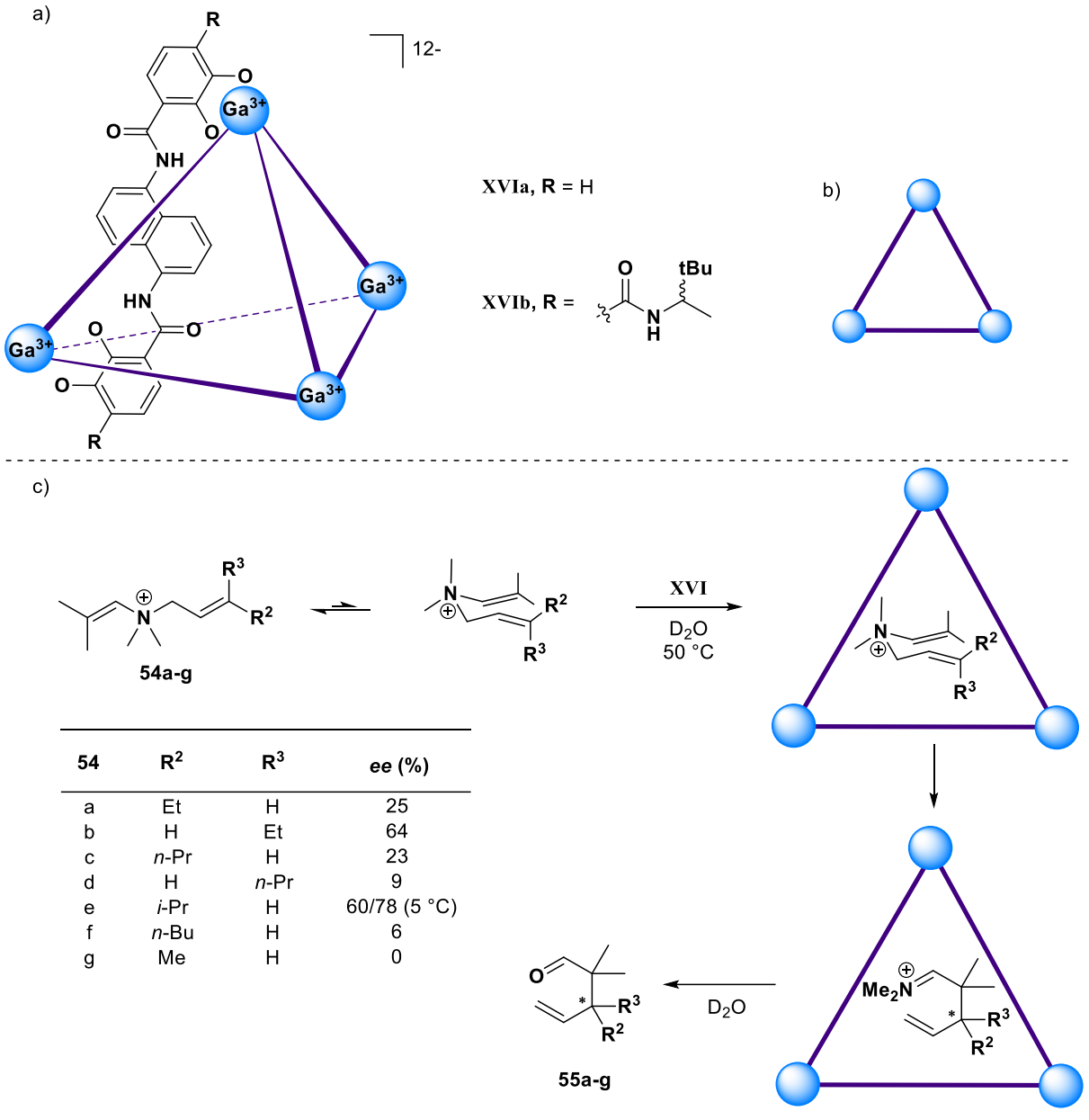


| 54 | $R^2$ | $R^3$ | ee (%) |
|---|---|---|---|
| a | Et | H | 25 |
| b | H | Et | 64 |
| c | *n*-Pr | H | 23 |
| d | H | *n*-Pr | 9 |
| e | *i*-Pr | H | 60/78 (5 °C) |
| f | *n*-Bu | H | 6 |
| g | Me | H | 0 |

**Scheme 16**. a) Self-assembled capsule **XVI**. b) Schematic 2D-representation of cage **XVI**. c) Enantioselective aza-COPE rearrangement of **54** to **55** inside tetrahedral supramolecular host **XVI.**

The PRINS-type cyclization of monoterpenes was also explored inside cage **XVIa** (Scheme 17).[115] Under acidic conditions, citronellal (**56**) undergoes cyclization to form compound **58**. However, in the presence of supramolecular catalyst **XVIa** followed by

elimination, the reaction results in diastereomers **57a-d** (Scheme 17a). Enantioselective PRINS-type cyclization was performed inside optically active capsule **XVIb** on the substrate **59**, yielding alcohols **60** and **61** (8:1 ratio), reaching 61% *ee* for alcohol **60** (Scheme 17b).[111]

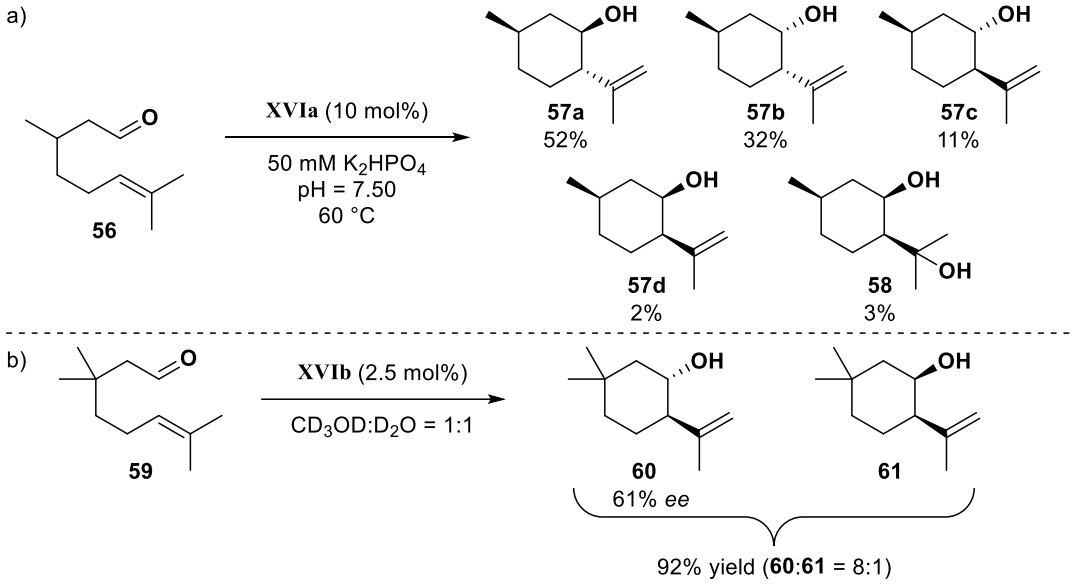


**Scheme 17**. a) Terpene-like cyclization of citronellal catalyzed by **XVIa**. b) Enantioselective PRINS-cyclization of **113** inside optically active supramolecular cage **XVIb**.

In 2016 MASTALERZ reported a chiral octameric host **XVII** with a volume of 2300 Å$^3$, which only self-assembles from enantiopure tris(isatin) **62** in apolar solvents (Scheme 18a).[116] The capsule **XVII**, which is held together by seventy-two NH−O and CH−O bonds forming a "closed-shell" hydrogen bond network, can encapsulate cationic guests (e.g., tetraalkylammonium salts) as well as neutral molecules (e.g., pyrene). STEFANKIEWICZ described enantiopure nanocapsule **XVIII**, which assembles from eight amino acid-functionalized trisubstituted benzene building blocks **63** held together *via* forty-eight hydrogen bonds (Scheme 18b).[117]

Self-sorting represents a powerful tool for the creation of chiral complex supramolecular structures.[118] The SZUMNA group has reported a dynamic formation of homo- or heterochiral hybrid peptidic resorcinarene-based capsules obtained by using the DCC approach.[119] Later the group utilized the DCC approach to construct intrinsically chiral cages (Scheme 18c).[120] The stepwise reaction of hydrazine with achiral tetraaldehyde resorcinarene-based building block **64** allowed the formation of chiral cage **XIX**, which structure was confirmed by X-ray crystallography. In the case of this structure, the chirality originates from the ordered distribution of the hydrazine moieties. The structure is additionally stabilized *via* a hydrogen-bonding network due to the presence of unprotected phenolic groups. The two

enantiomers of **XIX** were partially isolated by means of HPLC and characterized with CD spectroscopy. Further studies of the group afforded a nature-inspired rational design of chiral self-assemblies based on resorcinarenes with azapeptide moieties of different lengths.[121]

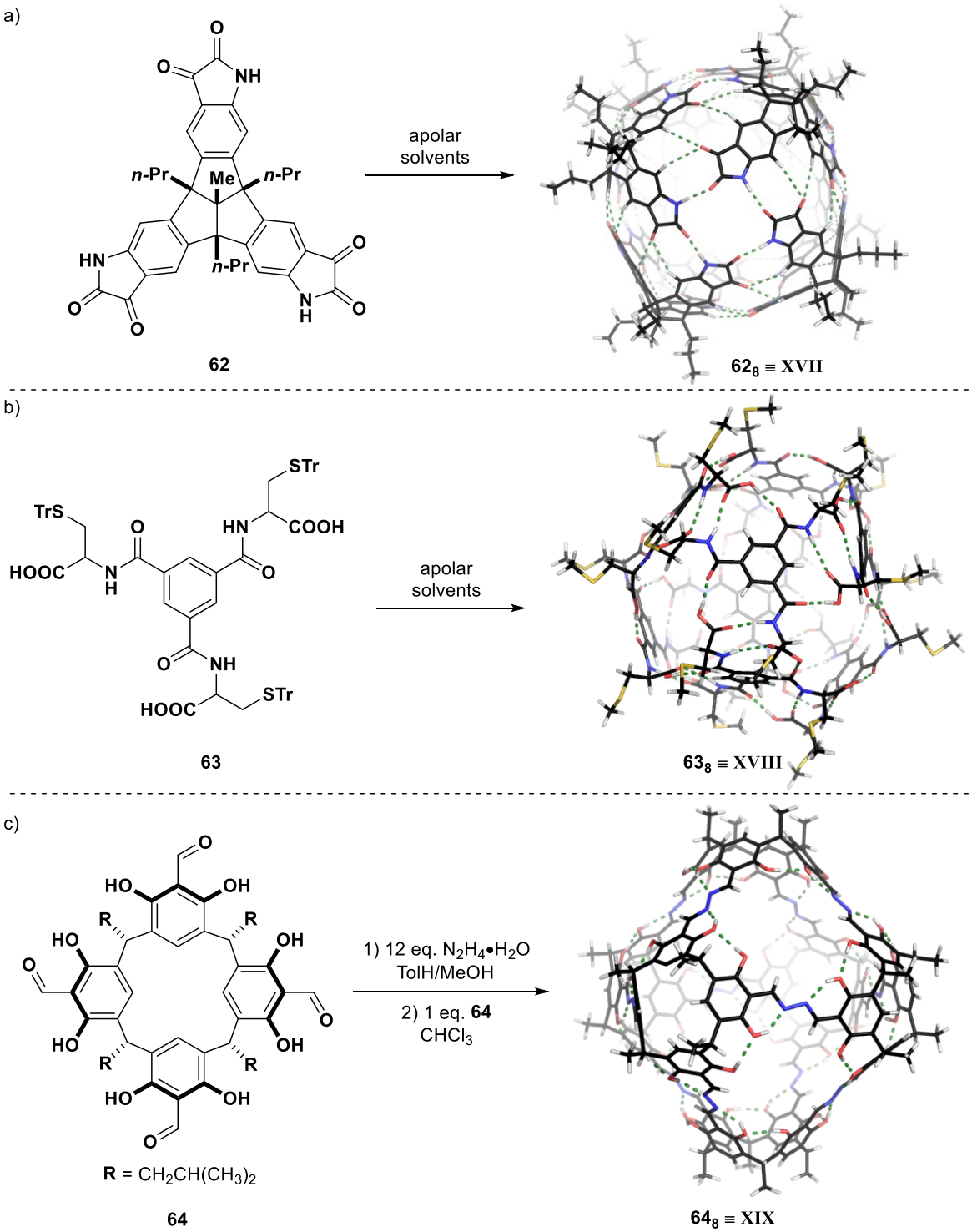


**Scheme 18**. a) Self-assembly of octameric capsule **XVII** form enantiopure **62**. b) Formation of chiral octamer **XVIII** from building block **63**. c) Self-assembly of chiral cage **XIX** from resorcinarene **64**. Feet (R) were omitted for clarity.

There are other examples of supramolecular systems successfully utilized to catalyze different reactions, however, their application in enantioselective catalysis is rather limited.[122,123]

## 1.3. Selected Reactions Inside Resorcinarene Capsule Leading to Formation of Chiral Products

At first glance, symmetry is a very common phenomenon in nature. However, on the molecular level, asymmetry is preferred. This fact is confirmed by amino acids and sugars, which exist in enantiopure forms in nature, the stereospecificity of enzyme-catalyzed reactions, and many other specific metabolic and regulatory biological processes. Of particular interest are chiral molecules for the pharmaceutical industry. Often only one enantiomer of the drug possesses the desired properties, while the second one either has no effect or can even cause undesired and/or serious side effects. The amount of enantiopure drugs introduced into the market is rising each year.[124]

In nature, stereoselective reactions involve enzymes, which can selectively bind and recognize substrate molecules producing the desired compound in enantiopure form. This makes asymmetric synthesis particularly interesting and important for research and industry alike.

Terpene natural products demonstrate a broad range of biological activities, making them perspective for the treatment of human diseases.[125–130] Terpene cyclization is one of the most complex transformations found in nature, which often leads to the formation of chiral products. Therefore, the possibility to conduct this reaction enantioselectively in a laboratory setting is especially relevant for chemists.

Iminium catalyzed reactions represent another important class of reactions leading to chiral product formation. Iminium catalysis proved to be an exceptional tool that was and is used for numerous different chemical transformations.[131]

Both terpene cyclization and iminium catalyzed reactions inside resorcinarene capsule **XII** are of particular interest for this work. Therefore, the following chapter will focus on these topics.

### *1.3.1. Terpene Cyclization*

The cyclization of terpenes is one of the most interesting enzyme-catalyzed reactions found in nature, especially because terpenes represent a highly diverse class of natural products, and many of them are biologically active.[127–129] Terpenes are categorized based on the number of carbon atoms/isoprene units: hemi- ($C_5$), mono- ($C_{10}$), sesqui- ($C_{15}$), di- ($C_{20}$), sester- ($C_{25}$), triterpenes ($C_{30}$), and other larger members. Despite this diversity, several acyclic terpene precursors stand out (Fig. 4), from which other terpenes are formed: geranyl diphosphate (**65**) (monoterpenes), farnesyl diphosphate (**66**) (sesquiterpenes), geranylgeranyl diphosphate (**67**) (diterpenes).[129]

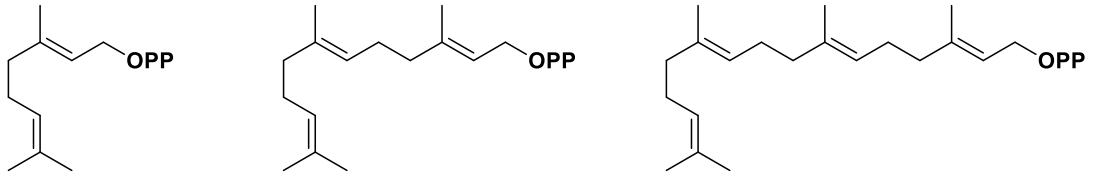


65 66 67

**Figure 4**. Acyclic precursors for the biosynthesis of complex terpenes.

Terpene cyclases perform the cyclization of these precursors in nature. There are two main biosynthetic pathways that have been described: "head-to-tail" terpene (HTT) cyclization, which is triggered by electrophilic activation of a terminal prenyl moiety, and "tail-to-head" terpene (THT) cyclization, which starts from allylic pyrophosphate group cleavage.[132] In both cases, the formed carbocation is intramolecularly attacked by a double bond to form a cyclic molecule. The produced carbocation can further go through additional transformations until the final product is released from the active enzyme pocket. This "non-stop" cyclization is very characteristic of terpene cyclases and hard to achieve with artificial catalysts.[133] Terpene cyclases also demonstrate notable selectivity and can efficiently transfer chirality onto a prochiral substrate due to specific configurations of the enzymes' active sites.

Scheme 19 illustrates the complexity of the process and the diversity of the formed products in the cyclization reaction of geranyl diphosphate (**68**).[127] Tail-to-head cyclization is initiated by the diphosphate group cleavage, producing cationic species **68a**, which undergoes isomerization of the double-bond configuration directly[92] or *via* the linalyl diphosphate (**69**), followed by a rotation of the double bond.[127] Resulting cation **68b** cyclizes to α-terpinyl cation (**70**), which can further undergo transformations producing a variety of products. Thus, elimination gives limonene (**71**) and terpinolene (**72**), and if 1,2- or 1,3-hydride shift was followed by elimination, it leads to the formation of α-terpinene (**73**), γ-terpinene (**74**) or α-phellandrene (**75**). In the presence of water, α-terpineol (**76**) can form, which is able to further

cyclize to eucalyptol (**77**). Besides eucalyptol, other bicyclic structures such as β-pinene (**78**), camphene (**79**), 3-carene (**80**), sabinene (**81**), sabinene hydrate (**82**), and *endo*-fenchol (**83**) can be formed during the reaction. At the same time, some acyclic products such as geraniol (**84**), nerol (**85**), linalool (**86**), (*E*)-β-ocimene (**87**), and myrcene (**88**) occur if the initial isomerization is followed by deprotonation or by an attack of water. Additional products, which result from the attack of the initially cleaved diphosphate group can be found. The absolute configuration of the product refers to the helical conformation fold of geranyl diphosphate (**65**) and determines the configuration of the created α-terpinyl cation (**70**). In the case of the formation of several products, all of them usually possess the same absolute configuration.

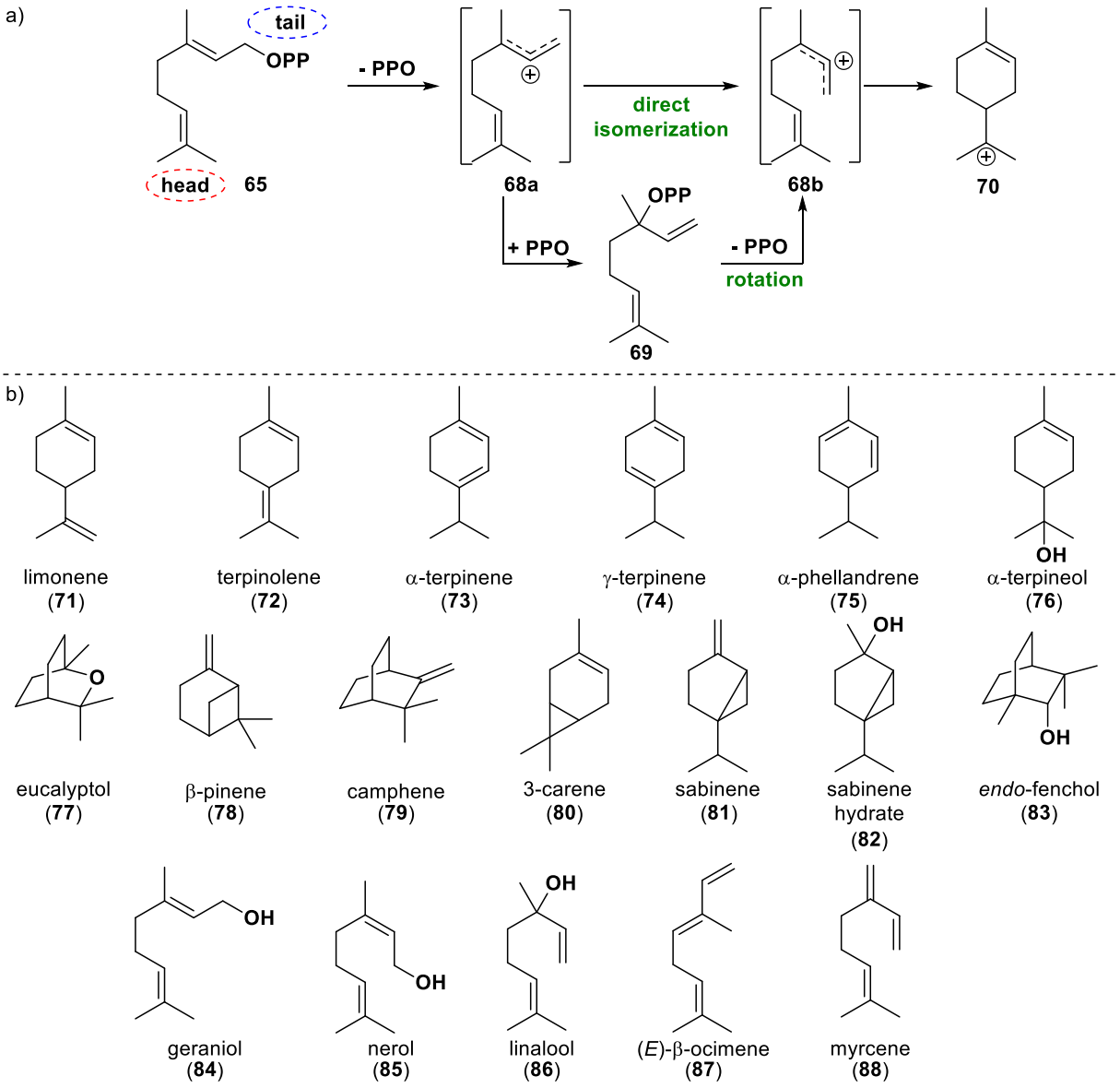


**Scheme 19**. a) Formation of the α-terpinyl cation (**70**) catalyzed by class I cyclases. b) Common cyclic and acyclic monoterpene products of the THT cyclization.

As one of the most diverse classes of organic compounds which possess various properties, including biological activity, terpenes are of great interest for synthetic chemistry. Therefore, a number of studies were performed in order to mimic the natural terpene cyclization process.[134] Most of the reported results regarding tail-to-head cyclizations of monoterpenes and sesquiterpenes proved to be difficult to reproduce and suffered from low yields and/or side-products through head-to-tail cyclizations.[92,135–139]

The first non-stop THT polycyclization in solution was reported in 2012 by SHENVI and co-workers.[132] They utilized a modified sesquiterpene **89** (Scheme 20a) with a vinyl epoxide moiety, which gets activated by aluminum LEWIS acids, and forms the bisabolyl cation (**90**). The cationic leaving group, which is covalently linked to the LEWIS acid, facilitates the cyclization cascade towards polycyclic compounds **91**–**93**. The JACOBSEN group has contributed to the field with the first catalytic enantioselective tail-to-head terpene cyclization in solution (Scheme 20b).[140] Based on the earlier published studies regarding utilization of thiourea derivatives for polyenes cyclization,[141] they described cyclization of the phenyl-substituted neryl chloride (**94**) in presence of catalyst **96** resulting mainly in derivatives of limonene **71** and terpinyl chloride (**95**) with high yields and enantioselectivity up to 93% *ee*. The presence of bulky aryl substituent on the substrate proved to be essential for steric and electronic reasons and for the stabilization of the positively charged intermediate by cation−π interactions between substrate and catalyst. The authors also presented a mechanism requiring two catalyst molecules, which explains why geranyl chloride derivatives due to unfavorable *E*-configuration of the double bond display weak reactivity and enantioselectivity in comparison to neryl chloride derivatives.

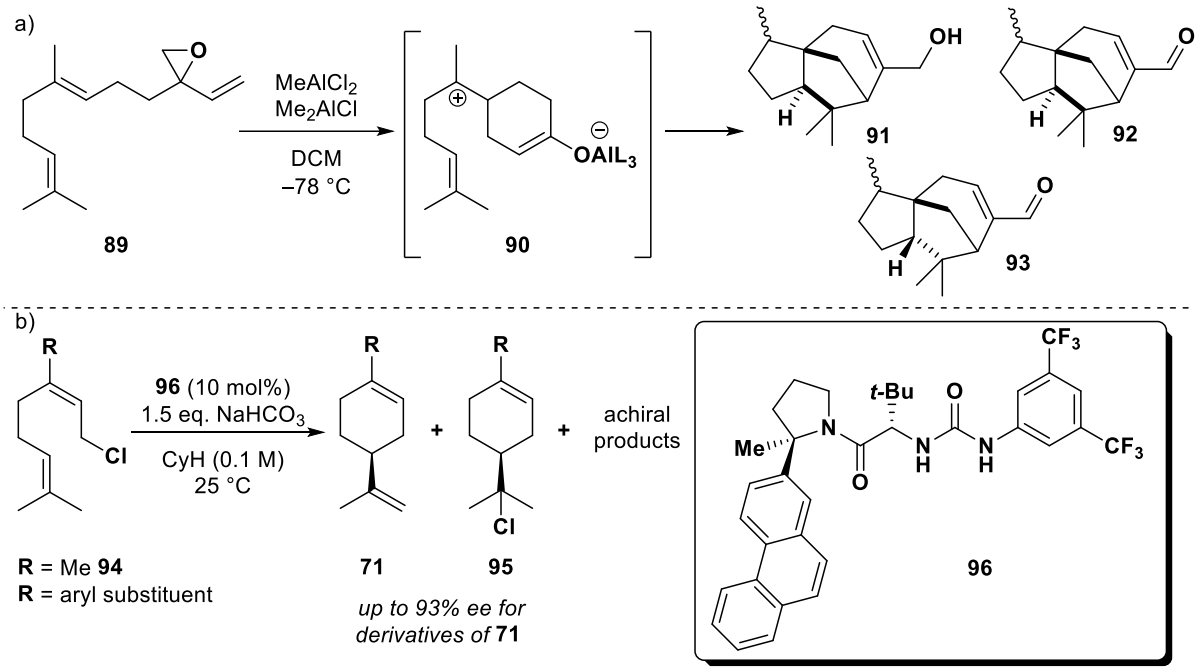


**Scheme 20**. a) Aluminum LEWIS acids activated tail-to-head cyclization of sesquiterpene **89**. b) Enantioselective tail-to-head cyclization of neryl chloride (**94**) and its derivatives with aryl substituents catalyzed by urea-based catalyst **96** reported by JACOBSEN.

The first example of successful THT cyclization inside a supramolecular capsule was published in 2015 by the TIEFENBACHER group reporting the utilization of resorcinarene hexamer **XII** as terpene cyclase mimetic.[92,93] THT cyclizations are difficult to control in solution due to potential side reactions of the cationic intermediates, which often leads to the formation of complex mixtures with traces of cyclic monoterpenes. However, supramolecular capsule **XII** was proved to activate commercially available monoterpenes such as nerol (**85**) or geranyl acetate (**97**) to promote their cyclization under mild conditions. Cyclization of nerol (**85**) with 10 mol% of **XII** and 3 mol% of HCl at 30 °C yields eucalyptol (**77**) as a major product and other monoterpenes (Scheme 21a). Such a direct cyclization to eucalyptol (**77**) utilizing artificial catalyst had not been described before. The reaction starts from the cleavage of leaving group, leading to the formation of α-terpineol (**76**) *via* α-terpinyl cation (**70**) followed by hydroalkoxylation (Scheme 21c). To prevent the quenching of the intermediate **70**, an acetate group was installed as a less nucleophilic leaving group, which led to the selective formation of α-terpinene (**73**) (up to 40% yield) from geranyl acetate (**97**) without the formation of other intermediates (Scheme 21b). The absence of other intermediates also observed for the cyclization of geraniol (**84**) speaks for the non-stop reaction mechanism, which is likely happening *via* the formation of the cation **98** due to the 1,2-hydride shift from intermediate **70**. This non-stop mechanism is facilitated by capsule **XII**, which stabilizes intermediary cations through cation-π interactions and protects them from the outside nucleophiles (e.g., water).

However, some alkylation products of the hexamer were identified in case of reactions with geranyl acetate (**76**) as a substrate. Geranyl acetate (**97**) cyclization indicates the importance of a direct isomerization from the *transoid* cation **68a** to the *cisoid* cation **68b** (not *via* the linalyl derivatives **99a**–**b)**, which had been previously considered as unlikely in the biosynthesis of terpenes.

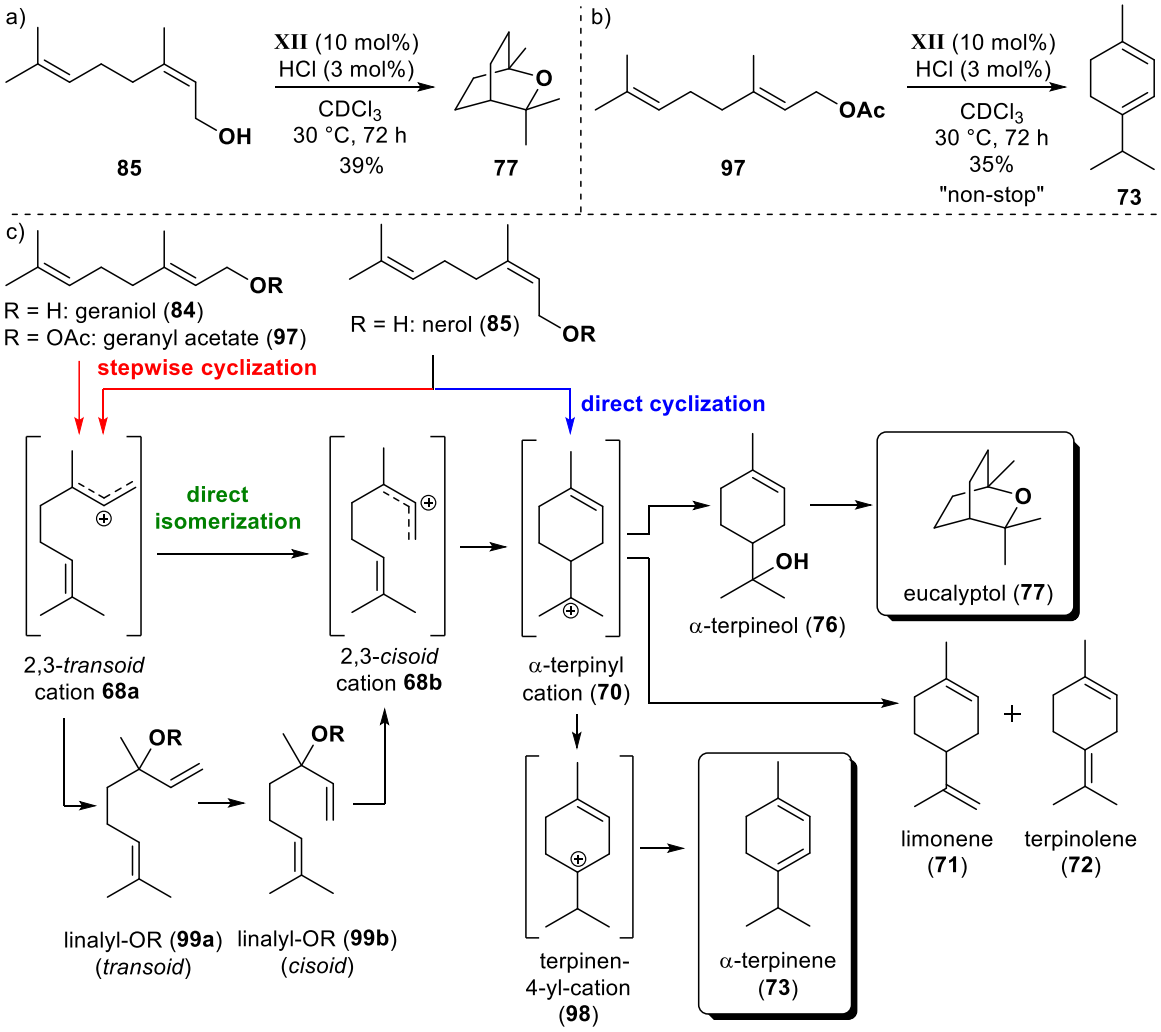


**Scheme 21**. a) Nerol (**85**) cyclization to eucalyptol (**77**) as the major product. b) Geranyl acetate (**97**) cyclization to α-terpinene (**73**) as the major product. c) Substrate-dependent reaction pathways of the THT cyclization catalyzed by capsule **XII**.

Kinetic studies allowed to hypothesize a mechanism (Scheme 22) and identify the key steps for THT cyclizations inside cavity **XII**: 1) substrate encapsulation; 2) protonation of the encapsulated substrate; 3) leaving group cleavage (rate-determining step) and stabilization of the formed ion pair inside the capsule.

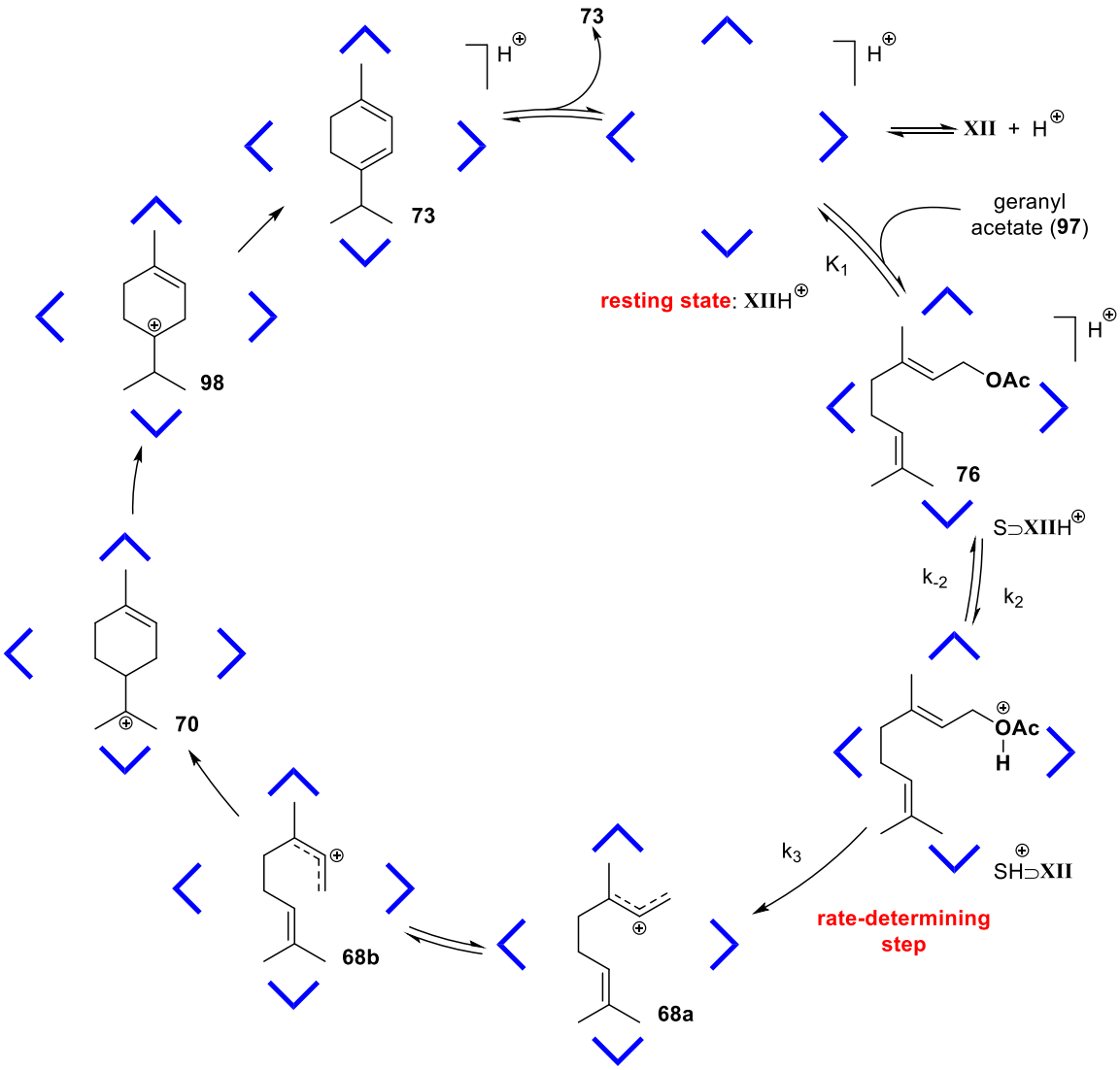


**Scheme 22**. Proposed mechanism of the acid-catalyzed cyclization of geranyl acetate (**97**) within the resorcinarene capsule **XII**.

Capsule **XII** has also been utilized for the cyclization of larger substrates. For example, isolongifolenone (**100**) can be successfully obtained from dihydro-β-ionone (**101**), which is in three steps converted into cyclization substrate cyclofarnesylacetate (**102**) (Scheme 23a).[142] The cyclization of **102** takes place inside capsule **XII** to give isolongifolene (**103**), which can be further oxidized to isolate isolongifolenone (**100**) with a 13% yield over five steps. Another report from the TIEFENBACHER group describes the total synthesis of δ-selinene (**104**) from nerol (**85**) with the capsule-catalyzed key cyclization step with substrate **106** (Scheme 23b).[143] The selectivity towards the formation of δ-selinene (**104**) is higher than in the reaction catalyzed by the corresponding natural cyclase. Extensive kinetic investigations proved that substrate encapsulation is a rate-determining step for sesquiterpene cyclizations in contrast to monoterpenes, where the reaction rate is controlled by the cleavage of the leaving group. Another application of hexamer **XII** which was recently found by TIEFENBACHER and

co-workers is the four-step synthesis of (−)-presilphiperfolan-1β-ol (**107**) from caryophyllene oxide (**108**) *via* the cyclization precursor **109** (Scheme 23c).[144] This approach also allows the synthesis of some artificial analogs, highlighting the advantages of supramolecular catalysis for the synthesis of natural products and their unnatural derivatives.

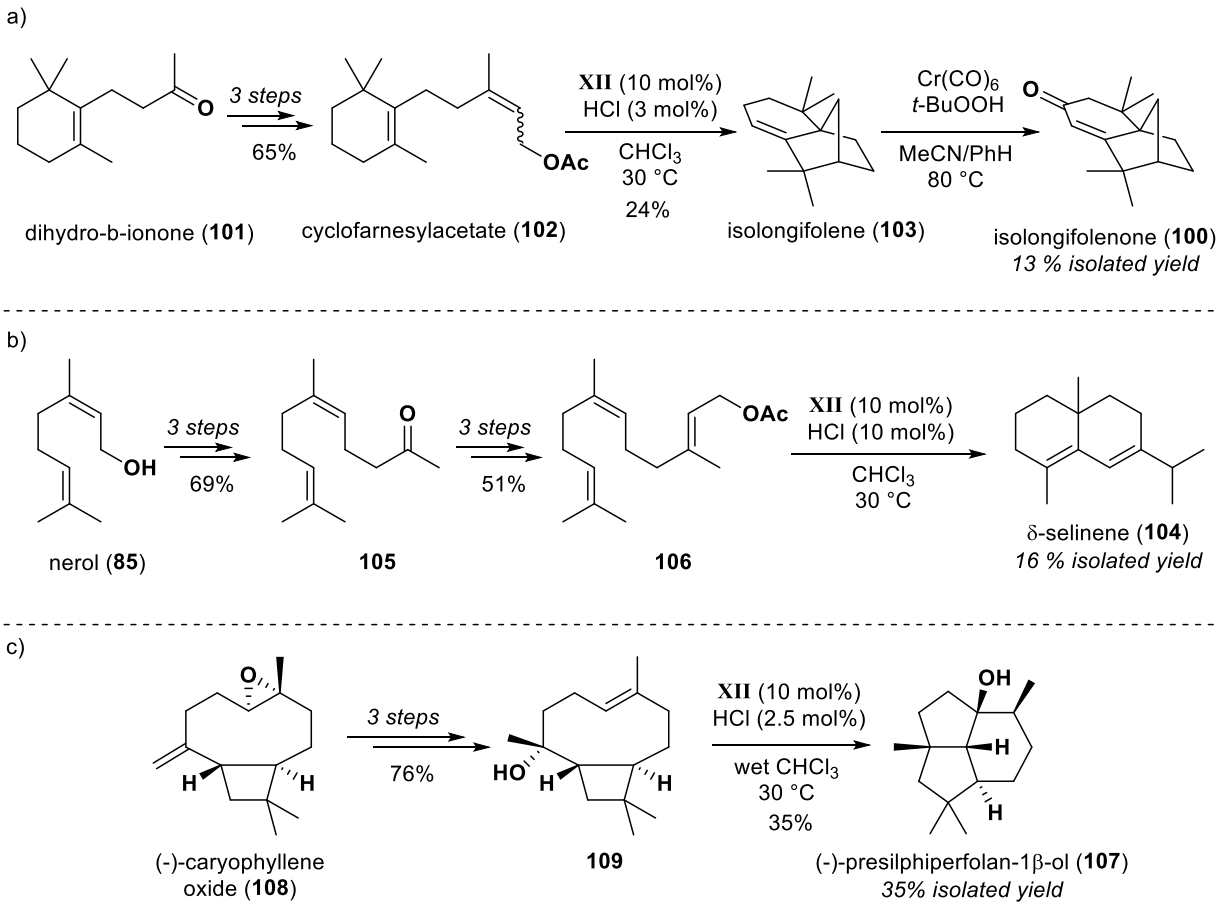


**Scheme 23**. a) Total synthesis of isolongifolenone (**100**) with a key step using capsule **XII**. b) Total synthesis of δ-selinene from nerol (**85**) utilizing **XII** for the final cyclization step. c) Four-step total synthesis of (–)-presilphiperfolan-1β-ol (**107**) starting from caryophyllene oxide (**108**) with the final cyclization step taking place inside supramolecular capsule **XII**.

A recent study by the TIEFENBACHER group allowed to establish the key requirements for terpene cyclization reactions inside supramolecular hosts.[145] The authors synthesized new resorcinarene derivatives **110**–**113**, which proved to assemble forming hexameric capsules. New assemblies based on these macrocycles were tested together with already known assemblies from **9b** and **10b** (Fig. 5) regarding their catalytic activity in THT cyclizations, ability to encapsulate terpene substrates and ion pairs, their response to acid addition, and the amount of water incorporated into hydrogen bond network.

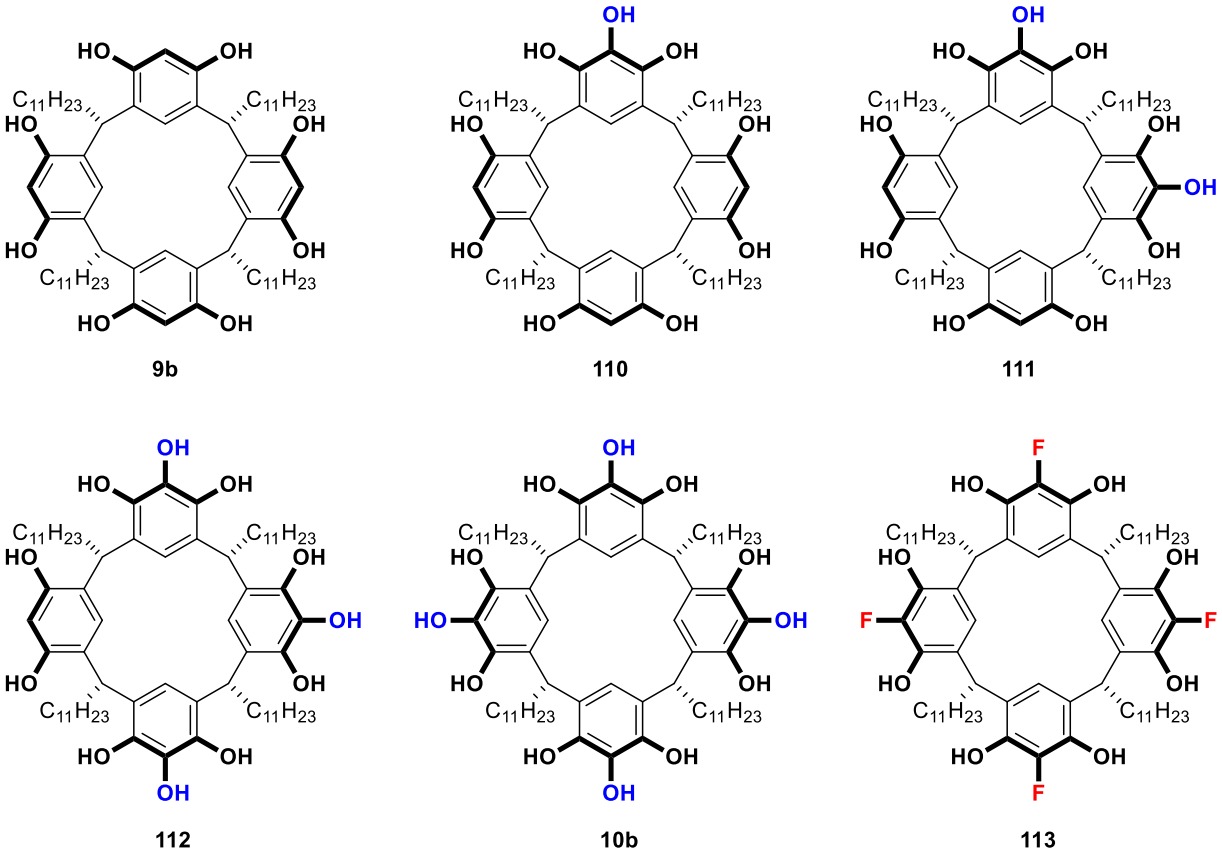


**Figure 5**. Resorcinarene-based macrocycles used by the TIEFENBACHER group to establish the requirements for terpene cyclization reactions inside supramolecular resorcinarene-based hosts.

The experimental results pointed out a correlation between the catalytic activity of the capsule and water as a part of the assembly, which was further confirmed by molecular dynamics simulations indicating the particular role of water in the protonation of the encapsulated substrate. The authors state that the incorporated water molecules act as a shuttle, which transfers the proton from the HCl co-catalyst to the encapsulated substrate initiating the cyclization process. These results are of particular importance for the further design of supramolecular catalysts, as they finally define the requirements for the catalytic activity of supramolecular structures for terpene cyclization reactions.

### *1.3.2. Iminium Catalysis*

First publications on asymmetrical organocatalytic reactions by LIST[146] and MACMILLAN[147] drew the chemists' attention and led to the so-called gold rush of organocatalysis.[148,149] The number of publications related to organocatalysts has significantly increased over the past years, underlining the importance of organocatalysis for scientific society. In 2021 LIST and MACMILLAN were awarded a Noble Prize for their invaluable contribution to the development of asymmetric organocatalysis. Organocatalysis has several advantages: 1) it offers alternative ways of making (chiral) molecules that do not rely on transition metals or enzymes; 2) it is considered as less sensitive towards air and moisture; 3) catalysts are relatively cheap, readily available, and have low toxicity. All these properties make organocatalysis especially beneficial for the pharmaceutical industry.

Iminium catalysis, in which iminium ions act as reactive intermediates in the catalytic cycle (Scheme 24), represents an important organocatalytic reaction and is particularly relevant for this work.[131] The catalytic cycle starts from an acid-induced condensation of α,β-unsaturated carbonyl compound **115** with chiral amine catalyst **114**, forming the iminium cation **116**. Nucleophile attacks the β-position of highly electrophilic iminium ion to form enamine compound **117**. Protonation of **117** and hydrolysis of **118** lead to the release of product **119**. Regenerated catalyst **114** can further participate in a new catalytic cycle.

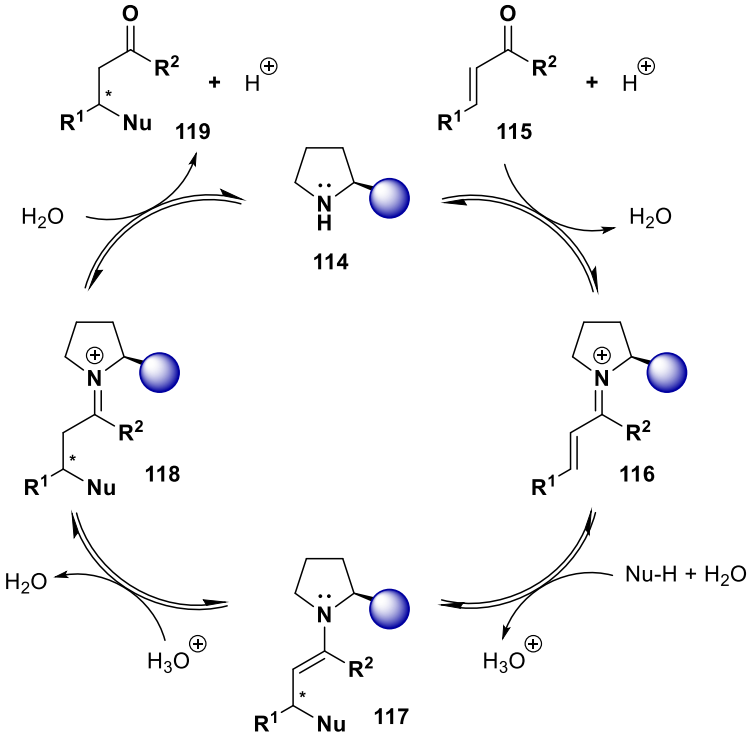


**Scheme 24.** General catalytic cycle of iminium catalysis in the presence of chiral aminocatalyst **114.**

Iminium catalysis has proved to be a useful tool for enantioselective functionalization of the β-position of aldehydes and ketones.[150–154] However, this chapter will focus on iminium-catalyzed reactions inside the supramolecular capsule **XII**, which is the main subject of the group's studies.

The first example of iminium catalysis inside supramolecular capsule **XII** was reported by TIEFENBACHER and co-workers.[155,156] The L-proline-catalyzed 1,4-reduction of α,β-unsaturated aldehydes **120** occurred with surprisingly high enantioselectivity in the presence of capsule **XII** (26 mol%) in comparison to a bulk solution (Scheme 25a). The observed modulation effect is attributed to the stereoselective binding of the encapsulated iminium intermediate to the capsule (Scheme 25b). The authors hypothesized that the less hindered side of the iminium ion experiences π-interactions with the capsule wall (Scheme 25c). Subsequent selective attack by HANTZSCH ester (**121**) delivers aldehyde **122**, favoring the (*S*)-enantiomer. Reactions with other proline derivatives **123b–c** (Scheme 25d) delivered enantioselectivity comparable to **123a** except for catalyst **123b**, which contains sterically shielding moiety. Further NMR studies proved that reaction indeed takes place inside **XII**.

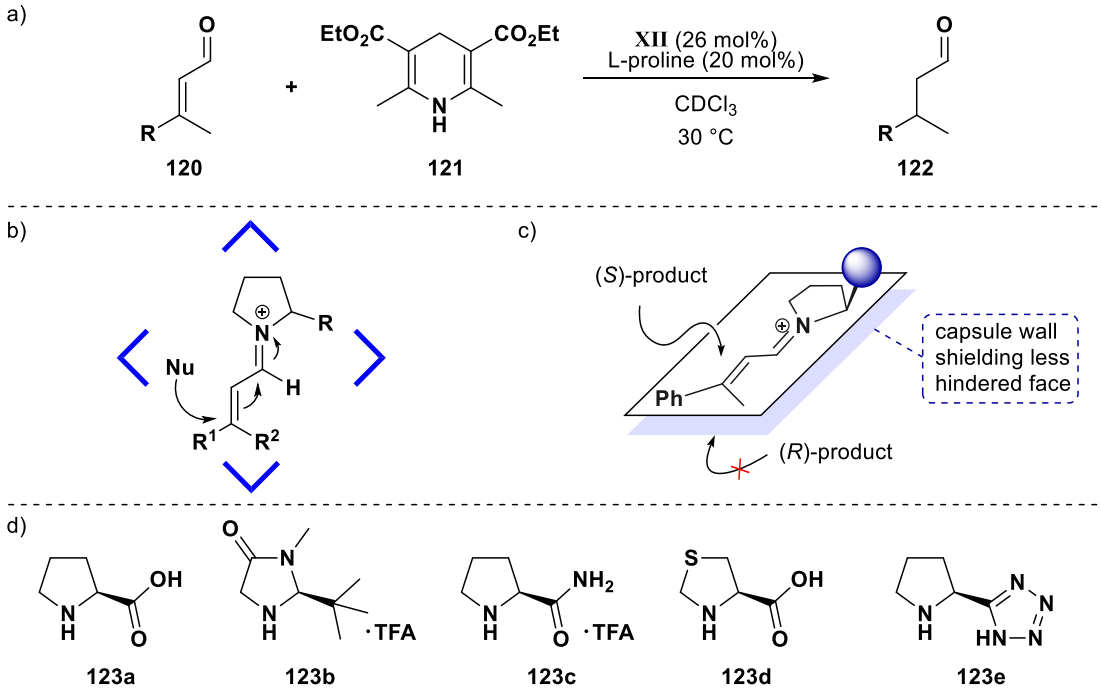


**Scheme 25**. a) Enantioselective iminium catalysis within hexamer **XII**. b) Encapsulated reactive iminium species within structure **XII**. c) Chiral induction, which is caused by the shielding of the bottom face by the capsule walls. d) Chiral aminocatalysts utilized for the study of iminium-catalyzed reduction inside capsule **XII**.

The expanded substrate scope (aldehydes **120a–j**, Fig. 6) confirmed the efficiency of this approach, delivering corresponding products with Δ*ee* up to 92% when comparing reactions with and without capsule **XII**.

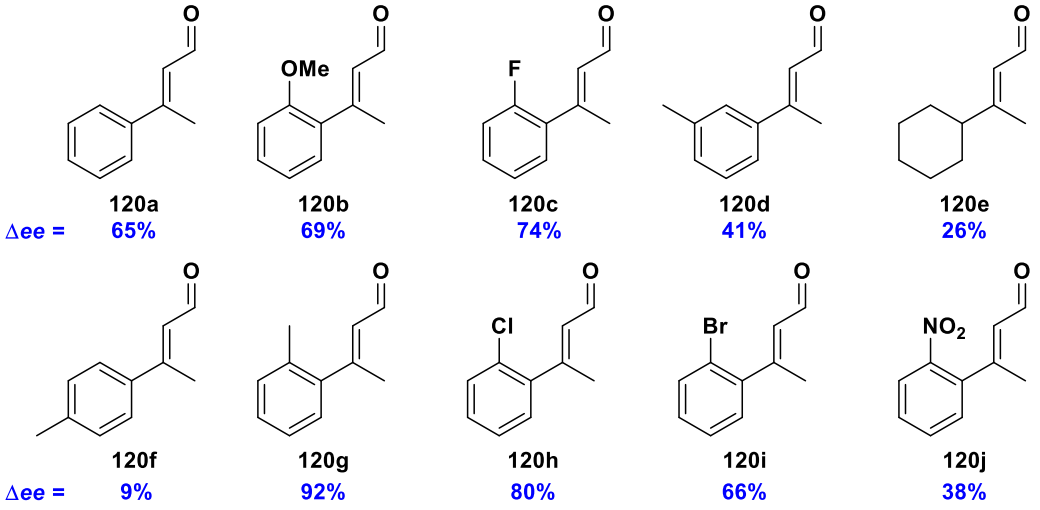


**Figure 6**. Substrate scope and Δ*ee* values for iminium-catalyzed 1,4-reduction inside supramolecular host **XII** reported by the TIEFENBACHER group.

Another remarkable example of an iminium-catalyzed reaction inside **XII** was reported by NERI and co-workers.[157] The authors showed that hexameric capsule **XII** is able to catalyze the 1,3-dipolar cycloaddition between nitrones **124** and unsaturated aldehydes (e.g., crotonaldehyde (**125**)) with a moderate to good control over the regio-, diastereo- and enantioselectivity of the reaction (Scheme 26a). Utilizing the same reaction conditions as the TIEFENBACHER group demonstrated for 1,4-reduction, NERI and co-workers achieved the best enantioselectivity (95% *ee*) for product **126a** (*endo*-isomer). The hypothesized mechanism involves stabilization of iminium intermediate by cation–π interactions with electron-rich aromatic cavity **XII** followed by reaction with nitrone inside the capsule, followed by the subsequent release of the products (Scheme 26b). The formation of iminium-intermediate inside capsule **XII** was also confirmed by *in silico* studies. The generality of the approach concerning the structure of nitrones **124** in terms of efficiency and selectivity was confirmed by the expansion of the substrate scope (Scheme 26a). In all cases, the reaction did not occur in the absence of capsule **XII** indicating the importance of supramolecular catalyst for the reaction to take place.

a)


**124a-f** **125** *endo*-**126a-f** *exo*-**126a-f**

| **124, 126** | **R$^1$** | **R$^2$** | **Yield (%)** | *endo*-**126**/*exo*-**126** | ***ee*** *endo*-**126**/*exo*-**126 (%)** |
|---|---|---|---|---|---|
| a | Me | Ph | 90 | 84/14 | 95 (4*R*)/0 |
| b | Bn | Ph | 91 | 39/58 | 68(4*R*)/39(3*R*) |
| c | Bn | 4-MeO-$C_6H_4$ | 75 | 57/43 | 56(4*R*)/50(3*R*) |
| d | Me | 4-Cl-$C_6H_4$ | 92 | 94/6 | 94(4*R*)/- |
| e | Me | 4-Me-$C_6H_4$ | 91 | 86/10 | 80(4*R*)/13(3*R*) |
| f | Bn | 4-Me-$C_6H_4$ | 85 | 63/37 | 77(4*R*)/50(3*R*) |

b)

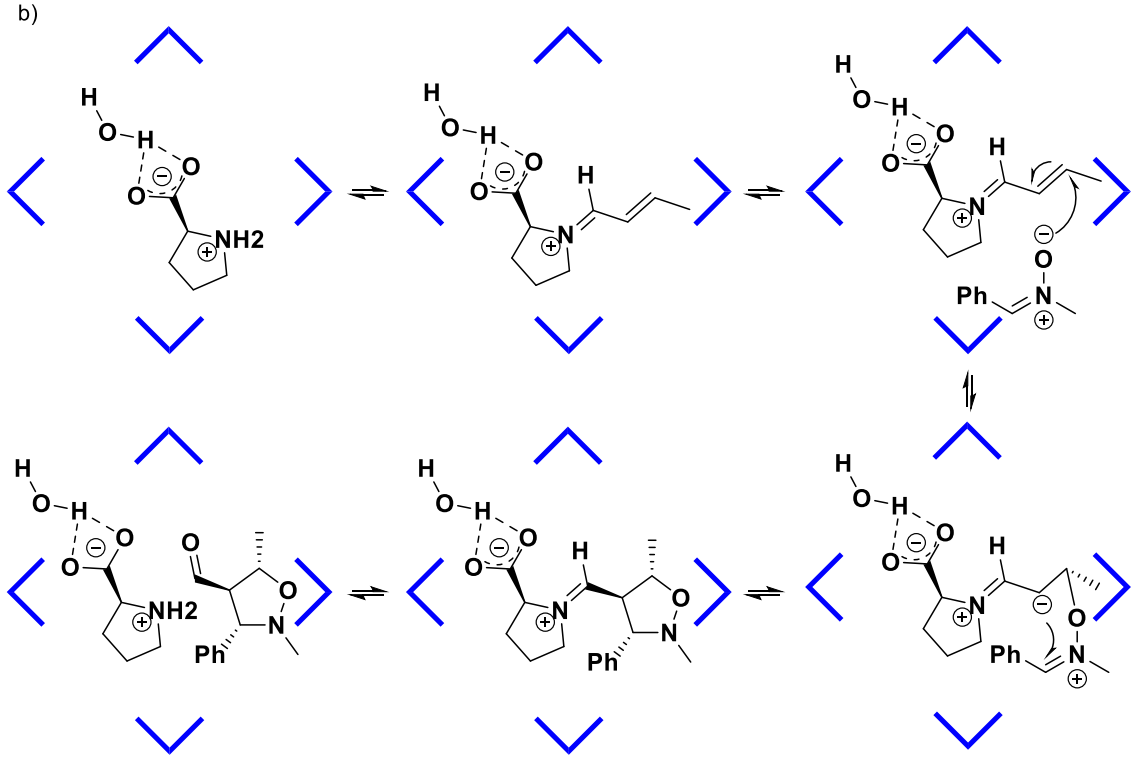

**Scheme 26**. a) Iminium-catalyzed 1,3-dipolar cycloaddition reaction inside supramolecular host **XII** reported by NERI. b) Proposed mechanism for 1,3-dipolar cycloaddition between nitrones and unsaturated aldehydes inside capsule **XII**.

# 2. OBJECTIVES OF THIS THESIS

Hexameric capsule **XII** has proved to serve as an efficient enzyme mimetic and catalyze a variety of chemical transformations. Successful tail-to-head terpene cyclization was also achieved by using **XII** as a catalyst. However, this reaction inside **XII** has never been done in an enantioselective fashion. Therefore, this work aims to develop a capsule **XII**-based supramolecular catalyst for enantioselective terpene cyclization.

The resorcin[4]arene building block **9** has to be modified in order to obtain chiral catalysts for achieving enantioselective transformations. This can be done *via* monofunctionalization to modify the upper rim of the resorcinarene (Scheme 27a) or to use optically active aldehydes for condensation with resorcinol to introduce chirality on the feet (Scheme 27b). In this work, we propose a synthesis of such derivatives and test their behavior in tail-to-head terpene cyclization reactions.

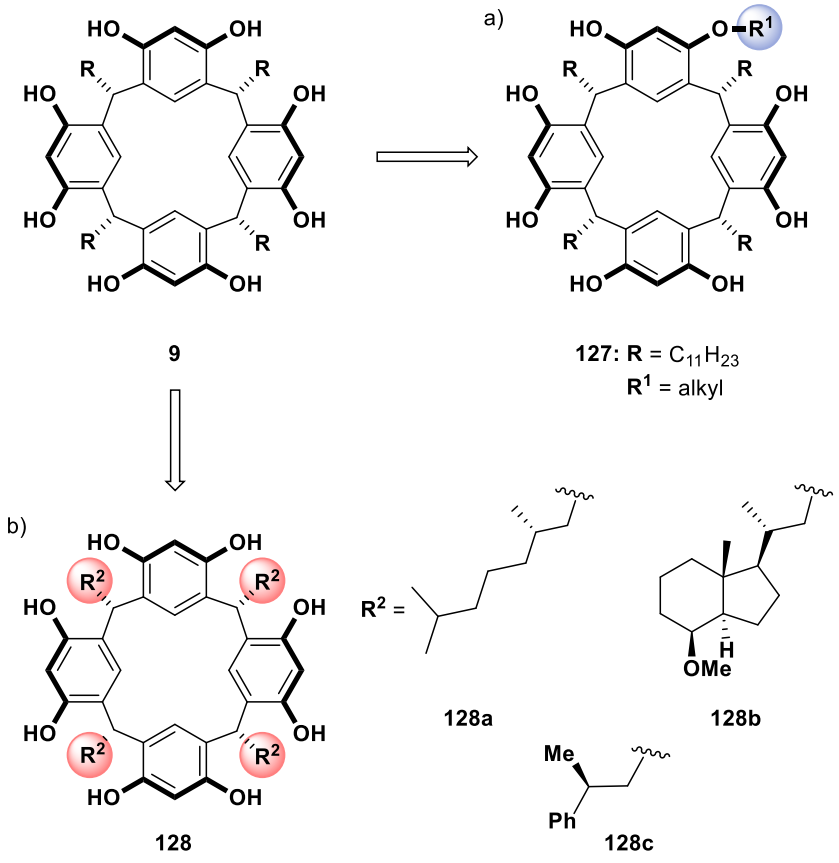


**Scheme 27.** a) Upper-rim monomodified resorcinarene with alkyl moieties. b) Resorcinarenes with chiral feet.

Iminium-catalyzed 1,4-reduction of α,β-unsaturated aldehydes enantioselectively occurs inside capsule **XII** due to the chiral co-catalyst L-proline, as it was shown by previous studies in our group. Later, we also demonstrated that the presence of HCl as a co-catalyst plays a crucial role

in various reactions catalyzed by capsule **XII**. However, the effect of HCl additive on iminium catalysis inside **XII** was never investigated. Therefore, another objective of this work is to explore the influence of HCl as a co-catalyst on the iminium-catalyzed reduction of α,β-unsaturated aldehydes inside capsule **XII**. In parallel, we also aim to optimize the conditions and examine other additives, which could increase the enantioselectivity of this transformation.

# 3. RESULTS AND DISCUSSION

## 3.1. Publication Summary

**Optimized iminium-catalyzed 1,4-reductions inside the resorcinarene capsule: achieving >90% ee with proline as catalyst**[158]

Previous reports by our group describe iminium-catalyzed enantioselective 1,4-reduction of α,β-unsaturated aldehydes inside capsule **XII** (Fig. 7). Later studies demonstrated the importance of HCl as a co-catalyst for a selection of capsule **XII**-catalyzed reactions, however, its influence on iminium catalysis inside **XII** was never explored before. Therefore, we aimed to (1) investigate the HCl role in iminium-catalysis inside capsule **XII**; (2) reduce the previously utilized 26 mol% of capsule catalyst, which was originally chosen to ensure complete encapsulation of 20 mol% L-proline (**123a**) and the formed iminium species; (3) optimize the reaction conditions in order to improve enantioselectivity.

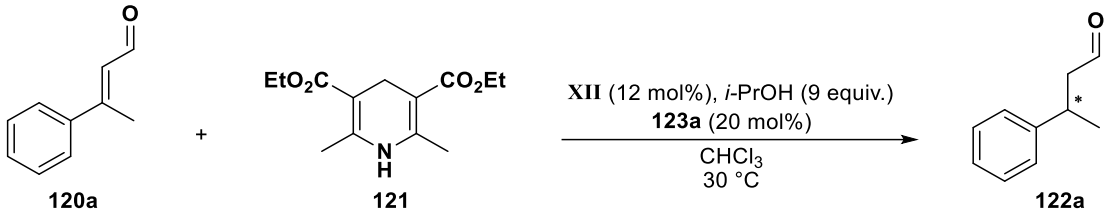


**Figure 7.** General scheme of iminium catalyzed 1,4-reduction inside capsule **XII**. Reproduced from Ref. [158] with permission from the Royal Society of Chemistry.

The first step of the study involved screening of different capsule **XII** loadings (8–26 mol%) to find the optimal amount of the catalyst. The peak selectivity (80% *ee*) was observed when utilizing 12 mol% of **XII**, while lower and higher capsule loadings led to a decreased enantioselectivity (Fig. 8a). This effect can be explained as follows: (1) at low capsule loading (8 – 10 mol%), the iminium reaction outside of the capsule decreases the *ee*; (2) at higher capsule loadings (14 – 26 mol%), the background reaction caused by the activation of the substrate by capsule itself leads to the formation of the racemic product. Since the previous study already established HANTZSCH ester (**121**) as the most optimal hydride source and L-proline (**123a**) as the most suitable chiral catalyst, in this work, only different aminocatalyst **100a** loadings were examined, indicating the optimum at 20 mol% of **123a**.

Investigation of the HCl influence was our next step. Its effect was studied with previously reported capsule **XII** loading of 26 mol% and the optimized 12 mol%. As shown in Fig. 8b, HCl does not provide better enantioselectivity of the reaction, which even drops with higher

acid loadings (>5 mol%). Thus, we could conclude that HCl is not required for the iminium-catalyzed 1,4-reduction inside capsule **XII**.

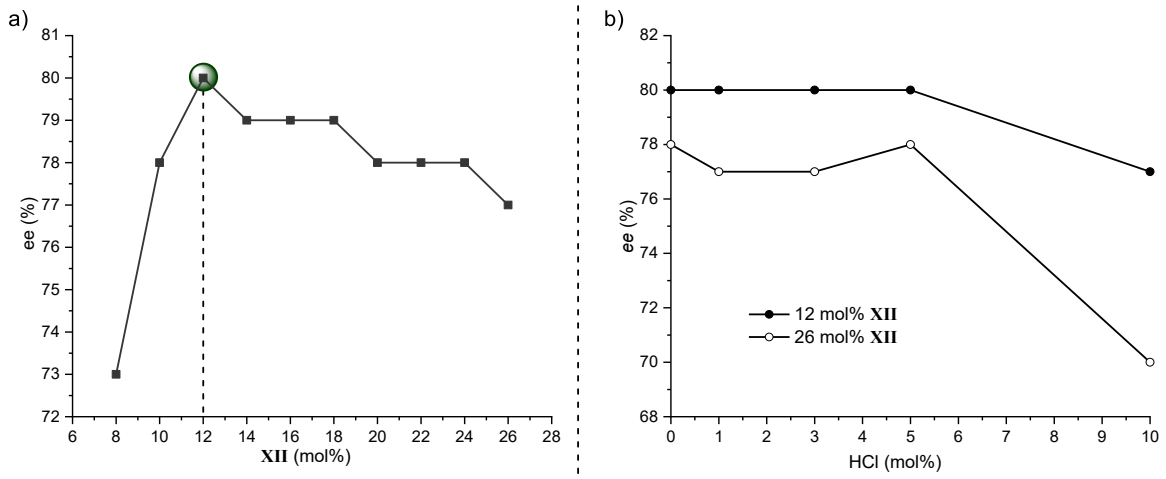


**Figure 8.** a) Optimization of the capsule **XII** loading (8–26 mol%) under the standard reaction conditions using aldehyde **120a**: 1 eq. **120a**, *c*(**120a**) = 0.15 M in chloroform, 1.5 eq. **121**, 0.2 eq. **123a**. The optimal amount of **XII** (12 mol%) is highlighted. b) Influence of the HCl content on the standard reaction utilizing either 12 or 26 mol% of capsule **XII**. Enantiomeric excesses were determined with chiral GC measurements. The values reported refer to measurements after 72 h of reaction time. Reproduced from Ref. [158] with permission from the Royal Society of Chemistry.

After establishing the optimal loadings of the capsule (12 mol%), L-proline (20 mol%), and HCl (none), we investigated other additives, which could influence the enantioselectivity of the reaction. Particularly interesting were alcohols as their interaction with resorcinarene-based capsules are well known and described in the literature. After performing the initial screening, which indicated 9 eq. of alcohol as an optimal amount of additive, several alcohols were tested (Table 1). As shown in Table 1, all the alcohol additives led to an increase of *ee*, with *i*-PrOH performing slightly better than other alcohols regarding yield and enantioselectivity.

**Table 1**. Optimization of the alcohol additive under the standard reaction conditions: 1 eq. **120a**, *c*(**120a**) = 0.15 M in chloroform, 12 mol% of **XII**, 1.5 eq. **121**, 0.2 eq. **123a**. Conversions, yields, and enantiomeric excesses were determined with achiral and chiral GC measurements. The values reported refer to measurements after 72 h of reaction time. Reactions were performed in triplicate, and standard deviations were determined. Reproduced from Ref. [158] with permission from the Royal Society of Chemistry.

| Entry | Alcohol | Conversion (%) | Yield (%) | *ee* (%) |
|---|---|---|---|---|
| 1 | – | 93 ± 1 | 89 ± 1 | 77 ± 1 (*S*) |
| 2 | MeOH | 93 ± 1 | 89 ± 1 | 80 ± 2 (*S*) |
| 3 | EtOH | 94 ± 2 | 89 ± 3 | 80 ± 2 (*S*) |
| 4 | *n*-PrOH | 94 ± 2 | 90 ± 1 | 80 ± 2 (*S*) |
| 5 | *i*-PrOH | 94 ± 2 | 91 ± 1 | 83 ± 2 (*S*) |
| 6 | *n*-BuOH | 94 ± 2 | 89 ± 2 | 80 ± 2 (*S*) |

The observed effect of *i*-PrOH additive in reactions with aldehyde **120a** was further explored on other substrates **120b–e** (Table 2). All the tested substrates were converted to the desired products with higher enantioselectivity in the presence of the *i*-PrOH additive. For two substrates (**120b** and **120c**), an unprecedented, at least for proline, enantioselectivity >90% *ee* was achieved. It is only possible in combination of proline with capsule **XII** and *i*-PrOH.

**Table 2.** Results of reactions with different substrates under optimized conditions: 1 eq. **120**, *c*(**120**) = 0.15 M in chloroform, 12 mol% **XII**, 1.5 eq. **121**, 0.2 eq. **123a**, 9 eq. *i*-PrOH, (bright-green). Comparison to reactions in the presence of 12 mol% of capsule **XII**, but the absence of *i*-PrOH (dark-green); reactions in the absence of capsule **XII**, and the presence of 9 eq. of *i*-PrOH (dark-grey); reactions in the absence of both capsule **XII** and *i*-PrOH (light-grey). Conversions, yields, and enantiomeric excesses were determined by GC measurements. The values reported refer to measurements after 72 h of reaction time. Reactions were performed in triplicate, and standard deviations were determined. Reproduced from Ref. [158] with permission from the Royal Society of Chemistry.

| Entry | Aldehyde | Capsule XII | *i*-PrOH | Yield (%) | *ee* (%) |
|---|---|---|---|---|---|
| 1 | 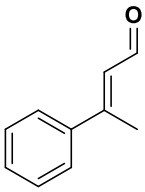 **120a** | yes | yes | 91 ± 1 | 83 ± 2 (*S*) |
| | | yes | no | 89 ± 1 | 77 ± 1 (*S*) |
| | | no | yes | 45 ± 7 | 1 ± 2 (*S*) |
| | | no | no | 50 ± 13 | 3 ± 2 (*S*) |
| 2 | 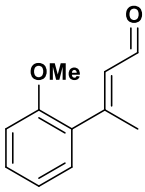 **120b** | yes | yes | 89 ± 7 | 92 ± 0 (*S*) |
| | | yes | no | 76 ± 4 | 83 ± 1 (*S*) |
| | | no | yes | 5 ± 0 | 5 ± 2 (*S*) |
| | | no | no | 5 ± 0 | 6 ± 1 (*S*) |
| 3 | 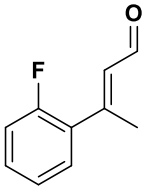 **120c** | yes | yes | 97 ± 0 | 92 ± 0 (*S*) |
| | | yes | no | 95 ± 2 | 88 ± 0 (*S*) |
| | | no | yes | 16 ± 2 | 6 ± 0 (*S*) |
| | | no | no | 15 ± 0 | 3 ± 1 (*S*) |
| 4 | 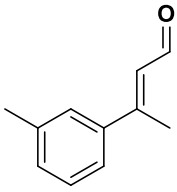 **120d** | yes | yes | 67 ± 2 | 57 ± 0 (*S*) |
| | | yes | no | 65 ± 1 | 55 ± 1 (*S*) |
| | | no | yes | 16 ± 1 | 3 ± 5 (*S*) |
| | | no | no | 18 ± 2 | 3 ± 1 (*S*) |
| 5 | 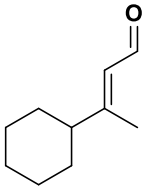 **120e** | yes | yes | 72 ± 1 | 58 ± 1 (*S*) |
| | | yes | no | 66 ± 9 | 55 ± 1 (*S*) |
| | | no | yes | 60 ± 0 | 30 ± 1 (*S*) |
| | | no | no | 61 ± 2 | 35 ± 0 (*S*) |

Next, we explored the influence of the alcohol additive on proline-proline interactions inside the capsule by performing a non-linear effect (NLE) study. For this case, we chose substrate **120e**, which shows the highest *ee* values in the reaction in the absence of capsule **XII** as can be seen in Table 2. In all the cases, the obtained linear graphs (Fig. 9) indicate no influence of *i*-PrOH on proline-proline interactions; therefore, it cannot be considered as a source of the increased enantioselectivity.

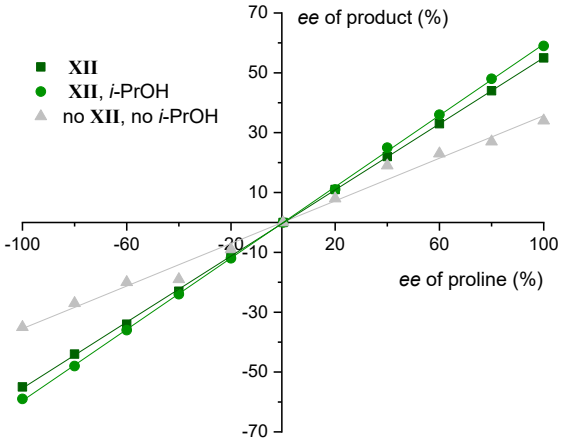


**Figure 9.** Non-linear effects study of iminium catalyzed 1,4-reduction under optimized conditions using aldehyde **120e**: 1 eq. **120e**, *c*(**120e**) = 0.15 M in chloroform, 1.5 eq. **121**, 0.2 eq. of proline (mixtures of L- and D-proline of different ratios). Different reaction conditions (absence/presence of **XII** and/or *i*-PrOH) were explored. Enantiomeric excesses were determined by chiral GC measurements. Reproduced from Ref. [158] with permission from the Royal Society of Chemistry.

Afterward, to elucidate the *i*-PrOH role, we investigated the initial rates and initial *ee*s of the reaction. Four reactions (presence/absence of capsule **XII**; presence/absence of alcohol additive) with substrate **120b**, which shows the fastest kinetics, were studied in parallel. Although reactions without capsule reach only 40-50% conversion, they are faster than reactions in the presence of capsule (Fig. 10a). Iminium catalysis inside capsule **XII** demonstrates slower kinetics since both the HANTZSCH ester and the iminium species need to be co-encapsulated for conversion. At the same time, we observed an increased reaction rate for the capsule-mediated reaction in the presence of alcohol, while in the absence of capsule **XII**, the alcohol additive suppressed the reaction rate. A different trend was observed when following the initial enantioselectivity of the reaction (Fig. 10b). While the influence of alcohol additive was negligible for the reactions without capsule, the capsule-mediated reaction benefited from the additive (92% *ee* vs. 84% *ee*).

We interpreted the results the following way: the increased enantioselectivity of capsule-mediated reaction with alcohol additive is likely a consequence of two effects: 1) the reduced background reaction of the free iminium species (grey lines in Fig. 10a) that leads to low *ee* values; 2) the increased reaction rate in the capsule (green lines in Fig. 10a). The

acceleration of the reaction in the presence of both alcohol and capsule (light-green line in Fig. 10a) likely stems from faster exchange kinetics of the reagents in/out of the capsule, as it is known that polar additives destabilize the hydrogen-bonding network. These results indicate that the proline-catalyzed reaction inside capsule **XII** is highly enantioselective and is only reduced to some extent by the racemic background reaction outside of the capsule.§

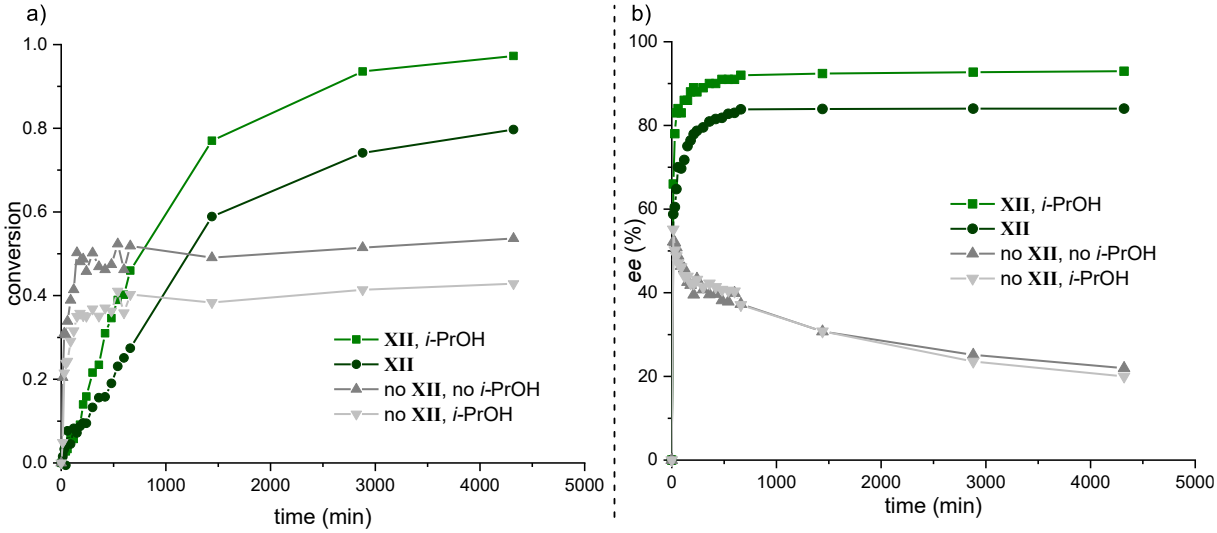


**Figure 10.** Influence of *i*-PrOH on the initial rates and enantiomeric excesses of the reaction under optimized conditions using aldehyde **120b**: 1 eq. **120b**, *c*(**120b**) = 0.15 M in chloroform, 1.5 eq. **121**, 0.2 eq. **123a**. Conversions and *ee*s were determined with achiral and chiral GC measurements, respectively. (a) Conversions of reactions in the presence/absence of capsule **XII** (12 mol% if present); the presence/absence of alcohol additive (9 eq. if present). (b) Enantiomeric excesses of reactions in the presence/absence of capsule **XII** (12 mol% if present); the presence/absence of alcohol additive (9 eq. if present). Reproduced from Ref. [158] with permission from the Royal Society of Chemistry.

In summary, we presented the optimized reaction conditions for the iminium-catalyzed 1,4-reduction of α,β-unsaturated aldehydes inside the supramolecular capsule **XII**. The capsule loading was successfully reduced from 26 to 12 mol%. We also established that HCl is not required as a co-catalyst. Furthermore, we found that alcohol additives have a beneficial role regarding the enantioselectivity of the reaction. For two substrates, products with unprecedented enantioselectivity of 92% *ee* were formed. The increased interactions inside the confined space of capsule **XII** lead to a dramatic increase in enantioselectivity, while proline itself performs poorly in solution. According to our initial hypothesis, the observed enantioselectivity stems from a selective shielding of one side of the iminium species by the inner wall of capsule **XII**. This study demonstrates that this enantioselectivity can be further increased by alcohol additives that not only decrease the background reaction but also accelerate the capsule-catalyzed process. We are convinced that these results not only strengthen our understanding of confinement catalysis but will also be transferable to other reaction classes.

## 3.2. Submitted Publication

The following section contains the submitted publication together with the supporting information, which is currently under review. Figures, numbering of compounds, and literature references correspond to those presented in the submitted manuscript.

**Chiral hexameric resorcin[4]arene capsule derivatives enable enantioselective tail-to-head terpene cyclizations**

**Abstract:** Molecular capsules enable the conversion of substrates inside a closed cavity, mimicking to some extent enzymatic catalysis. Chirality transfer from the molecular capsule onto the encapsulated substrate has been only studied in a few cases. Here we demonstrate that chirality transfer is possible inside a rather large molecular container of approximately 1400 Å$^3$. Specifically, we present (1) the first examples of optically active hexameric resorcin[4]arene capsules, (2) their ability to enantioselectively catalyze tail-to-head terpene cyclizations, and (3) the surprisingly high sensitivity of enantioselectivity on the structural modifications.

Self-assembled molecular capsules enable the temporary isolation of guest molecules from the bulk solvent inside a closed cavity space.[1] Such host-guest interactions have facilitated the acceleration of reactions, and if product inhibition is overcome, also catalytic turnover.[2] In a few cases, chirality transfer from the capsule onto the substrate even enabled enantioselective conversions.[2e, 3] Of particular interest for catalysis are capsules with a large inner cavity as they enable a wider reaction and substrate scope. However, as the cavity size increases, the substrate-host interactions naturally decrease as contacts from multiple sides become less likely. This raises the question of whether a chirality transfer from the capsule onto the substrate is still possible with large capsular host systems. Here we answer this question and report that enantioselective tail-to-head terpene cyclizations are indeed possible inside the large 1400 Å$^3$ volume of a molecular capsule.

The resorcin[4]arene capsule, first reported by the Atwood group,[4] is one of the best-studied examples in the field as it is readily available, and offers an unusually large cavity volume of approximately 1400 Å$^3$.[4-5] A crystal structure revealed the ability of resorcin[4]arene **1** (Fig. 1a) to self-assemble *via* sixty hydrogen bonds to a hexameric molecular capsule that also incorporates eight water molecules on its surface (Fig. 1b). Each of the six resorcin[4]arene units formally lies at a face of a cube, while the water molecules occupy the vertices. However, the symmetry is broken as the building blocks are slightly tilted (see for instance the highlighted blue resorcin[4]arene in Fig. 1b), producing a D2-symmetry and making the assembly chiral.

As building block **1** is achiral, a racemic capsule mixture is formed. Moreover, the two capsule enantiomers should rapidly interconvert (racemize) as only a slight rotation of each building block is required.[6] Although enantioenriched resorcin[4]arene derivatives have been described,[7] to our knowledge, there are no reports of such derivatives forming enantioenriched self-assembled capsules. This is most likely due to the steric bulk installed at the resorcin[4]arene rim in most literature examples that prevents self-assembly. Our group reported that the encapsulation of chiral, optically active amines induces some handedness onto the capsular system.[8] However, the uptake and protonation of the chiral amine prevent reactions from taking place inside the cavity. Hence, there are no reports about enantioselective catalysis inside the resorcin[4]arene container that involve a chirality transfer from the capsule onto the product. The few examples reported for enantioselective catalysis inside **I**, utilize a chiral co-catalyst (L-proline) that covalently transfers its chirality onto the product *via* iminium intermediates.[9] While there are no reports of enantioenriched capsule **I** derivatives, other enantioenriched molecular capsules that are catalytically active are known.[2e] The tetrahedral gallium-phenolate capsule, developed by the Raymond group,[10] was utilized for enantioselective aza-Cope[11] and Prins[12] cyclizations. A reasonable transfer of chirality (with *ee*s in the 60s) was achieved inside the relatively small capsular host that features a volume of up to approximately 400 Å$^3$.[3]

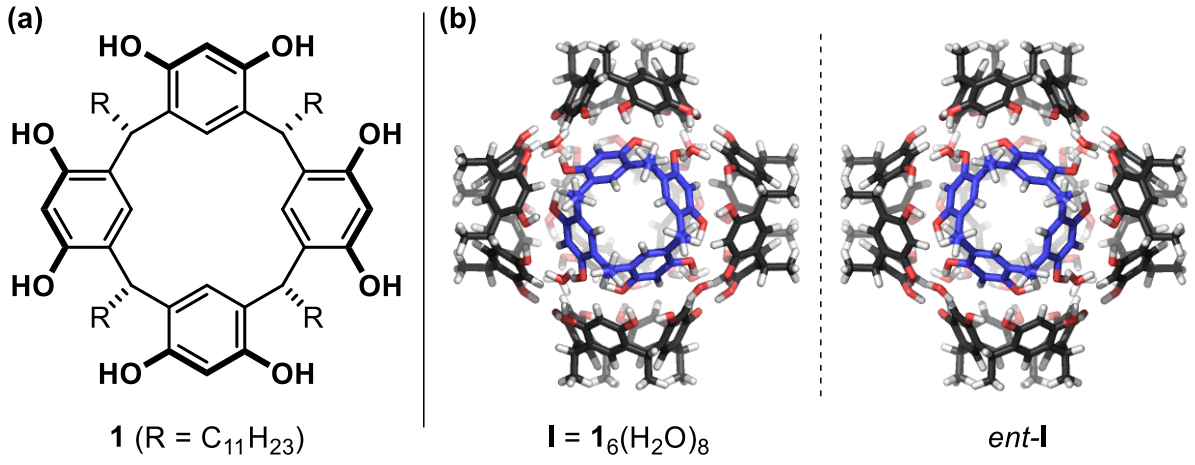


**Figure 1.** Self-assembly of resorcinarene **1** (a) into the chiral but racemic hexameric capsule **I** (b).

At the outset of this project, we envisioned two alternative strategies to turn the achiral resorcin[4]arene moiety **1** into a chiral derivative still able to assemble to a hexameric capsule. First, the installation of chiral residues at the R-"feet" of **1** was explored (Fig. 2a). Interestingly, chiral feet derivatives of **1** have been reported by the groups of Mattay and Rebek,[7i, 13]

however, their self-assembling properties to hexameric capsules remained unexplored. Derivatives **2a-b** were prepared according to the literature procedure from the respective chiral aldehydes ((*S*)-citronellal or vitamin D2) and resorcinol.[13] In addition, we prepared a third derivative, **2c**, *via* a similar strategy in three steps starting from (*S*)-3-phenyl butyric acid (see SI chapter 2). The second strategy involved breaking the symmetry of **1** *via* mono-phenol alkylation to produce derivatives **3a-c** (Fig. 2b). A monobenzylation of **1** has been reported by Konishi,[14] however, neither chiral resolution nor its self-assembling properties have been studied. While the monoalkylation strategy produced the desired chiral derivatives **3a-c** directly in one step from **1**, the separation of the enantiomers proved difficult. After extensive screening, separation *via* preparative HPLC using the Chiralpak IB N-5 column was successful. One enantiomer of each derivative (**3a-c**) was obtained in pure form and fully characterized (see SI chapter 2).

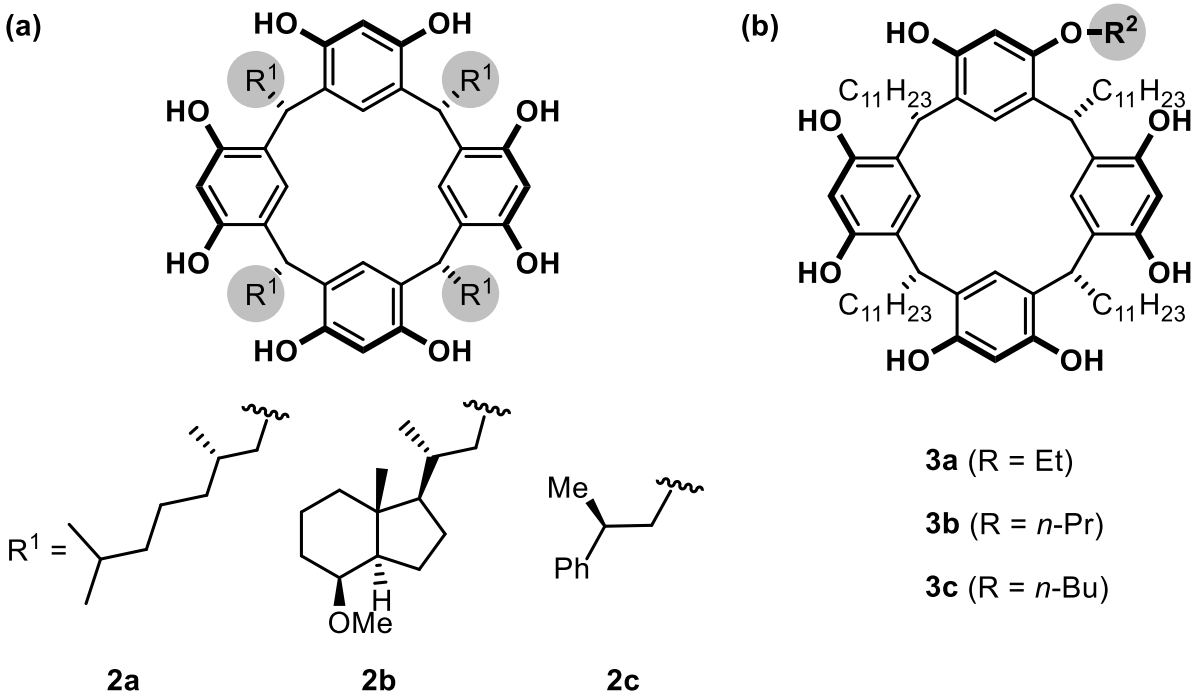


**Figure 2.** Chiral derivatives of resorcin[4]arene investigated. They either carry the chiral information at the feet (a), or at the rim of the macrocycle (b).

With six chiral, optically active resorcinarene derivatives in hand, their ability to self-assemble to hexametric capsules was explored. Diffusion ordered spectroscopy (DOSY) NMR has been established as a reliable tool to interrogate assembly sizes in solution as demonstrated conclusively by the Cohen group.[15] Accordingly, all derivatives (**2a**-**c**, **3a**-**c**) were studied under conditions typically utilized for catalysis inside capsule **I** (20 mM, $CDCl_3$, 30 °C). The

translational diffusion coefficients (D) obtained in these experiments are summarized in Table 1. The values obtained (0.23-0.27 $x10^{-9}$ $m^2s^{-1}$, entries 2-7) are in good agreement with the hexameric parent capsule **I** (0.23 $x10^{-9}$ $m^2s^{-1}$, entry 1). Smaller assemblies would have substantially larger diffusion coefficients.[16] Accordingly, we concluded that all derivatives likely self-assemble to hexameric capsules in chloroform solution. This result is not surprising for derivatives **2a-c**, as they feature the same hydrogen bonding motifs as the parent compound **1**. However, the results for **3a-c** are not obvious, as one hydrogen bond donor on each resorcin[4]arene is blocked and the formed alkyl ether moiety presents a steric disturbance to the elaborate hydrogen bond network of capsule **I**. However, we recently demonstrated in another context that the self-assembly process of **I** tolerates some covalent modifications close to the hydrogen bonding motifs.[17] Further evidence for the formation of hexameric capsules was obtained by the subsequent cyclization studies.

**Table 1.** Comparison of the diffusion coefficients of the assemblies formed from macrocycles **1** – **3c** (20 mM in $CDCl_3$).

| Entry | Compound | D [$\times10^{-9}$ $m^2/s$] |
|---|---|---|
| 1 | **1** | 0.23 |
| 2 | **2a** | 0.26 |
| 3 | **2b** | 0.23 |
| 4 | **2c** | 0.27 |
| 5 | **3a** | 0.25 |
| 6 | **3b** | 0.25 |
| 7 | **3c** | 0.26 |

Our group has demonstrated that tail-to-head monoterpene cyclizations performed inside capsule **I** display distinct product selectivities that differ from regular bulk solution reactivity.[18] For the study of enantioselective catalysis, the cyclization of nerol is best suited as it produces a chiral main product, α-terpineol (Figure 3). Besides the achiral products eucalyptol, α-terpinene, terpinolene, and γ-terpinene also chiral limonene is formed.

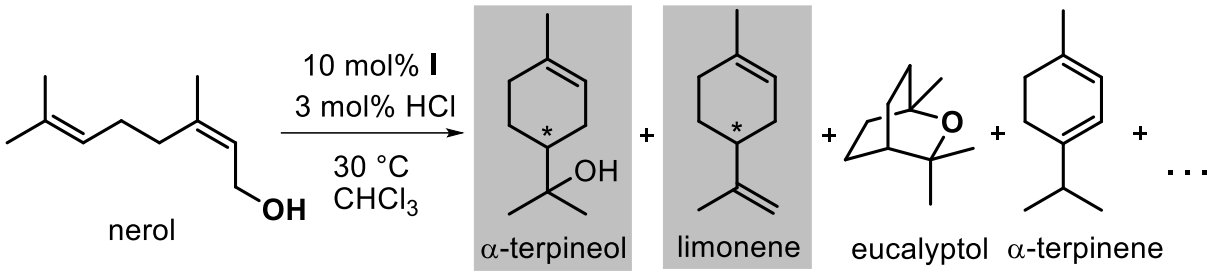


**Figure 3.** The capsule **I**-catalyzed cyclization of nerol produces two chiral products, α-terpineol and limonene, and was chosen to explore the potential for enantioselective catalysis inside the capsules formed from derivatives **2a-c** and **3a-c**.

Hence, nerol cyclization studies were performed with the chiral, optically active resorcin[4]arene derivatives **2a-c** and **3a-c** under the standard reaction conditions established for capsule **I**: 10 mol% capsule, 3 mol% HCl, 20 mM in $CDCl_3$, 30 °C. The reactions were monitored by achiral GC with a focus on the two chiral products of the cyclization, α-terpineol and limonene. The enantiomeric ratio of the products was determined by chiral GC measurement, utilizing commercially available samples of racemic and enantioenriched α-terpineol and limonene as reference compounds. The results of these studies are summarized in Table 2 and provide strong evidence for the self-assembly of hexameric capsules for all derivatives **2a-c** and **3a-c**. In all cases, significant amounts of α-terpineol are produced, in analogy to the parent system **I**, indicating that the conversion takes place inside a capsular host closely related to the parent hexameric host. The results concerning the optical activity of the products formed clearly demonstrate that the chiral feet derivatives **2a-c** are not suitable for transferring chirality onto the cyclization products. In all three cases (entries 1-3), no significant enantioselectivities were observed. Interestingly, the rim-functionalized derivatives **3a-c** displayed a different behavior. Ethyl derivative **3a** produced α-terpineol with some enantioselectivity (17 ± 1% *ee*, entry 4), favoring the (*S*)-enantiomer. The other chiral product, limonene, however, was produced in racemic form. Most interestingly, the monopropyl derivative **3b** performed best in catalysis, producing (*S*)-(–)-limonene and (*S*)-(–)-α-terpineol in 62% and 48% *ee*, respectively after 24h of reaction time. The enantioselectivity was also monitored during the reaction, and no significant changes in *ee* were observed (Fig. S12). This level of enantioselectivity is noteworthy, as it is comparable to that achieved for other reactions by the significantly smaller (approximately 400 $Å^3$) state-of-the-art capsule system.[11-12] Moreover, the Jacobsen group demonstrated how challenging the enantioselective catalysis of tail-to-head terpene cyclizations is.[19] State-of-the-art chiral urea catalysts enabled only modest levels of enantioselectivity of up to 34% *ee* for limonene. Non-natural modifications, like the

installation of an aryl group, on the nerol substrate were required to improve substrate catalyst recognition, highlighting the potential of enantioselective capsule catalysis for non-modified terpene substrates presented herein. To our knowledge, only chiral leaving groups were successful in performing such cyclizations on unmodified terpenes previous to this report.[20] Intriguingly, the slightly larger butyl derivative **3c** produced only racemic material (entry 6). To support this surprising finding by excluding potential signal overlap in the chiral GC, the other enantiomer of the best performing catalyst building block **3b** was isolated. When submitted to the standard reaction conditions, it indeed delivered the same high levels of enantioselectivity for the two main products, limonene and α-terpineol, however, as expected, favoring the other product enantiomer (entry 7).

**Table 2.** Results of the nerol cyclization reaction inside capsules based on resorcinarenes **2a** – **3c**. Reaction conditions: 10 mol% capsule, 3 mol% HCl, 20 mM in $CDCl_3$, 30 °C, 24h. Yields and enantiomeric excesses were determined by GC measurements. Reactions were performed in triplicate and standard deviations were determined.

| Entry | Capsule | α-terpineol | | limonene | |
|---|---|---|---|---|---|
| | | **Yield, %** | ***ee*, %** | **Yield, %** | ***ee*, %** |
| 1 | **2a** | 13 ± 3 | < 5% | 5 ± 1 | < 5% |
| 2 | **2b** | 34 ± 1 | 6 ± 0 (*S*) | 10 ± 1 | 6 ± 2 (*S*) |
| 3 | **2c** | 34 ± 3[a] | < 5%[a] | 9 ± 1[a] | < 5%[a] |
| 4 | (–)-**3a** | 16 ± 4[b] | 17 ± 1 (*S*) | 8 ± 2[b] | < 5% |
| 5 | (–)-**3b** | 47± 6 | 48 ± 1 (*S*) | 30± 3 | 62 ± 1 (*S*) |
| 6 | (–)-**3c** | 20 ± 1[b] | 5 ± 1 (*S*) | 10 ± 1[b] | < 5% |
| 7 | (+)-**3b** | 41 ± 1 | 46 ± 1 (*R*) | 26 ± 1 | 62 ± 1 (*R*) |

[a] The values are given after 10h of the reaction time. [b] The values are given after 8h of the reaction time.

The high sensitivity of product enantioselectivity on the structural modifications of the capsule building blocks was surprising to us. While the ethyl- and butyl-derivatives **3a** and **3c** failed to significantly transfer optical activity onto the products, the propyl-derivative **3b** did so rather

efficiently, especially when compared to the state-of-the-art results obtained in much smaller capsules. The relatively efficient transfer of chirality in such a large capsule was certainly not obvious a priori and might be related to the activation of the substrate close to the capsule surface.[21]

In conclusion, we presented the synthesis of four novel enantioenriched resorcin[4]arene building blocks, and demonstrated that these derivatives are able to self-assemble to hexameric capsules. To our knowledge, these are the first reports on enantioenriched hexameric resorcin[4]arene capsules. All capsules formed showed catalytic activity in the tail-to-head terpene cyclization of nerol. The derivatives that feature the chiral information outside of the capsule's surface failed to induce enantioselective terpene cyclizations. Apparently, the distance between the chiral information and the encapsulated substrate that is additionally shielded by the capsule walls prevents a transfer of chirality. However, two of the monoalkylated derivatives that carry the chiral information at the surface of the capsule, induced significant enantiomeric excesses of up to 62% *ee*. The enantioselectivities obtained are comparable to state-of-the-art results in smaller capsules for other reactions. As the resorcinarene hexamer capsule is quite large, which prevents efficient contact between multiple capsule walls and the substrate, such enantioselectivities were not expected a priori. The results obtained certainly augur well for performing enantioselective catalysis inside large molecular capsules. Future research will deal with optimizing chirality transfer and expanding the reaction scope.

**Acknowledgements**

This work was supported by funding from the European Research Council Horizon 2020 Programme [ERC Starting Grant 714620-TERPENECAT].

[1] a) M. M. Conn, J. Rebek, *Chem. Rev.* **1997**, *97*, 1647-1668; b) F. Hof, S. L. Craig, C. Nuckolls, J. J. Rebek, *Angew. Chem. Int. Ed.* **2002**, *41*, 1488-1508.

[2] a) M. D. Ward, C. A. Hunter, N. H. Williams, *Acc. Chem. Res.* **2018**, *51*, 2073-2082; b) Q. Zhang, L. Catti, K. Tiefenbacher, *Acc. Chem. Res.* **2018**, *51*, 2107-2114; c) V. Mouarrawis, R. Plessius, J. I. van der Vlugt, J. N. H. Reek, *Front. Chem.* **2018**, *6*; d) C. Gaeta, C. Talotta, M. De Rosa, P. La Manna, A. Soriente, P. Neri, *Chem. Eur. J.* **2019**, *25*, 4899-4913; e) M. Morimoto, S. M. Bierschenk, K. T. Xia, R. G. Bergman, K. N. Raymond, F. D. Toste, *Nat. Catal.* **2020**, *3*, 969-984; f) R. J. Hooley, *Synlett* **2020**, *31*,

1448-1463; g[1] a) M. M. Conn, J. Rebek, Chem. Rev. 1997, 97, 1647-1668; b) F. Hof, S. L. Craig, C. Nuckolls, J. J. Rebek, Angew. Chem. Int. Ed. 2002, 41, 1488-1508.

[3] C. J. Brown, F. D. Toste, R. G. Bergman, K. N. Raymond, *Chem. Rev.* **2015**, *115*, 3012-3035.

[4] L. R. MacGillivray, J. L. Atwood, *Nature* **1997**, *389*, 469-472.

[5] a) L. Avram, Y. Cohen, *J. Am. Chem. Soc.* **2002**, *124*, 15148-15149; b) L. Avram, Y. Cohen, J. Rebek, *Chemical communications (Cambridge, England)* **2011**, *47*, 5368-5375.

[6] D. Ajami, J. Rebek, *Nature Chemistry* **2009**, *1*, 87-90.

[7] a) Y.-i. Matsushita, T. Matsui, *Tetrahedron Lett.* **1993**, *34*, 7433-7436; b) U. Schneider, H.-J. Schneider, *Chem. Ber.* **1994**, *127*, 2455-2469; c) W. Iwanek, C. Wolff, J. Mattay, *Tetrahedron Lett.* **1995**, *36*, 8969-8972; d) W. Iwanek, J. Mattay, *Liebigs Annalen* **1995**, *1995*, 1463-1466; e) R. Arnecke, V. Böhmer, S. Friebe, S. Gebauer, G. J. Krauss, I. Thondorf, W. Vogt, *Tetrahedron Lett.* **1995**, *36*, 6221-6224; f) M. T. El Gihani, H. Heaney, A. M. Z. Slawin, *Tetrahedron Lett.* **1995**, *36*, 4905-4908; g) O. D. Fox, N. K. Dalley, R. G. Harrison, *Journal of inclusion phenomena and macrocyclic chemistry* **1999**, *33*, 403-414; h) C. Agena, C. Wolff, J. Mattay, *Eur. J. Org. Chem.* **2001**, *2001*, 2977-2981; i) M. Schiendorfer, J. Mattay, *Synthesis* **2005**, *2005*, 2701-2712; j) M. Klaes, B. Neumann, H.-G. Stammler, J. Mattay, *Eur. J. Org. Chem.* **2005**, *2005*, 864-868.

[8] C. H. Pollok, Q. Zhang, K. Tiefenbacher, C. Merten, *ChemPhysChem* **2017**, *18*, 1987-1991.

[9] a) T. M. Bräuer, Q. Zhang, K. Tiefenbacher, *Angew. Chem. Int. Ed.* **2016**, *55*, 7698-7701; b) T. M. Bräuer, Q. Zhang, K. Tiefenbacher, *Journal of the American Chemical Society* **2017**, *139*, 17500-17507; c) P. La Manna, M. De Rosa, C. Talotta, C. Gaeta, A. Soriente, G. Floresta, A. Rescifina, P. Neri, *Organic Chemistry Frontiers* **2018**, *5*, 827-837.

[10] D. L. Caulder, K. N. Raymond, *J. Chem. Soc., Dalton Trans.* **1999**, 1185-1200.

[11] C. J. Brown, R. G. Bergman, K. N. Raymond, *Journal of the American Chemical Society* **2009**, *131*, 17530-17531.

[12] C. Zhao, Q.-F. Sun, W. M. Hart-Cooper, A. G. DiPasquale, F. D. Toste, R. G. Bergman, K. N. Raymond, *Journal of the American Chemical Society* **2013**, *135*, 18802-18805.

[13] T. Amaya, J. Rebek, *Journal of the American Chemical Society* **2004**, *126*, 6216-6217.

[14] K. Hisatoshi, T. Takashi, O. Hiromichi, K. Kazuhiro, M. Osamu, *Chem. Lett.* **1996**, *25*, 685-686.

[15] L. Avram, Y. Cohen, *Chem. Soc. Rev.* **2015**, *44*, 586-602.

[16] L. Avram, Y. Cohen, *Org. Lett.* **2008**, *10*, 1505-1508.

[17] S. J. Nemat, K. Tiefenbacher, *Org. Lett.* **2021**, *23*, 6861-6865.

[18] a) Q. Zhang, K. Tiefenbacher, *Nature chemistry* **2015**, *7*, 197-202; b) Q. Zhang, L. Catti, J. Pleiss, K. Tiefenbacher, *Journal of the American Chemical Society* **2017**, *139*, 11482–11492.

[19] D. A. Kutateladze, D. A. Strassfeld, E. N. Jacobsen, *Journal of the American Chemical Society* **2020**, *142*, 6951-6956.

[20] a) S. Sakane, J. Fujiwara, K. Maruoka, H. Yamamoto, *Journal of the American Chemical Society* **1983**, *105*, 6154-6155; b) H. Nakamura, K. Ishihara, H. Yamamoto, *The Journal of Organic Chemistry* **2002**, *67*, 5124-5137.

[21] S. Merget, L. Catti, G. Piccini, K. Tiefenbacher, *Journal of the American Chemical Society* **2020**, *142*, 4400-4410.

Supporting Information

# Chiral hexameric resorcin[4]arene capsule derivatives enable enantioselective tail-to-head terpene cyclizations

*Daria Sokolova and Konrad Tiefenbacher**

# 1. General Information

**Experimental:** All reactions were carried out using standard SCHLENK techniques with Argon (Ar 4.6) as the inert gas. Unless indicated otherwise, glass equipment was dried under a high vacuum ($10^{-2}$ mbar) at 500-600 °C using a heat gun. Reactions at low temperatures were performed using cooling baths (−78 °C using dry ice/*i*PrOH, 0 °C using ice/water). Transfer of liquids with a volume ranging from 1 to 10 µL or from 10 to 100 µL was performed with a microman M1 pipette (Gilson, systematic error: 1.40% − 1.60%) equipped with 10 µL or 100 µL pipette tips, respectively.

**Sources of Chemicals:** Reagents (ACROS, ALFA AESAR, FLUOROCHEM, SIGMA-ALDRICH, VWR) were used as received without prior purification.

**Solvents:** Anhydrous solvents were purchased from ACROS; solvents for extractions, chromatography, filtrations, and non-anhydrous reactions were purchased from VWR as HPLC grade solvents; NMR solvents were purchased from CAMBRIDGE ISOTOPE LABORATORIES. All solvents were used as received without prior purification.

**Thin-Layer Chromatography (TLC):** Analytical thin-layer chromatography (TLC) was performed on MERCK silica gel 60 F254 glass-baked plates, which were analyzed by fluorescence detection with UV-light (λ = 254 nm, [UV]) and after exposure to standard staining reagents and subsequent heat treatment. The following staining solution was used: acidic cerium ammonium molybdate solution [CAM] (40 g ammonium heptamolybdate, 1.6 g cerium sulfate in 900 mL $H_2O$ with 100 mL conc. $H_2SO_4$).

**NMR-Spectroscopy:** $^{1}$H NMR spectra were recorded at 500 MHz on a BRUKER UltraShield 500 spectrometer. $^{13}$C NMR spectra were recorded at 126 MHz on a BRUKER UltraShield 500 spectrometer. Chemical shifts of $^{1}$H NMR and $^{13}$C NMR spectra (measured at 298 K) are given in ppm by using residual solvent signals as references ($CDCl_3$: 7.26 ppm and 77.16 ppm, respectively; acetone-$d_6$: 2.05 ppm and 29.84 respectively). Coupling constants (*J*) are reported in Hertz (Hz). Standard abbreviations indicating multiplicity were used as follows: s (singlet), brs (broad singlet), d (doublet), dd (doublet of doublets), t (triplet), h (septet), m (multiplet).

DOSY-NMR experiments were performed on a BRUKER Avance III HD four-channel NMR spectrometer operating at 600.13 MHz proton frequency. The instrument was equipped with a cryogenic 5mm four-channel QCI probe (H/C/N/F) with a self-shielded z-gradient. The experiments were performed at 298 K, and the temperature was calibrated using a methanol standard showing accuracy within +/– 0.2 K. For the PFGSE (pulsed-field gradient spin echo)

diffusion experiment, the sample was placed in a 3 mm outer diameter tube, which was then inserted in a standard 5 mm round-bottom tube and securely kept in place as depicted below.

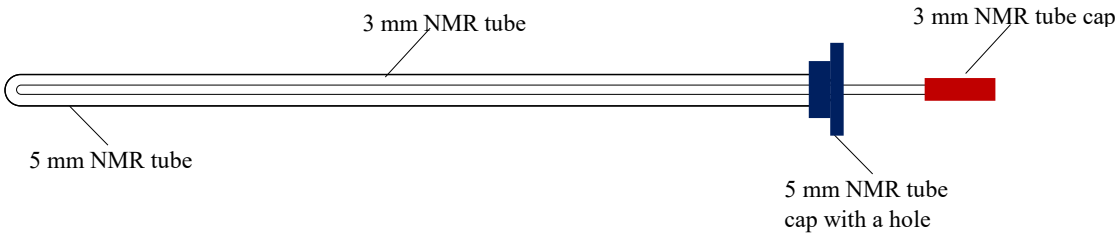


This setup ensured a negligible temperature gradient on the sample even inside a cryogenic probe. The PFGSE experiments were performed using a bipolar gradient pulse sequence.[1] The sigmoidal intensity decrease was fitted with a two-parameter fit ($I_0$ and diffusion coefficient D) with the DOSY routine implemented in topspin 3.6.1 [BRUKER Biospin GmbH]. A typically observed intensity decrease is depicted below.

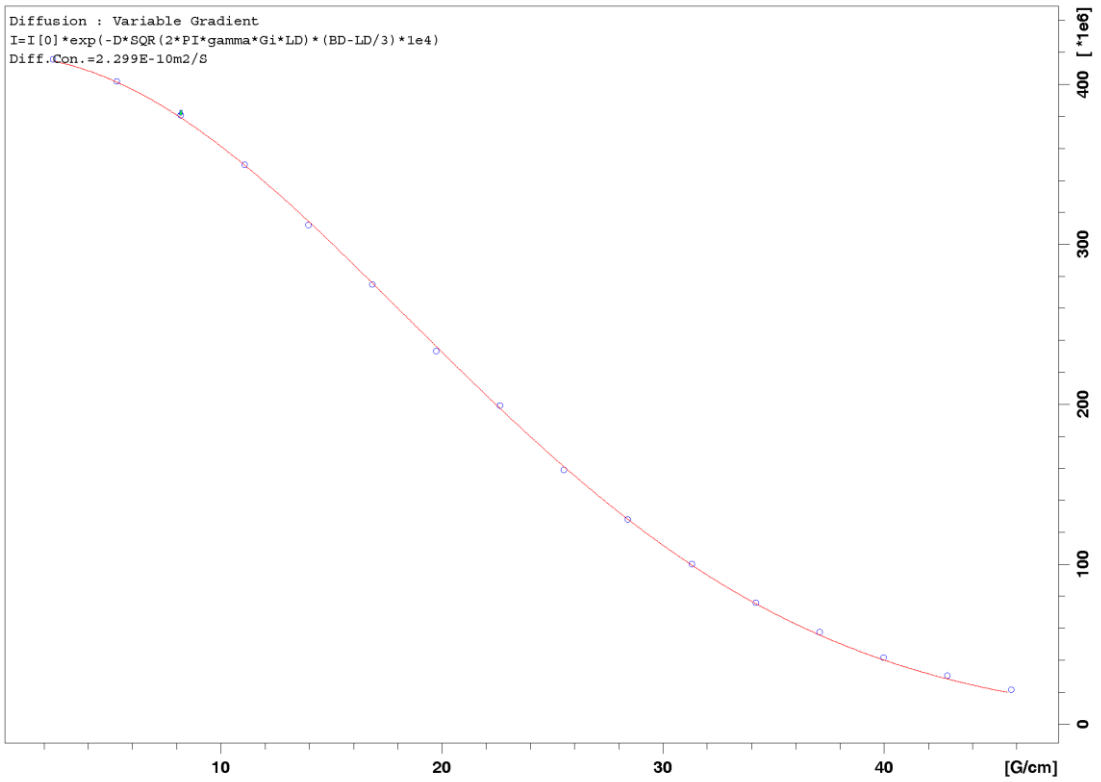


**High-Performance Liquid Chromatography:** HPLC was performed on an LC Prominence Liquid Chromatograph system by SHIMADZU equipped with a UV-Vis detector and an ELSD

unit. For analytical HPLC, a Chiralpak® IB N-5 (particle size: 5 µm; dimensions: 250 × 4.6 mm) DAICEL column was used. For preparative separation, a Chiralpak® IB N-5 (particle size: 5 µm; dimensions: 250 × 20 mm) DAICEL column was used.

**GC Analysis:** GC analyses were carried out on a SHIMADZU GC-2010 Plus instrument equipped with an FID detector and an Rtx-5 capillary column (length = 30 m). Hydrogen was used as the carrier gas, and the constant flow mode was used (flow rate = 40 mL/min) with a split ratio of 1:20. The following temperature program was used: 60 °C for 3 min, 15 °C $min^{-1}$ to 250 °C, and 250 °C for 5 min.

For the determination of enantiopurity *via* GC, a SHIMADZU GC-2010 Plus instrument equipped with an FID detector and an Rt-bDEXsm capillary column (length = 30 m) was used. Hydrogen was used as the carrier gas, and the constant-flow mode was used (flow rate = 50 mL/min) with a split ratio of 1:20. The following temperature program was used: 60 °C for 1 min, 5 °C $min^{-1}$ to 70 °C, 70 °C for 10 min, 5 °C $min^{-1}$ to 220 °C, 220 °C for 10 min.

**IR-Spectroscopy:** Infrared spectra were recorded on a BRUKER ALPHA spectrometer (attenuated total reflection, ATR). Only selected absorbances ($\tilde{\nu}_{max}$) are reported. Standard abbreviations indicating signal intensity were used as follows: s (strong), m (medium), w (weak), b (broad).

**ESI-HRMS:** High-resolution mass spectra were obtained using the electrospray ionization - time of flight (ESI-TOF) technique on a BRUKER maXis 4G mass spectrometer.

**Optical rotation:** Optical rotation was measured with an ANTON PAAR MCP 100 Modular Circular Polarimeter equipped with a Toolmaster™ sample cell (length: 1 dm; ø : 5 mm; temperature: 25 °C) operating on the sodium D-line (589 nm). The obtained values are reported as $[\boldsymbol{\alpha}]_{\boldsymbol{D}}^{\mathbf{25}}$ with the concentration c given in the unit 10 mg/mL.

## 2. Synthesis of Resorcinarene Derivatives

**Resorcinarene 1**[2]

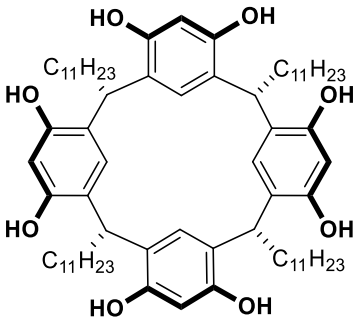


$C_{72}H_{112}O_8$
**M = 1105.68 g/mol**

A solution of resorcinol (71.6 g, 644 mmol, 1.0 eq.) in ethanol (270 mL) and conc. hydrochloric acid (90 mL) was prepared and cooled to 0 °C. A solution of dodecanal (151 mL, 125 g, 644 mmol, 1.0 eq.) in ethanol (180 mL) was added slowly over 40 minutes while the temperature was maintained at 0 °C. The resulting mixture was heated to 100 °C for 18 hours. After cooling the mixture to room temperature over four hours, the precipitate was collected by filtration and washed with cold methanol. The crude product was recrystallized from methanol (40 mL) and subsequently dried under vacuum to give a yellow powder. Subsequently, the material was suspended in MeOH/$H_2O$ (1:1, 10 mL/100 mg of macrocycle), sonicated for 20 minutes at room temperature, then filtered and washed with the MeOH/$H_2O$ (1:1) to remove any residual acid traces and give compound **1** (135 g, 122 mmol, 76%) as a beige powder. The spectroscopic data matches the reported literature values.[2]

**$^1$H-NMR:** (500 MHz, acetone-$d_6$) $\delta$ [ppm] = 8.44 (s, 8H), 7.54 (s, 4H), 6.24 (s, 4 H), 4.31 (t, $J$ = 7.9 Hz), 2.36 – 2.24 (m, 8H), 1.47 – 1.20 (m, 72H), 0.95 – 0.79 (m, 12H).

**(*S*)-(–)-citronellal-derived resorcinarene 2a**

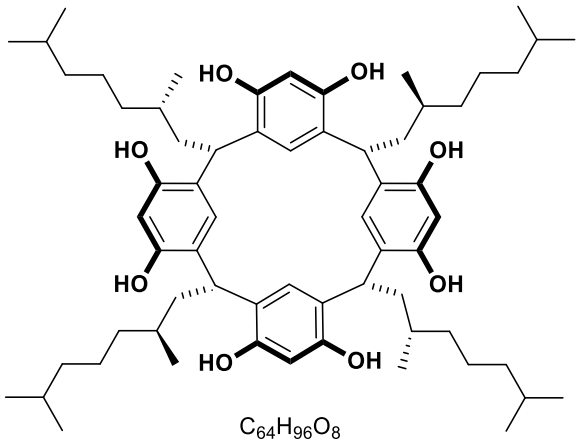


Resorcin[4]arene **2a** (1.12 g, 1.06 mmol, 45% over 2 steps) was obtained from commercial (*S*)-(–)-citronellal (SIGMA-ALDRICH) according to the literature known procedure; the spectroscopic data matches the reported literature values.[3]

**Optical rotation:** $[\alpha]_D^{25}$(C = 1.0, $CHCl_3$ ): –4.8°.

**$^1$H NMR** (500 MHz, acetone-$d_6$, 298 K): $\delta$[ppm] = 8.48 (s, 8H), 7.42 (s, 4H), 6.26 (s, 4H), 4.51 (dd, $J$ = 9.7, 6.3 Hz, 4H), 2.54 – 2.37 (m, 4H), 1.92 – 1.79 (m, 4H), 1.68 – 1.53 (m, 4H), 1.49 – 1.12 (m, 28H), 1.06 – 0.70 (m, 36H).

**Vitamin D2-derived resorcinarene 2b**

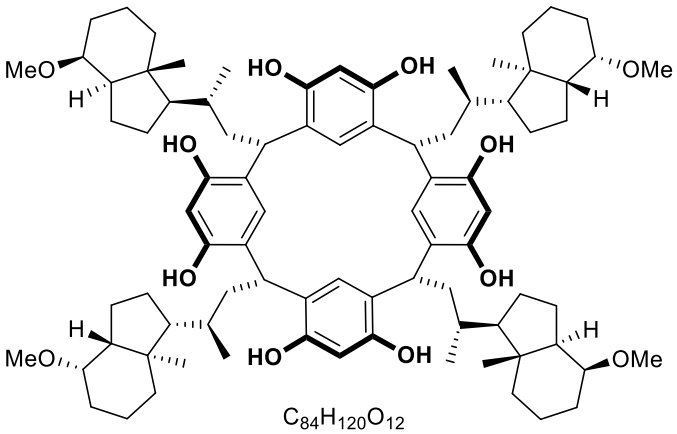


Resorcinarene **2b** (94.3 mg, 71.3 µmol, 45% over the last step) was obtained from commercial Vitamin D2 (SIGMA-ALDRICH) according to the literature known procedure; the spectroscopic data matches the reported literature values.[3]

**Optical rotation:** $[\alpha]_D^{25}$(C = 0.5, $CHCl_3$ ): +39.8°.

**$^1$H NMR** (500 MHz, acetone-$d_6$, 298 K): $\delta$[ppm] = 8.32 – 8.62 (m, 8H), 7.33 (s, 4H), 6.26 (s, 4H), 4.55 (dd, $J$ = 12.5, 3.0 Hz, 4H), 3.59 – 3.49 (m, 4H), 3.29 (s, 12H), 3.00 (t, $J$ = 12.8 Hz, 4H), 2.53 – 2.39 (m, 4H), 2.03 – 1.14 (m, 52H), 0.97 (d, $J$ = 6.2 Hz, 12H), 0.88 (s, 12H).

**(*S*)-3-phenylbutyric acid-derived resorcinarene 2c**

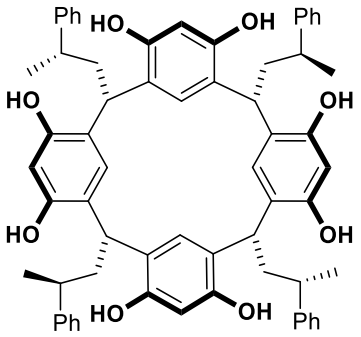


$C_{64}H_{64}O_8$
**M = 961.21 g/mol**

To a suspension of $LiAlH_4$ (1.28 g, 33.7 mmol, 1.5 eq.) in THF (80 mL) was added (*S*)-3-phenylbutyric acid (3.69 g, 22.5 mmol, 1.0 eq.) as a solution in THF (20 mL) at 0 °C. After 2 h of stirring at room temperature, the completion of the reaction was confirmed by TLC. The reaction was diluted with 50 mL of $Et_2O$ and cooled down to 0 °C. $H_2O$ (1.3 mL) was slowly added to the reaction mixture, followed by the addition of a 15% aqueous solution of NaOH (1.3 mL) and an additional portion of $H_2O$ (3.9 mL). After that, the reaction mixture was warmed up to room temperature and stirred for 15 min. $MgSO_4$ was added to the reaction mixture, stirred for 15 min, and filtered. The filtrate was concentrated *in vacuo* to give (*S*)-3-phenylbutanol (3.31 g, 22.0 mmol, 98%) as a colorless oil, which was used further without purification. The spectroscopic data matches the reported literature values.[4]

**$^1$H NMR** (500 MHz, $CDCl_3$, 298 K): $\delta$ [ppm] = 7.34 – 7.27 (m, 2H), 7.24 – 7.17 (m, 3H), 3.65 – 3.49 (m, 2H), 2.96 – 2.83 (m, 1H), 1.91 – 1.81 (m, 2H), 1.28 (d, $J$ = 7.0 Hz, 3H).

A solution of oxalyl chloride (3.07 g, 24.2 mmol, 2.07 ml, 1.1 eq.) in anhydrous DCM (81 mL) was cooled to –78 °C. A solution of DMSO (3.78 g, 48.4 mmol, 3.44 mL, 2.2 eq.) in anhydrous DCM (12 mL) was added, and the resulting mixture was stirred for 15 min at –78 °C. A solution of (*S*)-3-phenylbutanol (3.31 g, 22.0 mmol, 1.0 eq.) in anhydrous DCM (27 mL) was added dropwise over 25 min and stirred for additional 15 min at –78 °C. $Et_3N$ (11.4 g, 113 mmol, 15.6 mL, 5.1 eq.) was added, and the reaction mixture was stirred for 5 min at the same temperature. After warming up to room temperature, $H_2O$ (130 mL) was added; the organic layer was washed with brine (390 mL), 1% aqueous solution of $H_2SO_4$ (100 mL), $H_2O$ (130 mL), 4% aqueous solution of $NaHCO_3$ and dried over $Na_2SO_4$. After filtration, the solvent was removed *in vacuo* to give (*S*)-3-phenylbutanal (3.17 g, 21.4 mmol, 97%) as a colorless oil. The spectroscopic data matches the reported literature values.[4]

**$^1$H NMR** (500 MHz, $CDCl_3$, 298 K): $\delta$ [ppm] = 9.72 (t, $J$ = 2.0 Hz, 1H), 7.35 – 7.28 (m, 2H), 7.25 – 7.19 (m, 3H), 3.36 (h, $J$ = 7.1 Hz, 1H), 2.80 – 2.71 (m, 1H), 2.70 – 2.62 (m, 1H), 1.32 (d, $J$ = 6.9 Hz, 3H).

The mixture of (*S*)-3-phenylbutanal (3.17 g, 21.4 mmol, 1.0 eq.) and resorcinol (2.36 g, 21.4 mmol, 1.0 eq.) was dissolved in a mixture of ethanol (150 mL) and concentrated HCl (25 mL) at room temperature. The reaction mixture was heated to 100 °C for 13.5 h. After cooling down to room temperature, $H_2O$ (220 mL) was added. The formed precipitate was filtered and recrystallized from $CH_3CN$ to give a beige solid. Subsequently, the material was suspended in $CH_3CN/H_2O$ (1:1, 10 mL/100 mg of product), sonicated for 20 minutes at room temperature, then filtered and washed with the $CH_3CN/H_2O$ (1:1) to remove any residual acid traces to yield compound **2c** (1.73 g, 1.80 mmol, 34%) as a light beige solid.

**TLC**: $R_f$ = 0.43 ($CHCl_3$/MeOH = 12.5:1) [UV, CAM]

**Optical rotation:** $[\alpha]_D^{25}$ (C = 1.0, $CHCl_3$ ): +19.1°.

**$^1$H NMR** (500 MHz, acetone-$d_6$, 298 K): $\delta$ [ppm] = 8.47 (s, 4H), 8.43 (s, 4H), 7.67 (s, 4H), 7.30 – 7.22 (m, 8H), 7.18 (m, 12H), 6.25 (s, 4H), 4.46 (m, 4H), 2.69 (m, 4H), 2.62 (m, 4H), 2.28 (m, 4H), 1.25 (d, $J$ = 6.8 Hz, 12H).

**$^{13}$C NMR** (126 MHz, acetone-$d_6$, 298 K): $\delta$ [ppm] = 152.92, 152.71, 149.18, 129.30, 127.99, 126.68, 126.17, 125.79, 124.40, 103.77, 42.58, 38.65, 32.03, 21.75.

**IR** (ATR): $\tilde{\nu}$ [$cm^{-1}$] 3240 (w), 2958 (w), 1618 (s), 1492 (s), 1448 (m), 1376 (m), 1292 (m), 1165 (m), 1083 (m), 698 (s), 524 (s).

**HRMS** (ESI): calcd. for $C_{64}H_{64}NaO_8^+$ [$(M + Na)^+$]: 983.4493, found: 983.4480.

**Ethylresorcinarene 3a**

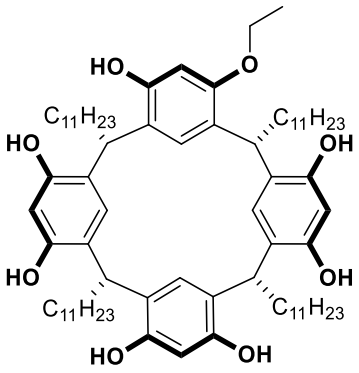


$C_{74}H_{116}O_8$
**M = 1133.73 g/mol**

Resorcinarene **1** (2.00 g, 1.81 mmol, 1.0 eq.) was dissolved in a 2:1 mixture of DMF (15 mL) and THF (7.5 mL). *t*BuOK (224 mg, 2.00 mmol, 1.1 eq.) was added in one portion at room temperature, and the mixture was stirred for 30 minutes. Ethyl iodide (312 mg, 163 µL, 2.00 mmol, 1.1 eq.) was added, and the reaction mixture was stirred at 110 °C for 15 h. After cooling down to room temperature, $H_2O$ (40 mL) was added, and the mixture was extracted with diethyl ether (3 × 75 mL). The organic layer was washed with $H_2O$ (5 × 75 mL), dried over $Na_2SO_4$, filtered, and concentrated. The crude product was purified *via* column chromatography (DCM/EtOAc = 4:1) to yield compound **3a** (874 mg, 771 µmol, 42%) as a beige solid (racemic mixture).

**TLC**: $R_f$ = 0.24 (DCM/EtOAc = 4:1) [UV, CAM]

**$^1$H NMR** (500 MHz, acetone-$d_6$, 298 K): $\delta$ [ppm] = 8.45 (brs, 6H), 7.57 (s, 1H), 7.56 (s, 1H), 7.52 (s, 1H), 7.50 (s, 1H), 7.25 (s, 1H), 6.37 (s, 1H), 6.27 (s, 1H), 6.23 (s, 1H), 6.15 (s, 1H), 4.38 – 4.27 (m, 4H), 4.10 – 4.00 (m, 2H), 2.36 – 2.20 (m, 8H), 1.43 (t, $J$ = 7.0 Hz, 3H), 1.40 – 1.23 (m, 72H), 0.94 – 0.85 (m, 12H).

**$^{13}$C NMR** (126 MHz, acetone-$d_6$, 298 K): $\delta$ [ppm] = 153.98, 153.93, 153.01, 153.00, 152.93, 152.68, 152.64, 152.47, 126.50, 126.08, 126.03, 125.69, 125.42, 125.20, 125.18, 125.13, 124.96, 124.77, 124.61, 124.60, 103.88, 103.75, 103.51, 101.09, 65.40, 34.91, 34.47, 34.41, 34.40, 34.36, 34.34, 34.31, 34.02, 30.64, 30.62, 30.62, 30.60, 30.55, 30.54, 30.52, 30.48, 30.17, 29.06, 29.03, 29.01, 23.38, 14.81, 14.41.

**IR** (ATR): $\tilde{\nu}$ [cm$^{-1}$] 3278 (m), 2921 (s), 2852 (s), 1619 (m), 1498 (m), 1446 (m), 1294 (m), 1162 (m), 1034 (w), 903 (w), 721 (w).

**HRMS** (ESI): calcd. for $C_{74}H_{115}O_8^-$ [$(M - H)^-$]: 1131.8597, found: 1131.8603.

One enantiomer of **3a** was resolved by preparative HPLC using the Chiralpak® IB N-5 (particle size: 5 µm; dimensions: 250 × 20 mm) DAICEL column. 1 mL of a solution of racemic mixture in DCM (30 mg/mL) was eluted by DCM/EtOAc using the following gradient program (flow rate: 15 mL/min, λ = 285 nm): 2 min DCM/EtOAc = 99:1, 44 min DCM/EtOAc = 99:1 → 80:20, 4 min DCM/EtOAc = 1:99, 5 min DCM/EtOAc = 99:1. The product was obtained as white solid.

The collected fractions were analyzed by analytical HPLC using the Chiralpak® IB N-5 (particle size: 5 µm; dimensions: 250 × 4.6 mm) DAICEL column using the following gradient program (flow rate: 1.5 mL/min, λ = 285 nm): 2 min DCM/EtOAc = 99:1, 14 min DCM/EtOAc = 99:1 → 80:20, 4 min DCM/EtOAc = 1:99, 2 min DCM/EtOAc = 99:1. Chromatograms of the racemic mixture and the isolated enantiomer of **3a** are shown in Fig. S1.

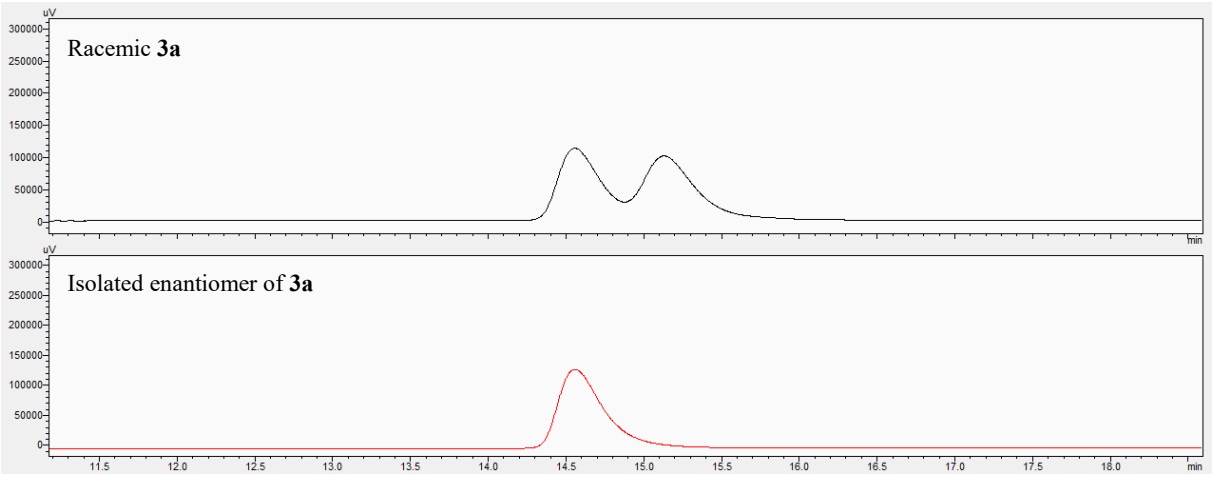


**Figure S1.** Chromatograms of the racemic mixture and isolated enantiomer of **3a**.

**Optical rotation value for isolated enantiomer:** $[\alpha]_D^{25}$(C = 1.0, $CHCl_3$ ): –4.8°.

**Propylresorcinarene 3b**

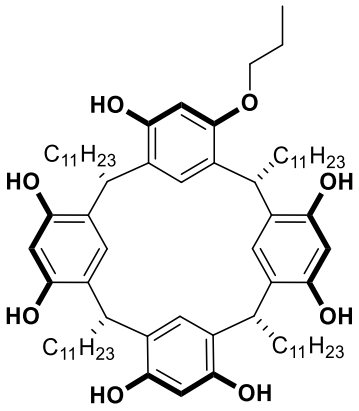


$C_{75}H_{118}O_8$
**M = 1147.76 g/mol**

Resorcinarene **1** (5.00 g, 4.52 mmol, 1.0 eq.) was dissolved in a 2:1 mixture of DMF (25 mL) and THF (12.5 mL). *t*BuOK (659 mg, 5.88 mmol, 1.3 eq.) was added in one portion at room temperature, and the mixture was stirred at 145 °C for 45 minutes. After cooling down to room temperature, *n*-propyl iodide (1.00 g, 574 µL, 5.88 mmol, 1.3 eq.) was added, and the reaction mixture was stirred at 130 °C for 15 h. After cooling down to room temperature, $H_2O$ (80 mL) was added, and the mixture was extracted with diethyl ether (3 × 150 mL). The organic layer was washed with $H_2O$ (5 × 150 mL), dried over $Na_2SO_4$, filtered, and concentrated. The crude product was purified *via* column chromatography (DCM/Acetonitrile = 7:3 → 7:4) to yield compound **3b** (1.98 g, 1.73 mmol, 38%) as a beige solid (racemic mixture).

**TLC**: $R_f$ = 0.38 (DCM/Acetonitrile = 7:4) [UV, CAM]

**$^1$H NMR** (500 MHz, acetone-$d_6$, 298 K): $\delta$ [ppm] = 8.54 (s, 1H), 8.50 (s, 1H), 8.48 (s, 1H), 8.45 (s, 1H), 8.42 (s, 1H), 8.35 (s, 1H), 7.58 (s, 1H), 7.55 (s, 1H), 7.52 (s, 1H), 7.49 (s, 1H), 7.24 (s, 1H), 6.39 (s, 1H), 6.28 (s, 1H), 6.22 (s, 1H), 6.15 (s, 1H), 4.42 – 4.27 (m, 4H), 4.05 – 3.98 (m, 1H), 3.94 – 3.86 (m, 1H), 2.37 – 2.18 (m, 8H), 1.91 – 1.80 (m, 2H), 1.31 (s, 72H), 1.07 (t, $J$ = 7.4 Hz, 3H), 0.95 – 0.83 (m, 12H).

**$^{13}$C NMR** (126 MHz, acetone-$d_6$, 298 K): $\delta$ [ppm] = 154.17, 153.97, 153.10, 153.06, 153.04, 152.73, 152.69, 152.49, 126.56, 126.23, 126.09, 125.81, 125.50, 125.26, 125.20, 125.08, 124.90, 124.82, 124.62, 124.60, 103.91, 103.83, 103.55, 101.22, 71.52, 34.99, 34.54, 34.50, 34.47, 34.41, 34.40, 34.36, 33.94, 32.77, 30.69, 30.68, 30.66, 30.60, 30.59, 30.55, 30.48, 30.46, 30.30, 30.23, 30.15, 29.99, 29.84, 29.11, 29.09, 29.00, 23.44, 23.15, 14.48, 10.89.

**IR** (ATR): $\tilde{\nu}$ [$cm^{-1}$] 3256 (m), 2922 (s), 2852 (s), 1619 (m), 1497 (m), 1448 (m), 1292 (m), 1167 (m), 1089 (m), 904 (w), 836 (m), 721 (w).

**HRMS** (ESI): calcd. for $C_{75}H_{118}NaO_8^+$ [$(M + Na)^+$]: 1169.8719, found: 1169.8696.

Both enantiomers of **3b** were resolved by preparative HPLC using the Chiralpak® IB N-5 (particle size: 5 µm; dimensions: 250 × 20 mm) DAICEL column. 1 mL of a solution of racemic mixture in DCM (30-40 mg/mL) was eluted by DCM/EtOAc using the following gradient program (flow rate: 15 mL/min, λ = 285 nm): 2 min DCM/EtOAc = 99:1, 44 min DCM/EtOAc = 99:1 → 80:20, 4 min DCM/EtOAc = 1:99, 5 min DCM/EtOAc = 99:1. Both enantiomers were obtained as white solids.

The collected fractions were analyzed by analytical HPLC using the Chiralpak® IB N-5 (particle size: 5 µm; dimensions: 250 × 4.6 mm) DAICEL column using the following gradient program (flow rate: 1.5 mL/min, λ = 285 nm): 2 min DCM/EtOAc = 99:1, 14 min DCM/EtOAc = 99:1 → 80:20, 4 min DCM/EtOAc = 1:99, 2 min DCM/EtOAc = 99:1. Chromatograms of the racemic mixture and the isolated enantiomers of **3b** are shown in Fig. S2.

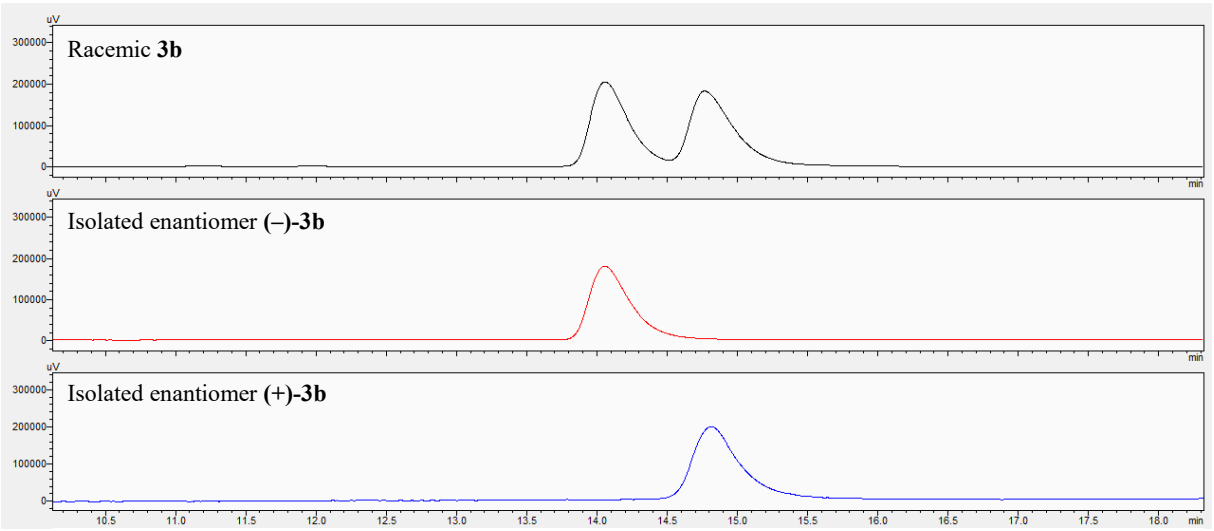


**Figure S2.** Chromatograms of the racemic mixture and isolated enantiomers of **3b**.

**Optical rotation values of the isolated enantiomers:**

**(–)-3b:** $[\alpha]_D^{25}$(C = 0.1, $CHCl_3$ ): –4.3°.

**(+)-3b:** $[\alpha]_D^{25}$(C = 0.1, $CHCl_3$ ): +4.4°.

**Butylresorcinarene 3c**

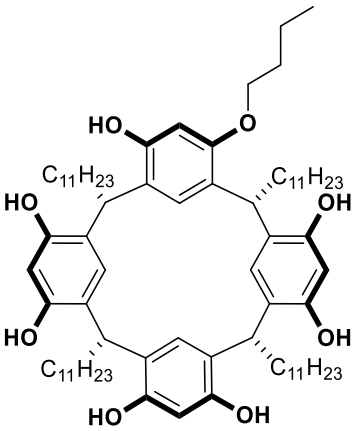


$C_{76}H_{120}O_8$
**M = 1161.79 g/mol**

Resorcinarene **1** (2.00 g, 1.81 mmol, 1.1 eq.) was dissolved in a 2:1 mixture of DMF (15 mL) and THF (7.5 mL). *t*BuOK (224 mg, 2.00 mmol, 1.1 eq.) was added in one portion at room temperature, and the mixture was stirred for 30 minutes. *n*-Butyl iodide (368 mg, 227 µL, 2.00 mmol, 1.1 eq.) was added the reaction mixture was stirred at 110 °C for 15 h. After cooling down to room temperature, $H_2O$ (40 mL) was added, and the mixture was extracted with diethyl ether (3 × 75 mL). The organic layer was washed with $H_2O$ (5 × 75 mL), dried over $Na_2SO_4$, filtered, and concentrated. The crude product was purified *via* column chromatography (DCM/EtOAc = 4:1) to yield compound **3c** (902 mg, 776 µmol, 43%) as a brown solid (racemic mixture).

**TLC**: $R_f$ = 0.19 (DCM/EtOAc = 4:1) [UV, CAM]

**$^1$H NMR** (500 MHz, acetone-$d_6$, 298 K): $\delta$ [ppm] = 8.62 – 8.23 (m, 6H), 7.58 (s, 1H), 7.55 (s, 1H), 7.53 (s, 1H), 7.50 (s, 1H), 7.23 (s, 1H), 6.40 (s, 1H), 6.28 (s, 1H), 6.22 (s, 1H), 6.15 (s, 1H), 4.41 – 4.26 (m, 4H), 4.10 – 4.02 (m, 1H), 4.00 – 3.92 (m, 1H), 2.40 – 2.15 (m, 8H), 1.90 – 1.73 (m, 2H), 1.64 – 1.47 (m, 2H), 1.46 – 1.21 (m, 72H), 0.99 (t, $J$ = 7.4 Hz, 3H), 0.94 – 0.82 (m, 12H).

**$^{13}$C NMR** (126 MHz, acetone-$d_6$, 298 K): $\delta$ [ppm] = 154.14, 153.92, 153.04, 152.99, 152.68, 152.63, 152.42, 126.50, 126.20, 126.06, 125.78, 125.45, 125.21, 125.15, 125.04, 124.86, 124.78, 124.57, 124.54, 103.85, 103.77, 103.48, 101.19, 69.69, 34.91, 34.48, 34.45, 34.42, 34.35, 34.31, 33.88, 32.72, 31.87, 30.63, 30.60, 30.54, 30.53, 30.49, 30.40, 30.17, 29.06, 29.03, 28.94, 23.38, 19.94, 14.43, 14.14.

**IR** (ATR): $\tilde{\nu}$ [$cm^{-1}$] 3263 (m), 2921 (s), 2852 (s), 1619 (m), 1498 (m), 1448 (m), 1293 (m), 1167 (m), 1089 (m), 1041 (m), 837 (m), 720 (w).

**HRMS** (ESI): calcd. for $C_{76}H_{119}O_8^-$ [$(M - H)^-$]: 1159.8910, found: 1159.8927.

One enantiomer of **3c** was resolved by preparative HPLC using the Chiralpak® IB N-5 (particle size: 5 µm; dimensions: 250 × 20 mm) DAICEL column. 1 mL of a solution of racemic mixture in DCM (30 mg/mL) was eluted by DCM/EtOAc using the following gradient program (flow rate: 15 mL/min, λ = 285 nm): 2 min2 min DCM/EtOAc = 99:1, 44 min DCM/EtOAc = 99:1 → 80:20, 4 min DCM/EtOAc = 1:99, 5 min DCM/EtOAc = 99:1. The product was obtained as white solid.

The collected fractions were analyzed by analytical HPLC using the Chiralpak® IB N-5 (particle size: 5 µm; dimensions: 250 × 4.6 mm) DAICEL column using the following gradient program (flow rate: 1.5 mL/min, λ = 285 nm): 2 min DCM/EtOAc = 99:1, 14 min DCM/EtOAc = 99:1 → 80:20, 4 min DCM/EtOAc = 1:99, 2 min DCM/EtOAc = 99:1. Chromatograms of the racemic mixture and the isolated enantiomer of **3c** are shown in Fig. S3.

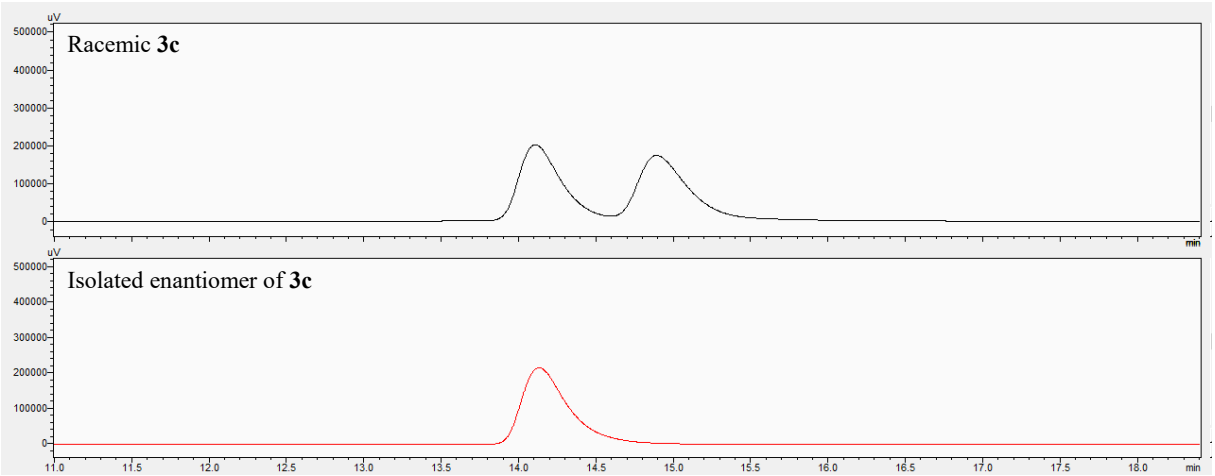


**Figure S3.** Chromatograms of racemic mixture and isolated enantiomer of **3c**.

**Optical rotation value of the isolated enantiomer:** $[\alpha]_D^{25}$(C = 1.0, $CHCl_3$ ): –0.4°.

## 3. Cyclization Studies

**Preparation and titration of HCl stock solution in chloroform:** HCl stock solution in chloroform was prepared by passing HCl gas, generated by the dropwise addition of concentrated $H_2SO_4$ to dry NaCl, through chloroform for approximately 30 min. The concentration of HCl in the resulting solution was determined as follows: HCl stock solution in chloroform (100 µL) was added to a solution of phenol red in EtOH (0.002 wt%, 2.5 mL) *via* a Microman M1 pipette equipped with a plastic tip. Upon addition, the solution turned from yellow (neutral) to pink (acidic). The resulting solution was then titrated with a 0.1 M ethanolic solution of triethylamine. At the equivalence point, the solution turned from pink to yellow. The HCl stock solution was kept in the fridge, and the titration was repeated immediately before each use.

**General procedure for nerol (NOH) cyclization reactions:** The corresponding resorcinarene (2.75 µmol, 0.1 eq. of the corresponding capsule) was dissolved in 50 µL of $CDCl_3$ in a GC vial (2 mL) with a micro insert (VWR, 15 mm top, 0.1 mL) as shown in Fig. S4. To this solution, NOH (708 µg, 4.59 µmol, 1.0 eq.) as a stock solution in $CDCl_3$ was added, followed by the addition of *n*-decane (1.34 µL, 6.89 µmol, 1.5 eq.). Additional chloroform was added to bring the total volume to 137.5 µL. An aliquot (2 µL) of the reaction mixture was diluted with 0.3 mL of *n*-hexane (containing 0.08% DMSO). The diluted sample was put in the freezer for at least 15 min, centrifuged to remove the corresponding resorcinarene, and subjected to GC analysis (initial sample). HCl stock solution in chloroform (0.03 eq.) was added to the reaction mixture, and the mixture was briefly shaken. The sealed GC vial was kept at 30 °C (±1 °C) using a thermostated heating block made from aluminum. Further samples were taken at the indicated times and analyzed by gas chromatography. Conversions and yields were calculated by employing the equations described in our previous work[5] and plotted against time (see profiles for the nerol cyclization reactions inside supramolecular capsules based on resorcinarenes **2a-3c** below; only chiral products are depicted). Enantiomeric excesses were determined with chiral GC measurements (see Table 2 of the manuscript).

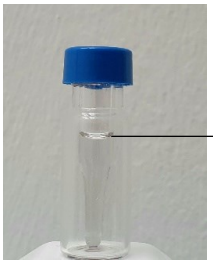


**Figure S4.** Standard GC vial with a glass micro insert used for cyclization studies.

Reactions were performed in triplicates, and standard deviations were determined using the following equations:

$$\text{mean value:} \quad \bar{x} = \frac{1}{n}\sum_{i=1}^{n} x_i$$

$$\text{standard deviation:} \quad \mathrm{S} = \sqrt{\frac{1}{n-1}\sum_{i=1}^{n}(x_i - \bar{x})^2}.$$

**Reaction profiles for the nerol cyclization reactions**

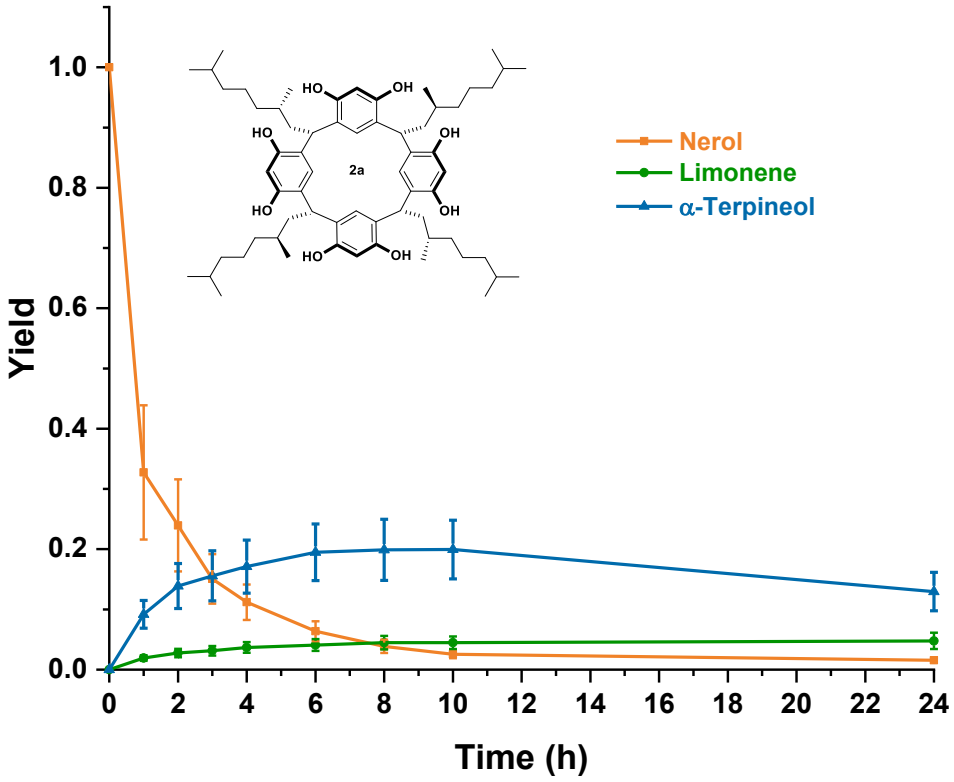


**Figure S5.** Reaction profile of nerol cyclization with **2a**; only chiral products are depicted.

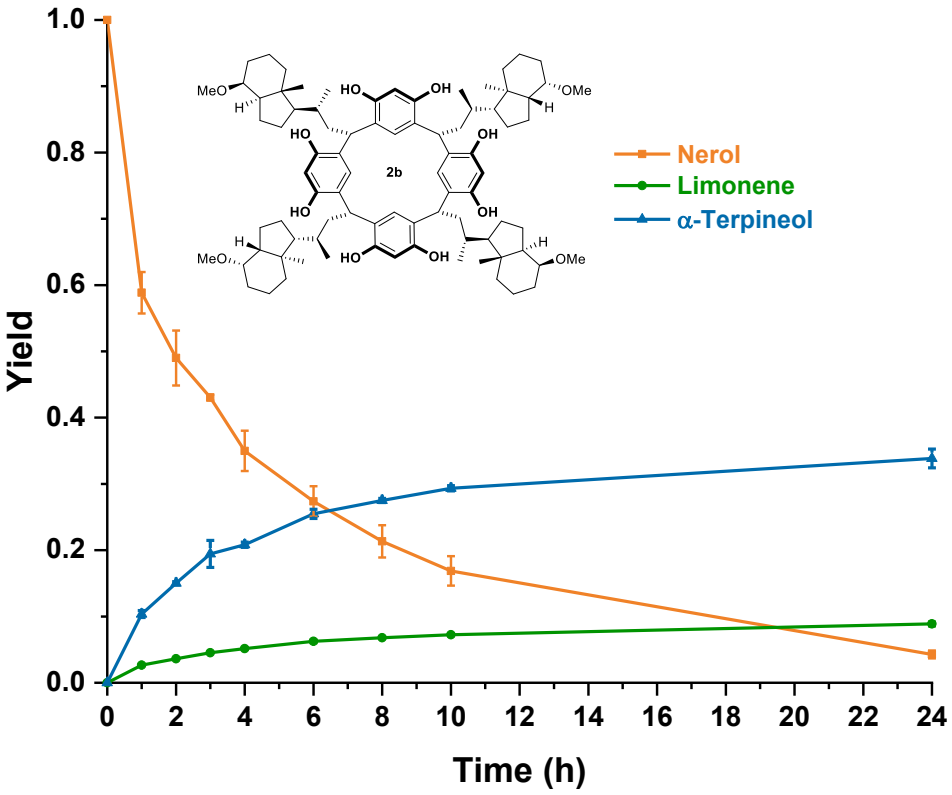


**Figure S6.** Reaction profile of nerol cyclization with **2b**; only chiral products are depicted.

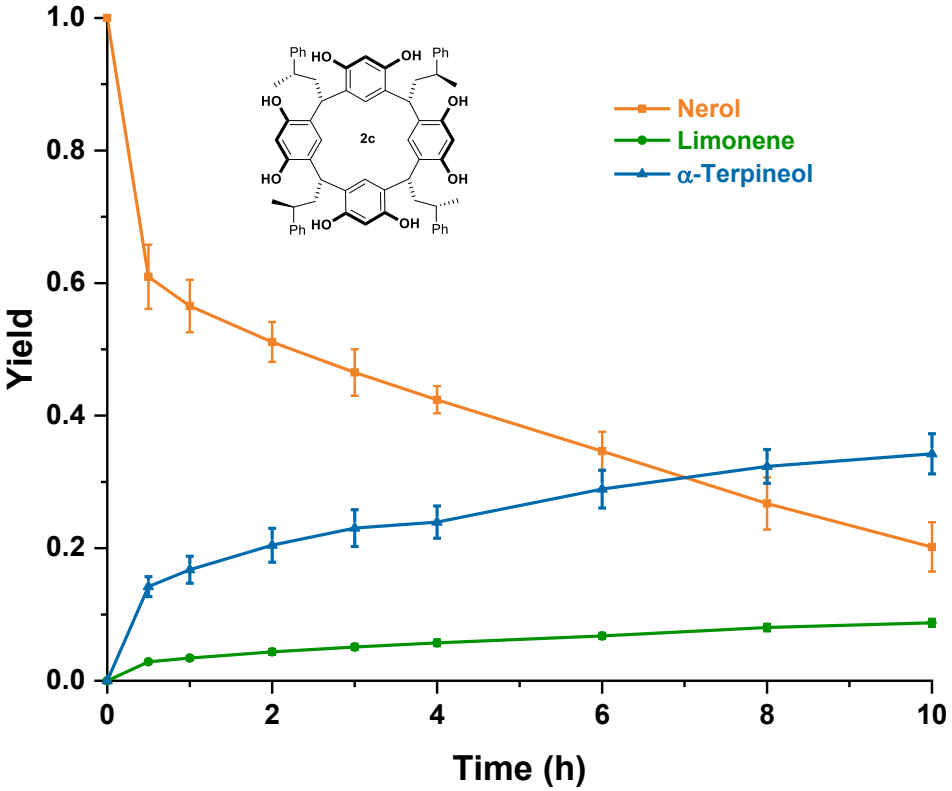


**Figure S7.** Reaction profile of nerol cyclization with **2c**; only chiral products are depicted.

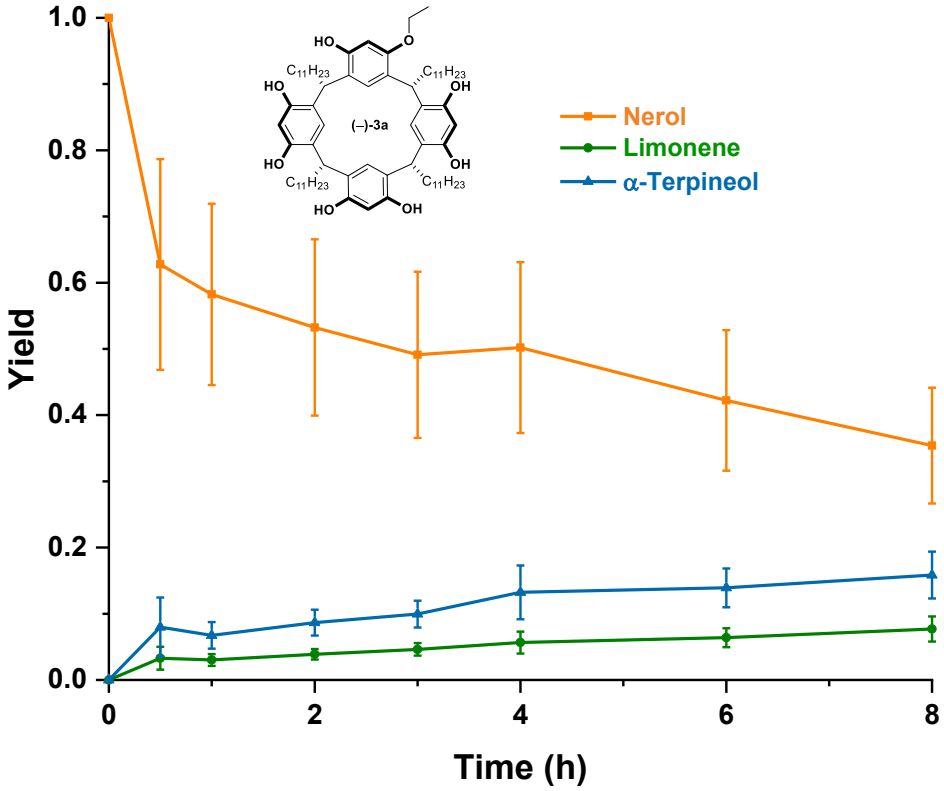


**Figure S8.** Reaction profile of nerol cyclization with **(–)-3a**; only chiral products are depicted.

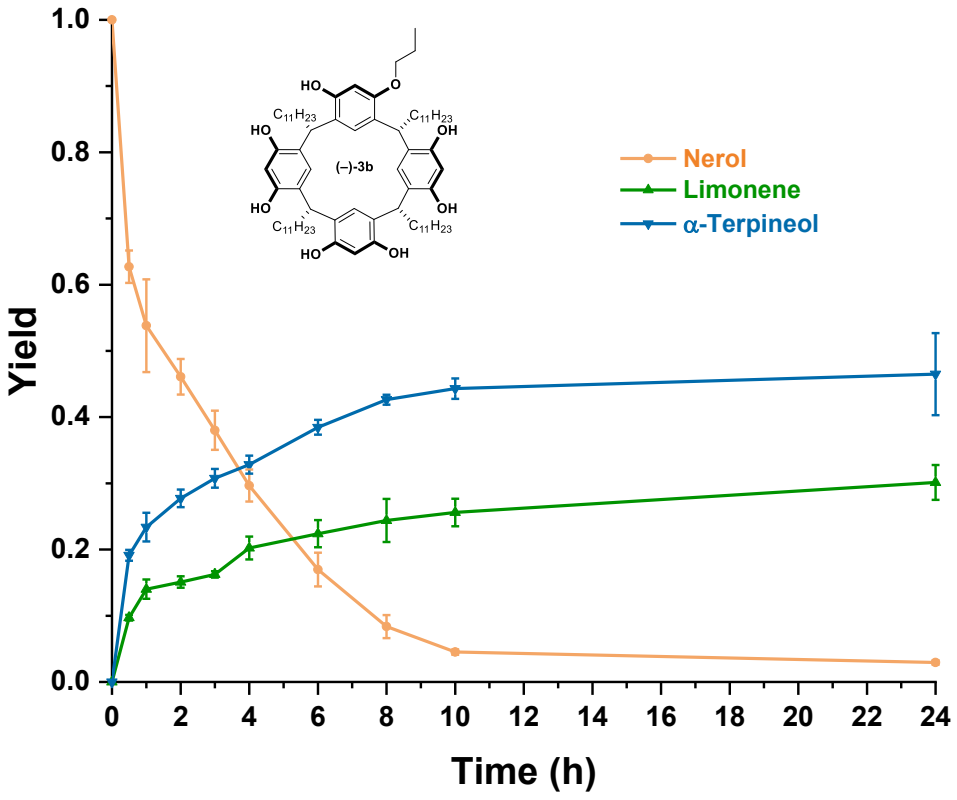


**Figure S9.** Reaction profile of nerol cyclization with **(–)-3b**; only chiral products are depicted.

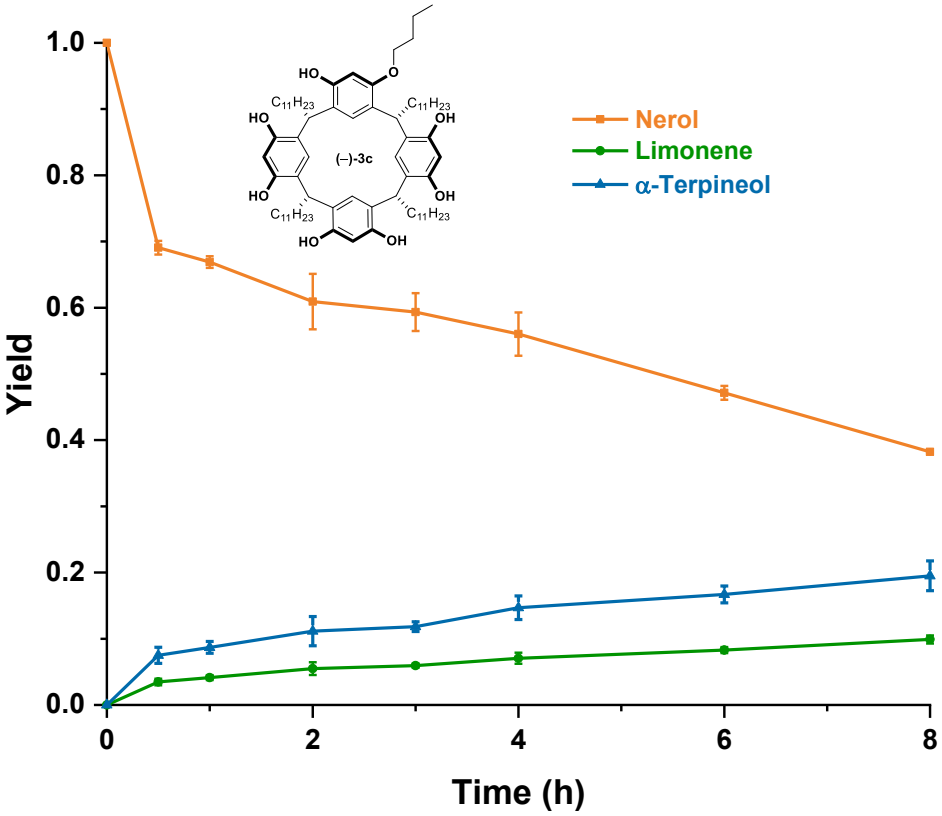


**Figure S10.** Reaction profile of nerol cyclization with **(–)-3c**; only chiral products are depicted.

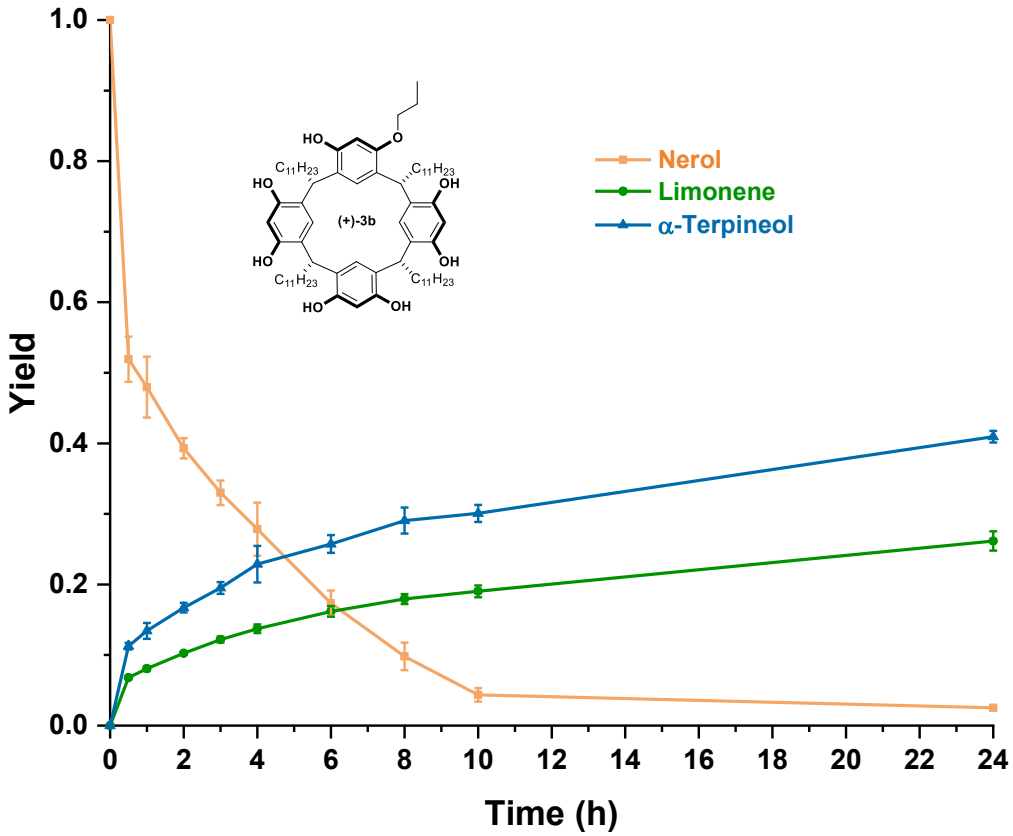


**Figure S11.** Reaction profile of nerol cyclization with **(+)-3b**; only chiral products are depicted.

**Observation of the enantiomeric excess of limonene and α-terpineol over time for the nerol cyclization reaction with (–)-3b**

No significant changes were observed. In previous work, we demonstrated that both compounds will convert further to achiral products.[97] Therefore, some small changes in *ee* over time are expected.

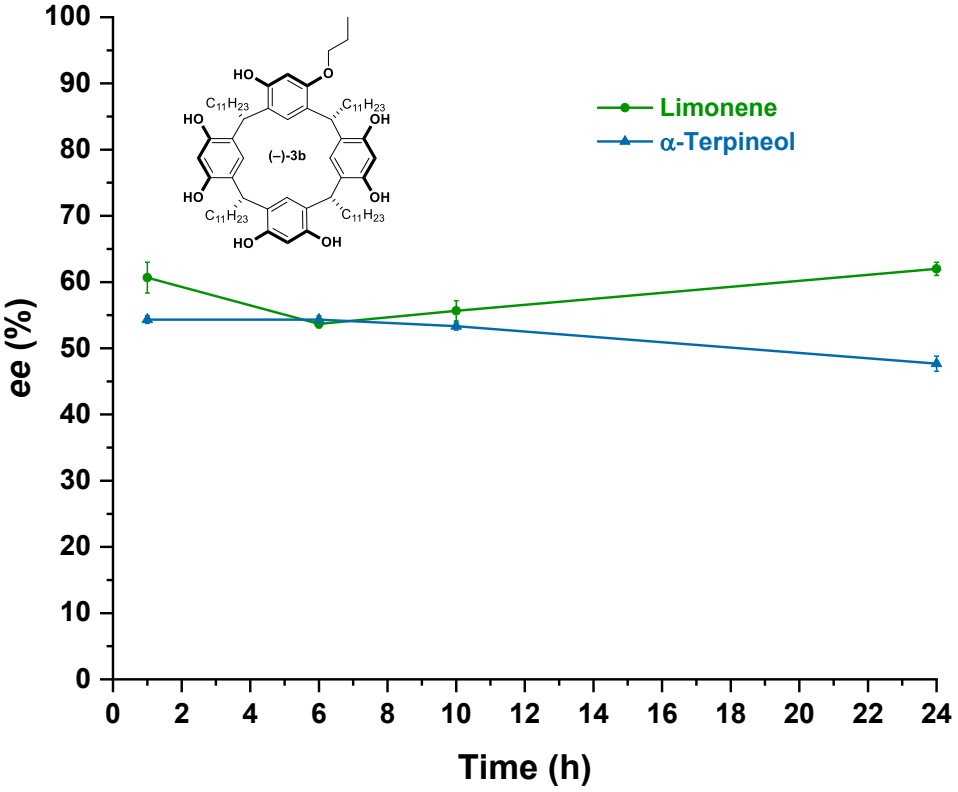


**Figure S12.** Observation of the enantiomeric excess of limonene and α-terpineol over time for the nerol cyclization reaction with **(–)-3b**.

**Determination of the configuration of products:** The configuration of the formed cyclization products, limonene and α-terpineol, was determined by chiral GC measurements. As references, the commercially available racemic mixture and the enantiopure sample were analyzed and compared with chromatograms of the reaction mixture. Chiral GC traces of commercial samples of limonene and α-terpineol and the cyclization reactions of NOH inside the enantioenriched capsules based on resorcinarene **3b** are shown in Fig. S13 and S14.

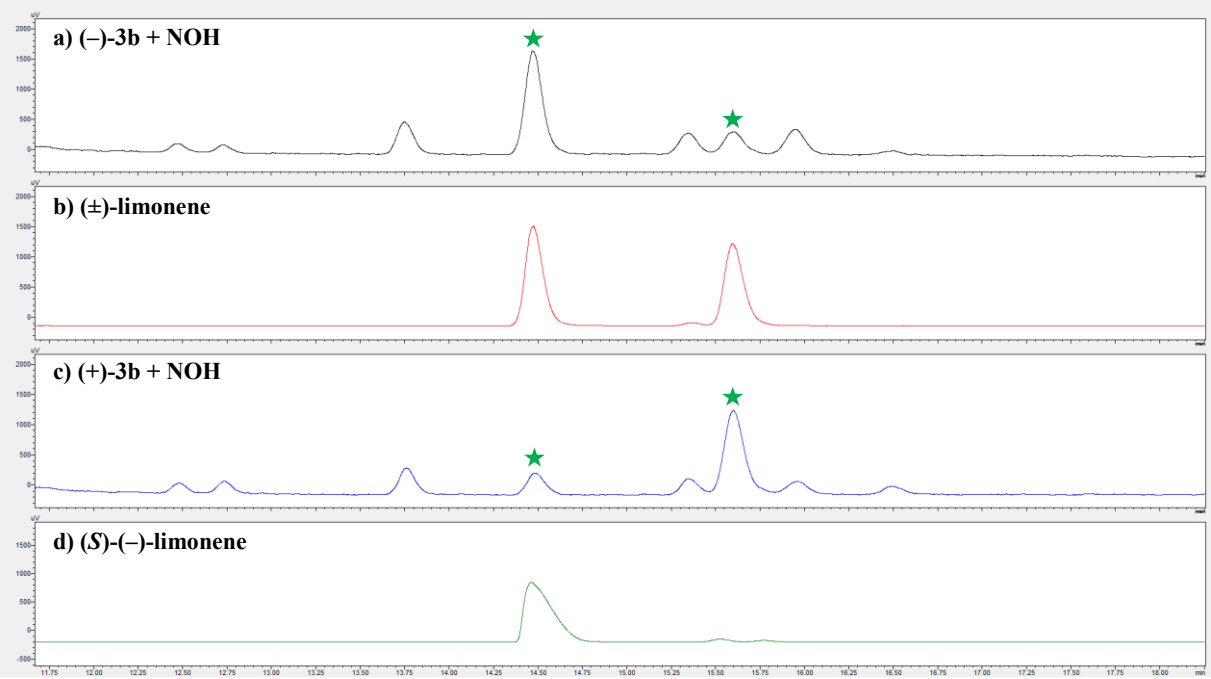


**Figure S13.** GC-traces of a) reaction mixture of the NOH cyclization with **(–)-3b** after 24 h; b) commercial sample of (±)-limonene; c) reaction mixture of the NOH cyclization with **(+)-3b** after 24 h; d) commercial sample of (*S*)-(–)-limonene.

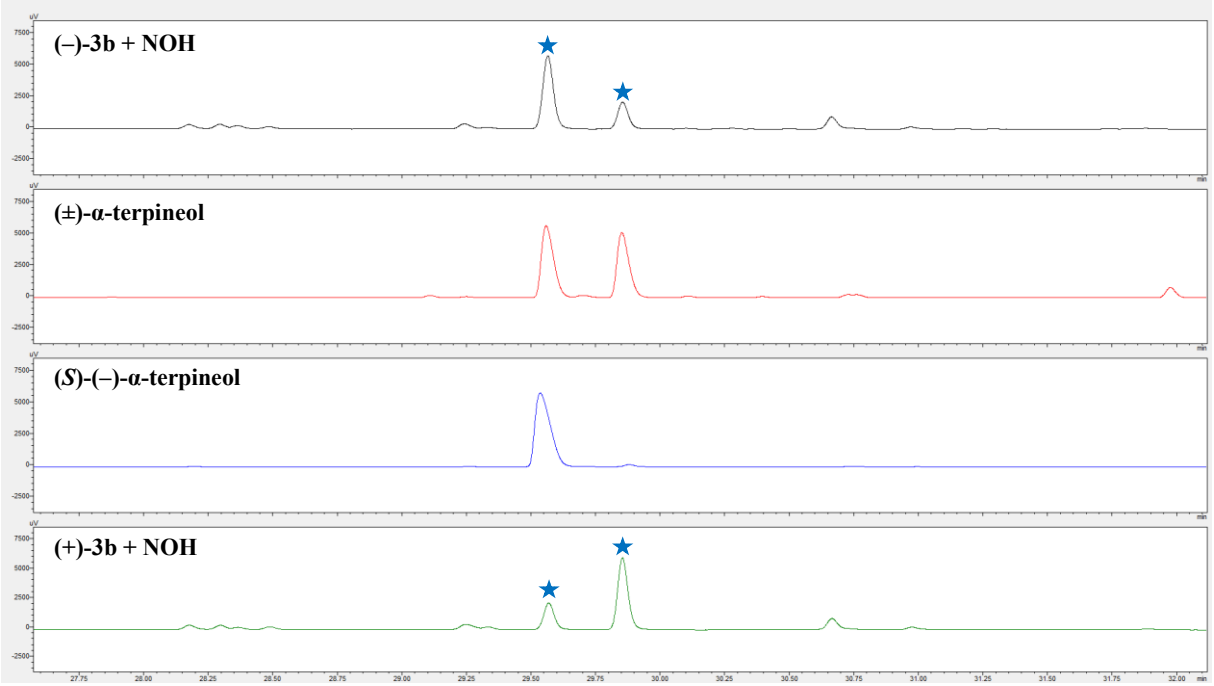


**Figure S14.** GC-traces of a) reaction mixture of the NOH cyclization with **(–)-3b** after 24 h; b) commercial sample of (±)-α-terpineol; c) reaction mixture of the NOH cyclization with **(+)-3b** after 24 h; d) commercial sample of (*S*)-(–)- α-terpineol.

# 4. NMR Spectra of New Compounds

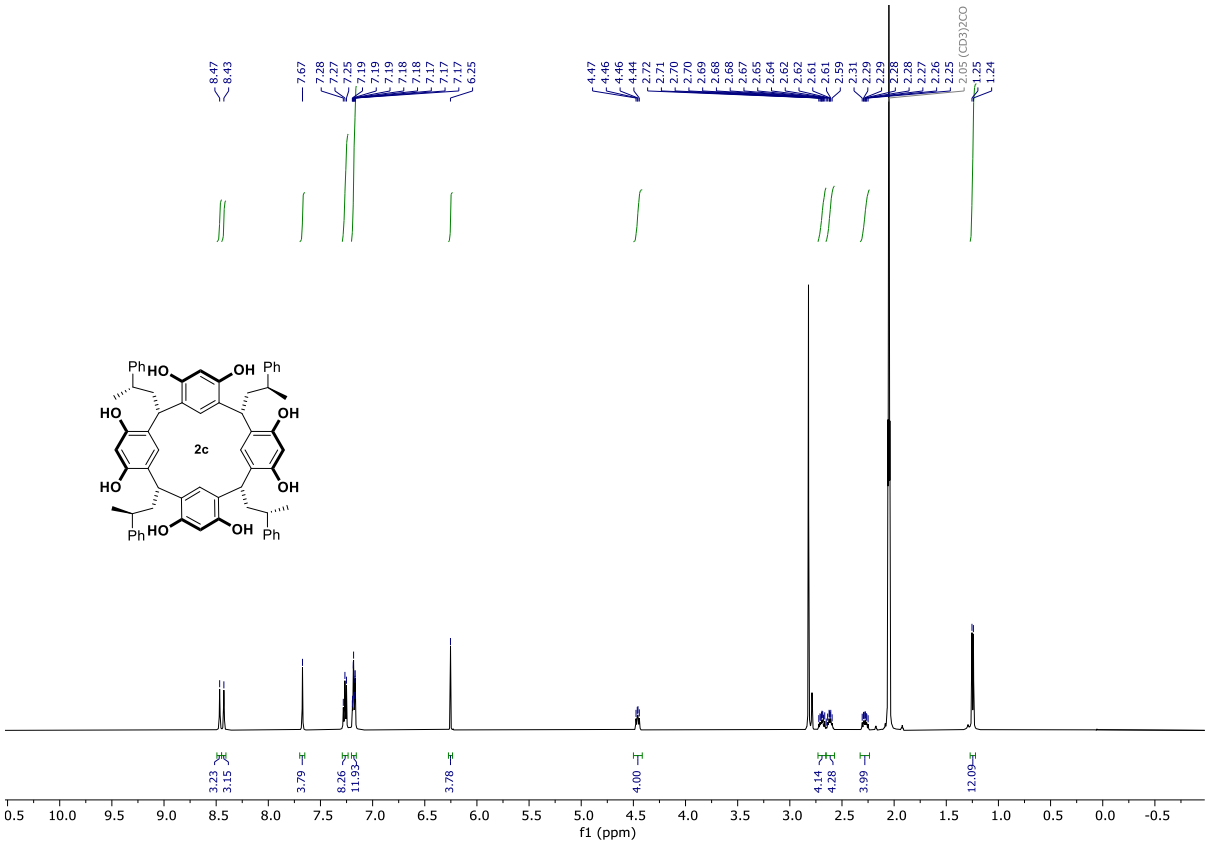


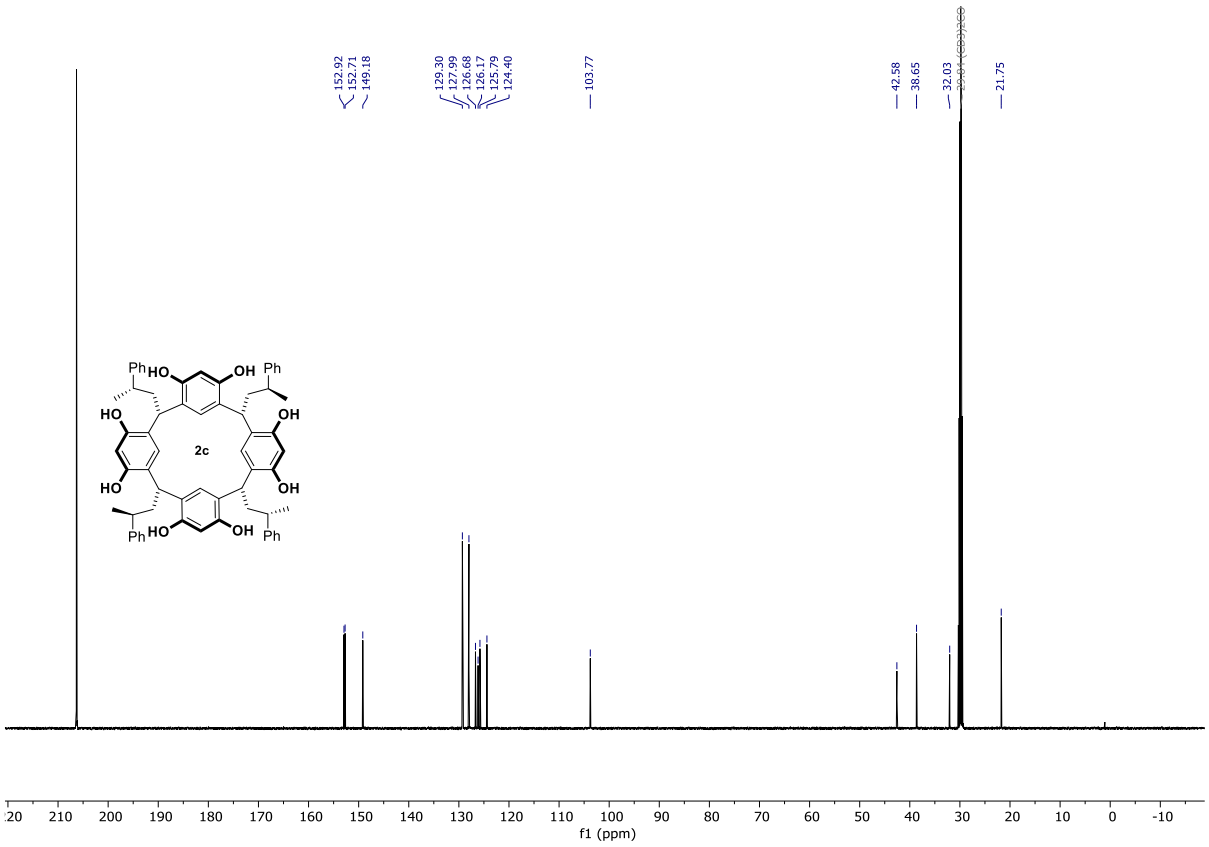

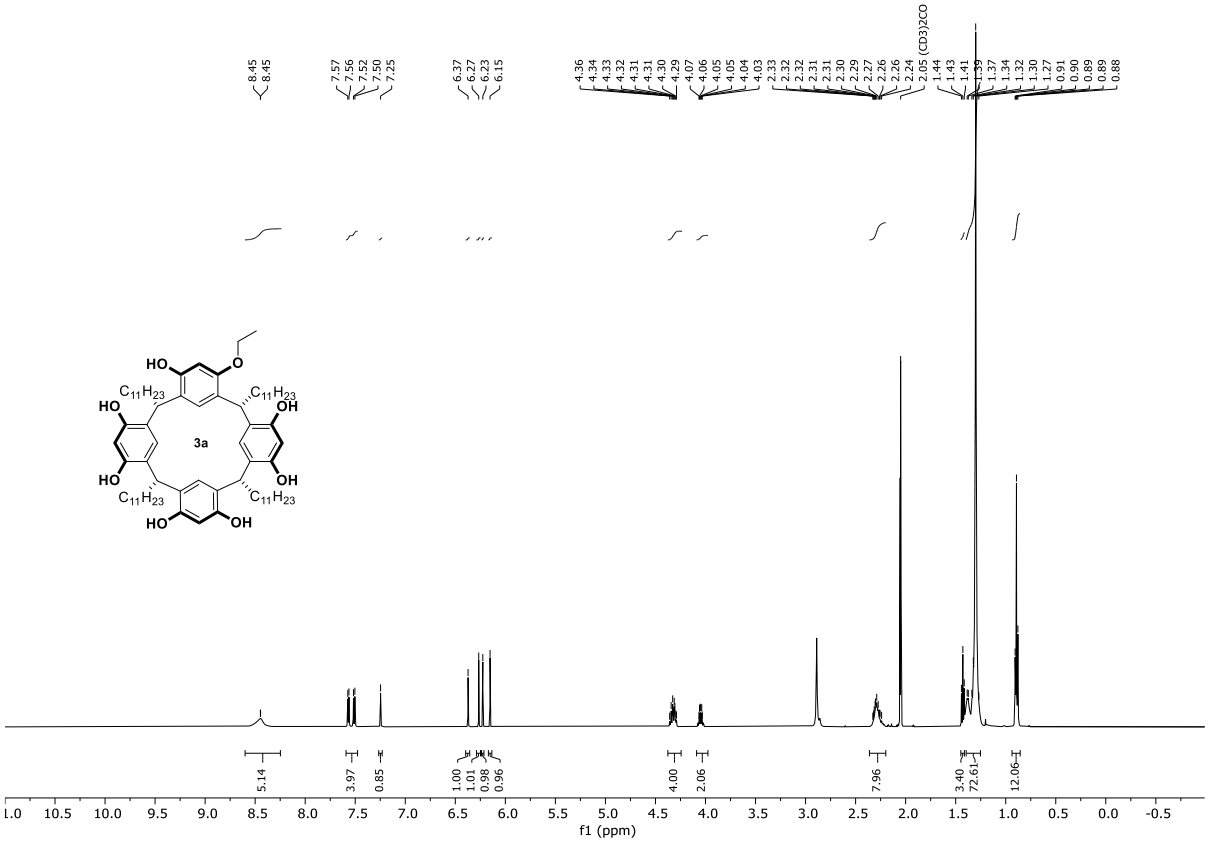
8.45
8.45
7.57
7.56
7.52
7.50
7.25
6.37
6.27
6.23
6.15
4.36
4.34
4.33
4.32
4.31
4.31
4.30
4.29
4.07
4.06
4.05
4.05
4.04
4.03
2.33
2.32
2.32
2.31
2.31
2.30
2.29
2.27
2.26
2.26
2.24
2.05 ((CD3)2CO
1.44
1.43
1.41
1.39
1.37
1.34
1.32
1.30
1.27
0.91
0.90
0.89
0.89
0.88
HO
O
C11H23
C11H23
HO
OH
3a
HO
OH
C11H23
C11H23
HO
OH
5.14
3.97
0.85
1.00
1.01
0.98
0.96
4.00
2.06
7.96
3.40
72.61
12.06
f1 (ppm)

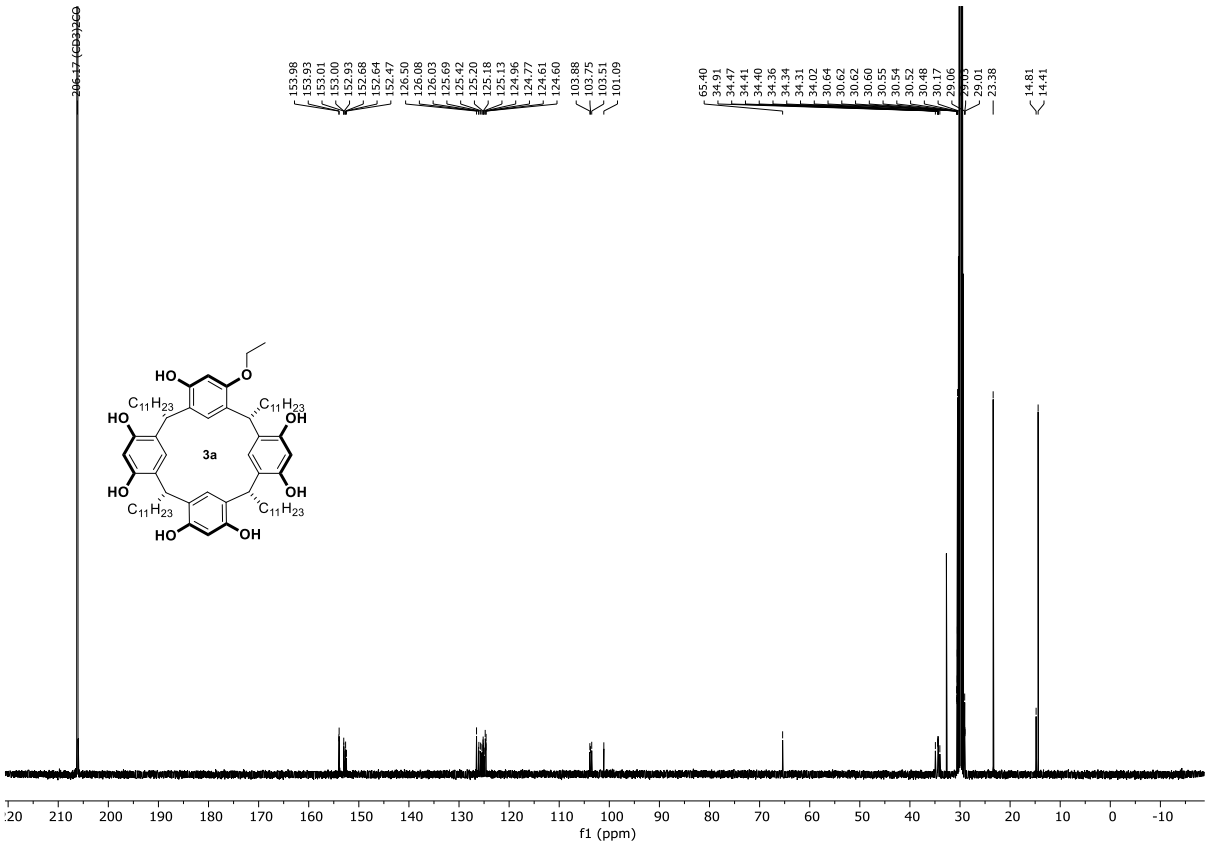
206.17 ((CD3)2CO
153.98
153.93
153.01
153.00
152.93
152.68
152.64
152.47
126.50
126.08
126.03
125.69
125.42
125.20
125.18
125.13
124.96
124.77
124.61
124.60
103.88
103.75
103.51
101.09
65.40
34.91
34.47
34.41
34.40
34.36
34.34
34.31
34.02
30.64
30.62
30.62
30.60
30.55
30.54
30.52
30.48
30.17
29.06
29.03
29.01
23.38
14.81
14.41
HO
O
C11H23
C11H23
HO
OH
3a
HO
OH
C11H23
C11H23
HO
OH
f1 (ppm)

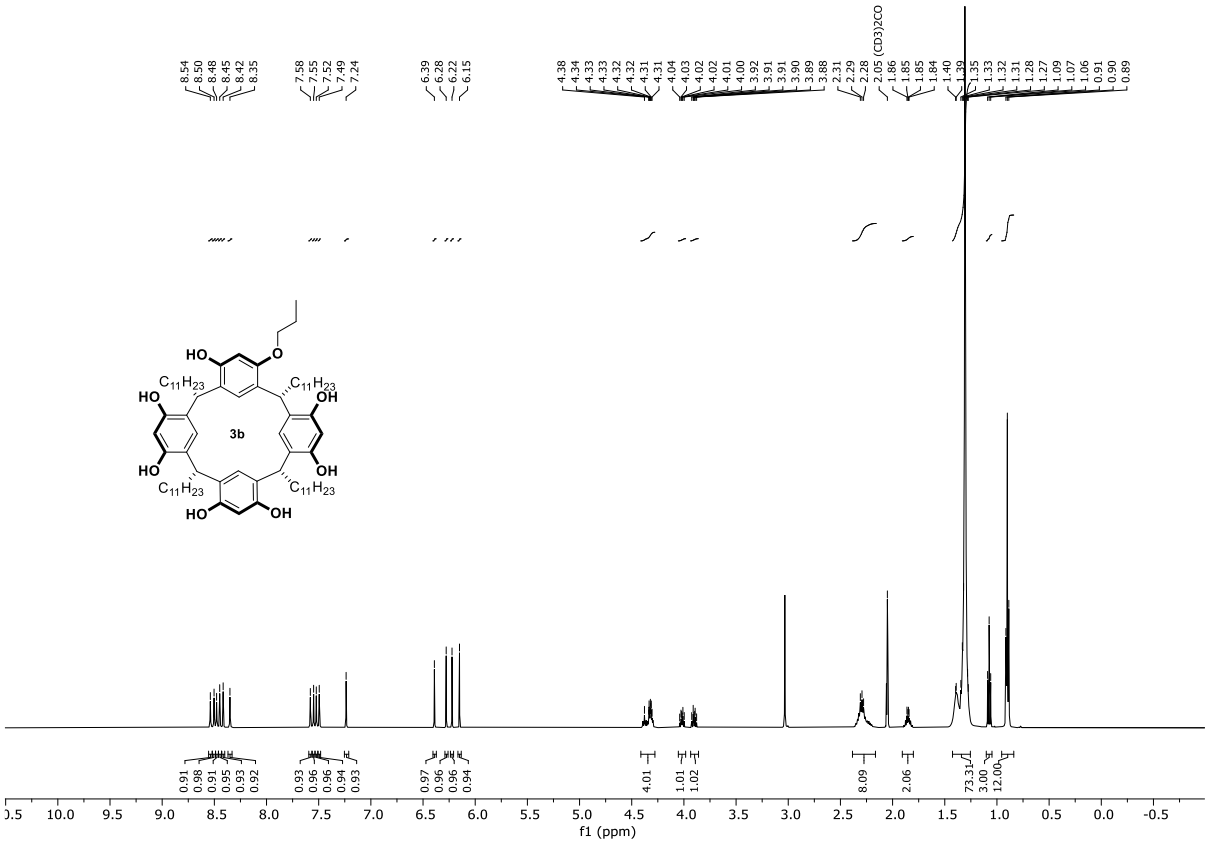
8.54
8.50
8.48
8.45
8.42
8.35
7.58
7.55
7.52
7.49
7.24
6.39
6.28
6.22
6.15
4.38
4.34
4.33
4.32
4.32
4.31
4.31
4.04
4.03
4.02
4.01
4.00
3.92
3.91
3.91
3.90
3.89
3.88
2.31
2.29
2.28
2.05 (CD3)2CO
1.86
1.85
1.85
1.84
1.40
1.38
1.35
1.33
1.32
1.31
1.28
1.27
1.09
1.07
1.06
0.91
0.90
0.89
3b
0.91
0.98
0.91
0.95
0.93
0.92
0.93
0.96
0.96
0.94
0.93
0.97
0.96
0.96
0.94
4.01
1.01
1.02
8.09
2.06
73.31
3.00
12.00
f1 (ppm)

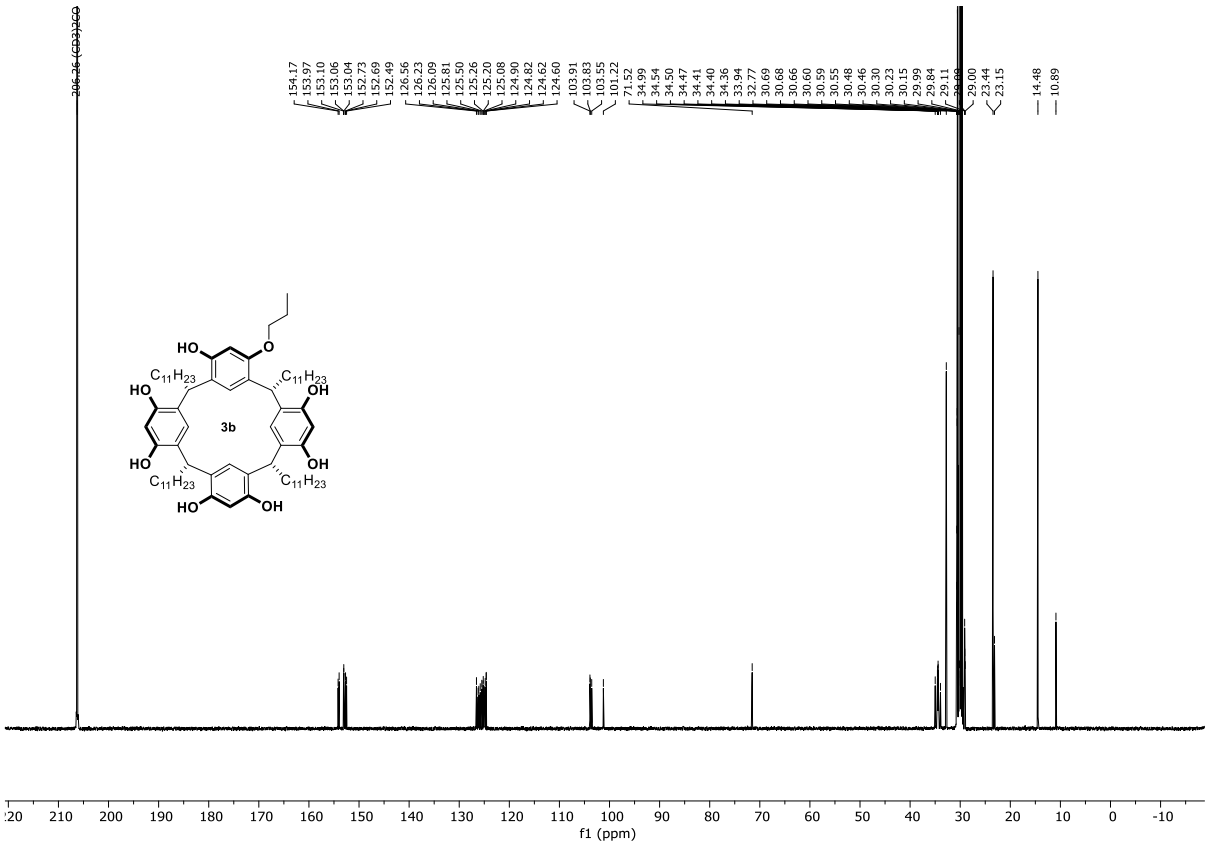
206.26 (CD3)2CO
154.17
153.97
153.10
153.06
153.04
152.73
152.69
152.49
126.56
126.23
126.09
125.81
125.50
125.26
125.20
125.08
124.90
124.82
124.62
124.60
103.91
103.83
103.55
101.22
71.52
34.99
34.54
34.50
34.47
34.41
34.40
34.36
33.94
32.77
30.69
30.68
30.66
30.60
30.59
30.55
30.48
30.46
30.30
30.23
30.15
29.99
29.84
29.11
29.00
23.44
23.15
14.48
10.89
3b
f1 (ppm)

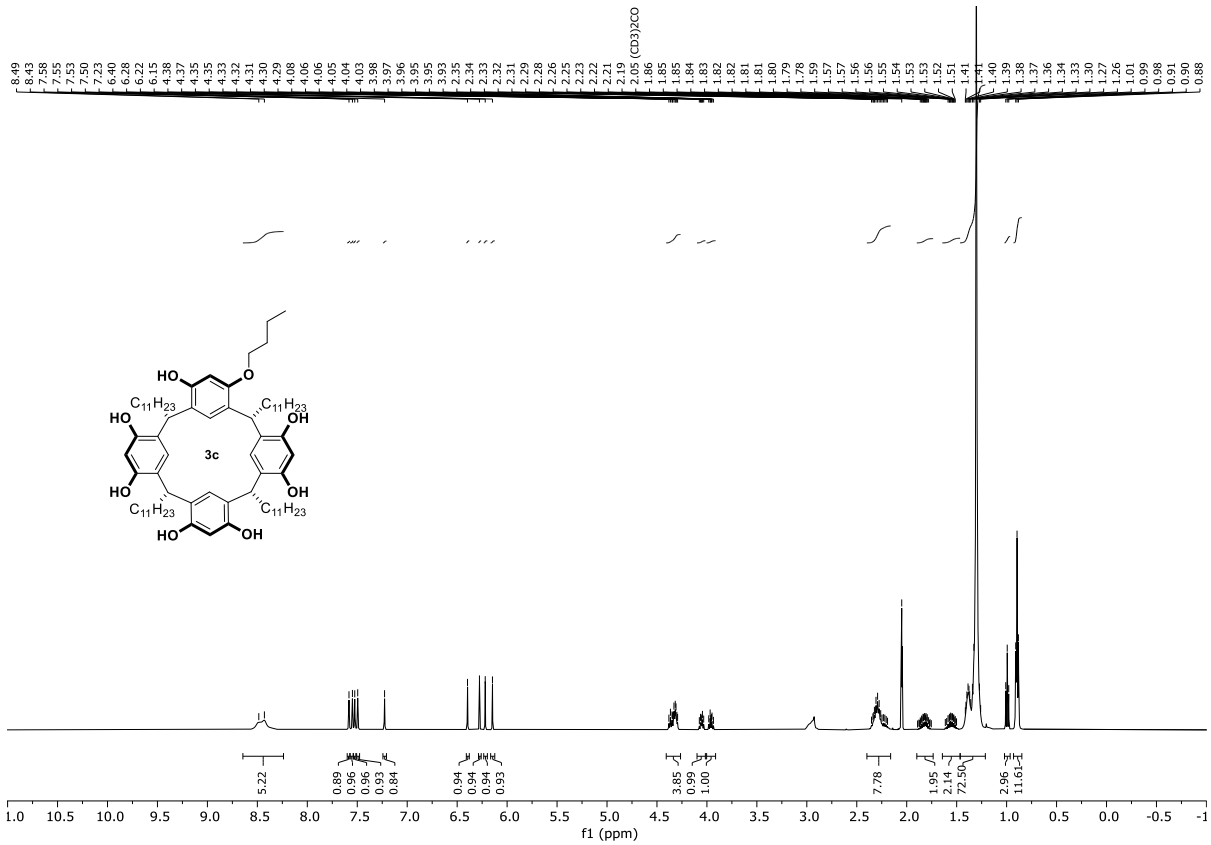
3c
f1 (ppm)

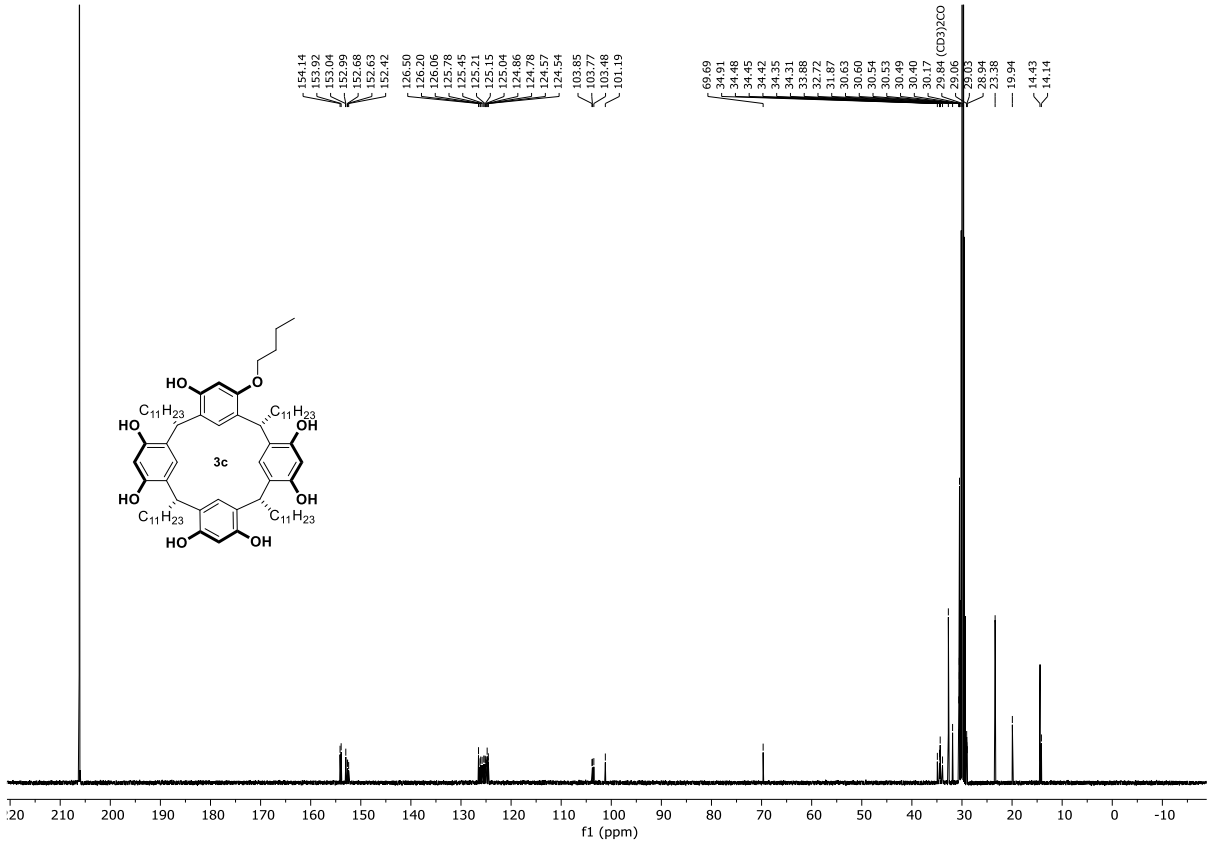
3c
f1 (ppm)

# 5. Chiral GC Traces of Selected Reactions

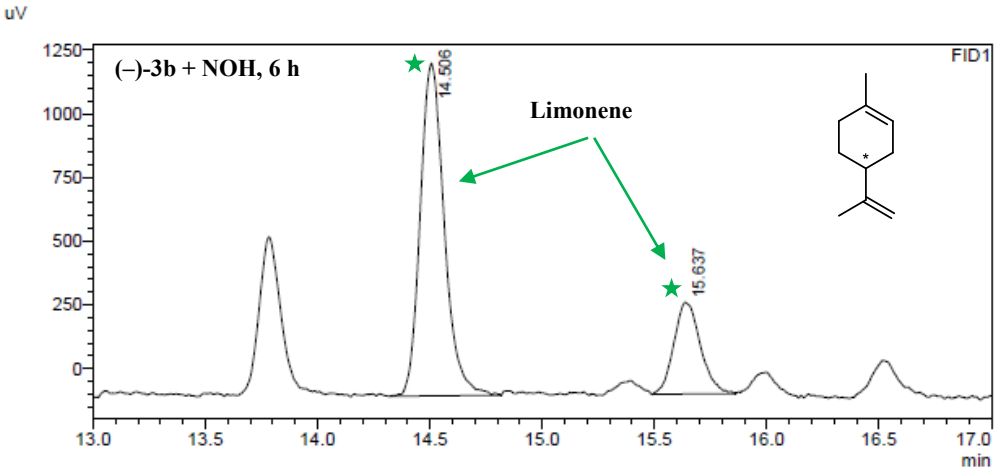


FID1

| Peak# | Ret. Time | Area | Area% |
|---|---|---|---|
| 1 | 14.506 | 9733 | 76.691 |
| 2 | 15.637 | 2958 | 23.309 |
| Total | | 12692 | 100.000 |

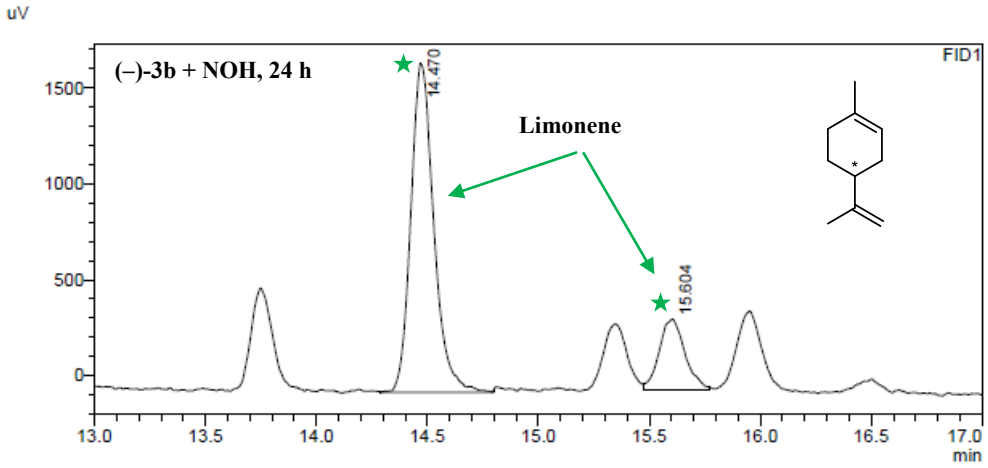


FID1

| Peak# | Ret. Time | Area | Area% |
|---|---|---|---|
| 1 | 14.470 | 12378 | 80.359 |
| 2 | 15.604 | 3025 | 19.641 |
| Total | | 15404 | 100.000 |

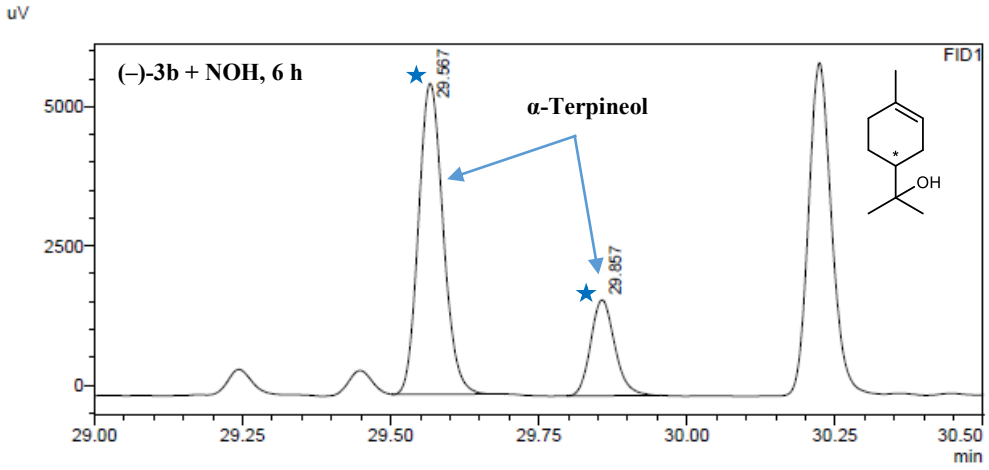


FID1

| Peak# | Ret. Time | Area | Area% |
|---|---|---|---|
| 1 | 29.567 | 16150 | 76.782 |
| 2 | 29.857 | 4884 | 23.218 |
| Total | | 21033 | 100.000 |

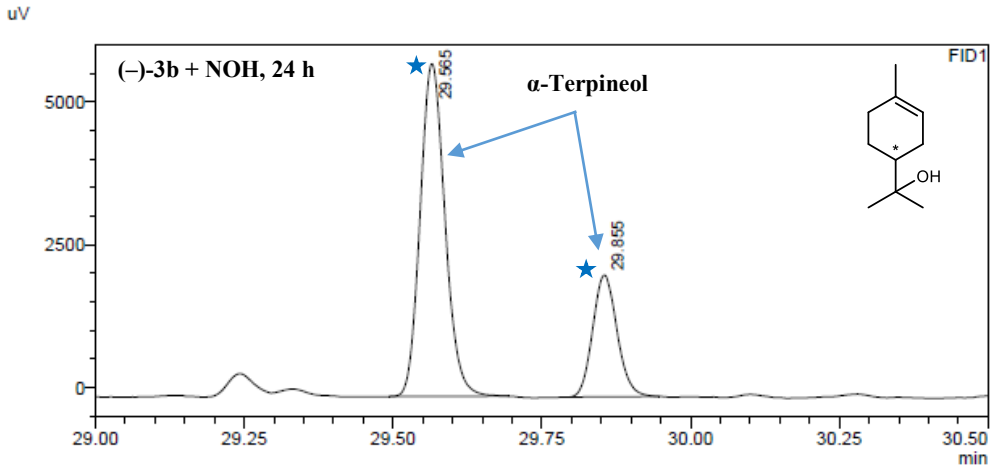


FID1

| Peak# | Ret. Time | Area | Area% |
|---|---|---|---|
| 1 | 29.565 | 16875 | 73.502 |
| 2 | 29.855 | 6083 | 26.498 |
| Total | | 22958 | 100.000 |

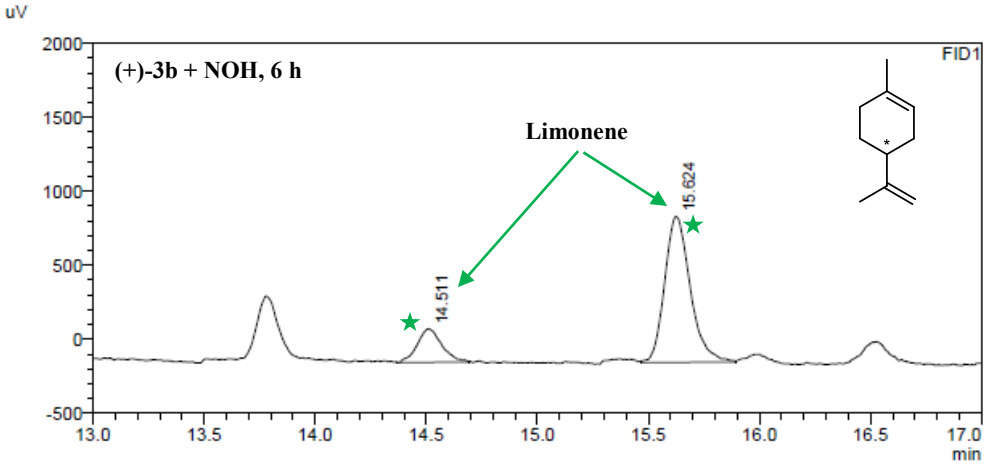


FID1

| Peak# | Ret. Time | Area | Area% |
|---|---|---|---|
| 1 | 14.511 | 1743 | 18.051 |
| 2 | 15.624 | 7912 | 81.949 |
| Total | | 9655 | 100.000 |

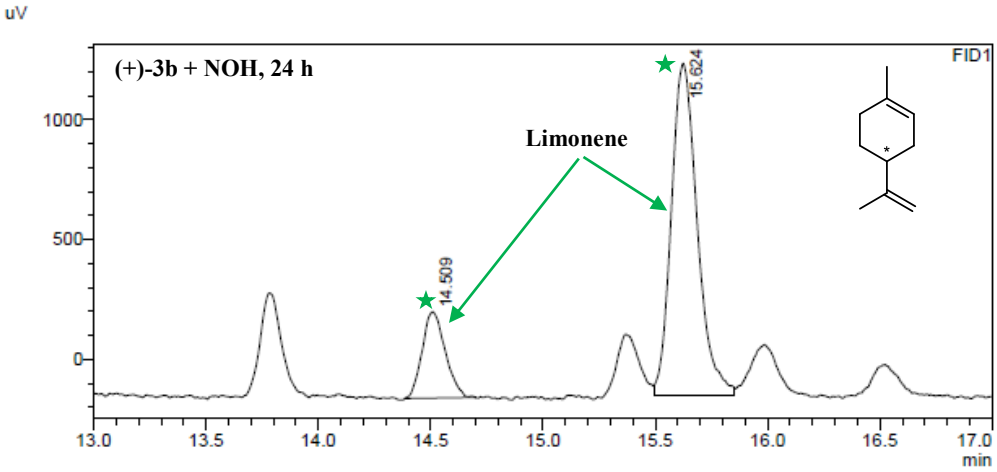


FID1

| Peak# | Ret. Time | Area | Area% |
|---|---|---|---|
| 1 | 14.509 | 2574 | 18.689 |
| 2 | 15.624 | 11199 | 81.311 |
| Total | | 13773 | 100.000 |

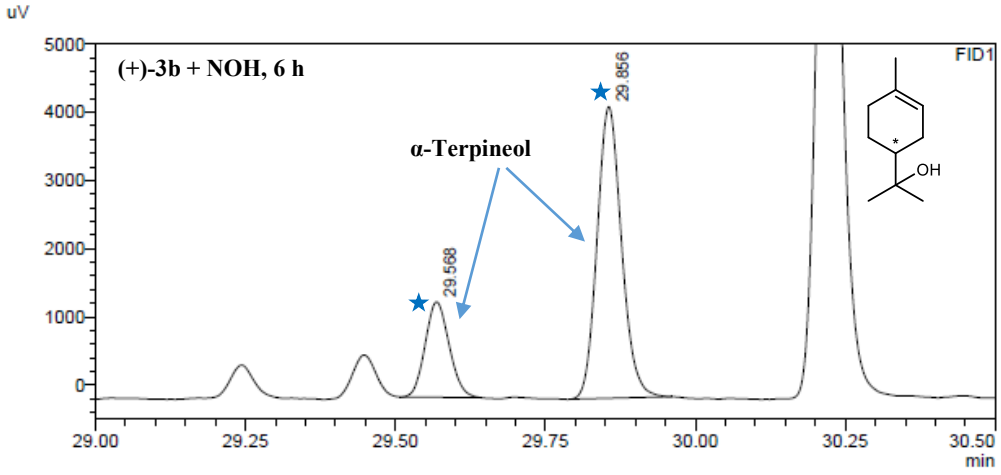


FID1

| Peak# | Ret. Time | Area | Area% |
|---|---|---|---|
| 1 | 29.568 | 3883 | 24.247 |
| 2 | 29.856 | 12131 | 75.753 |
| Total | | 16014 | 100.000 |

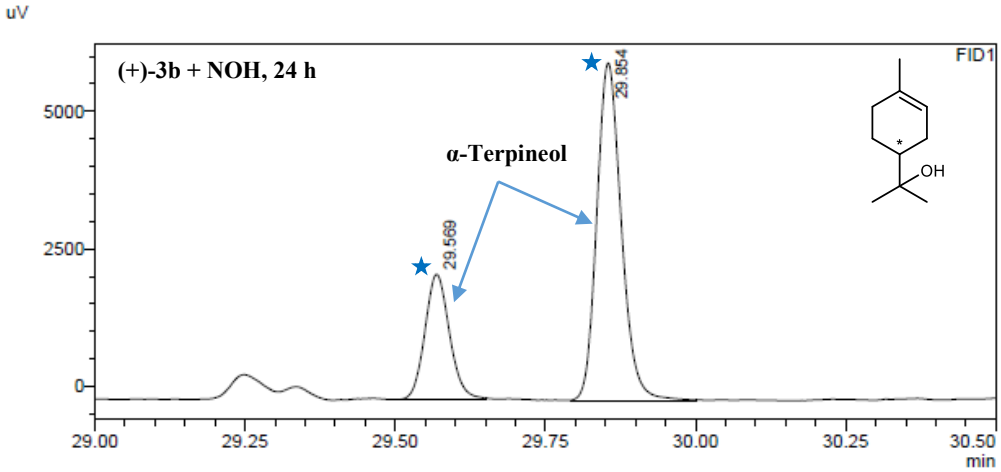


FID1

| Peak# | Ret. Time | Area | Area% |
|---|---|---|---|
| 1 | 29.569 | 6571 | 27.386 |
| 2 | 29.854 | 17422 | 72.614 |
| Total | | 23992 | 100.000 |

## 6. References

[1] D. H. Wu, A. Chen, C. S. Johnson, *J. Magn. Reson. Ser. A* **1995**, *115*, 260–264.

[2] I. Elidrisi, S. Negin, P. V. Bhatt, T. Govender, H. G. Kruger, G. W. Gokel, G. E. M. Maguire, *Org. Biomol. Chem.* **2011**, *9*, 4498–4506.

[3] T. Amaya, J. Rebek, *J. Am. Chem. Soc.* **2004**, *126*, 6216–6217.

[4] T. Lee, J. Bryan Jones, *J. Am. Chem. Soc.* **1996**, *118*, 502–508.

[5] Q. Zhang, K. Tiefenbacher, *Nat. Chem.* **2015**, *7*, 197–202.

# 4. SUMMARY AND OUTLOOK

Enantioselective transformations are of particular interest for chemistry. Acting as an enzyme mimetic, the hexameric resorcinarene-based capsules are able to catalyze various reactions, often requiring HCl as a co-catalyst. However, only a few enantioselective transformations inside such supramolecular capsules are known. For instance, iminium-catalyzed 1,4-reduction of α,β-unsaturated aldehydes inside the supramolecular capsule **XII** delivers high enantioselectivity with up to 92% Δ*ee* in comparison to reactions in bulk solution. The role of HCl as a co-catalyst was never explored for this transformation inside capsule **XII**, however, it could potentially have a beneficial effect.

We set out to review the effect of HCl additive on iminium catalysis inside **XII** and explore other additives which could increase the enantioselectivity. In this work, we present the optimized reaction conditions for the iminium-catalyzed 1,4-reduction of α,β-unsaturated aldehydes inside the supramolecular capsule **XII** (Scheme 28). We established that HCl is not required as a co-catalyst for this process. Moreover, we successfully reduced the previously reported capsule loading of 26 mol% to 12 mol%. In parallel, we demonstrated that enantioselectivity can be increased by using an alcohol additive, which plays a dual role: 1) it reduces the background reaction outside of the capsule; 2) it accelerates the capsule-catalyzed transformation. For two substrates, we reported unprecedented enantioselectivity of 92% *ee*. The obtained results consolidate our understanding of catalysis inside confined spaces and will be transferred to other classes of reactions.

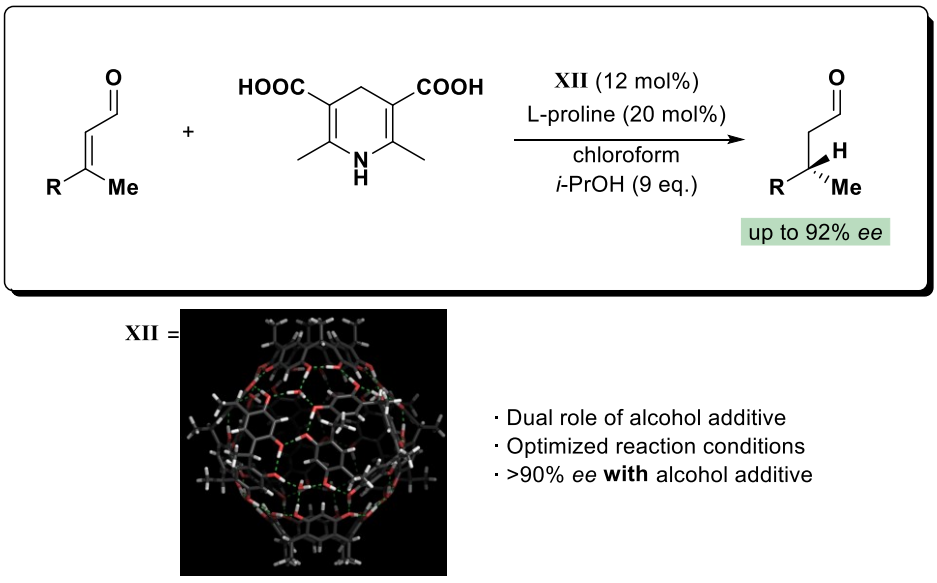


**Scheme 28.** a) Optimized conditions for iminium-catalyzed reduction of α,β-unsaturated aldehydes inside the supramolecular capsule **XII**.

One of the most complex chemical transformations found in nature – tail-to-head terpene cyclization – can take place inside capsule **XII**. Even though this reaction leads to the formation of chiral products, it has not been reported to occur in an enantioselective fashion inside resorcinarene capsules. Therefore, we aimed to develop a supramolecular resorcin[4]arene-based catalyst to perform enantioselective tail-to-head terpene cyclization.

As a result, in this work, we present the synthesis of novel optically active resorcin[4]arenes, which can self-assemble into hexameric supramolecular capsules. Chirality was introduced by cyclization of resorcinol with optically active aldehydes and by monoalkylation of the achiral resorcin[4]arene (Fig. 11), followed by separation of enantiomers by HPLC. All the obtained capsules based on building blocks **127**-**128** demonstrated catalytic activity in the tail-to-head terpene cyclization with nerol as a substrate. However, in the case of derivatives **128a**-**c**, the chiral information is too far from the encapsulated substrate, and these derivatives failed to induce enantioselective cyclization. Two monoalkylated derivatives **127a**-**b** that carry the chiral information at the surface of the capsule are able to induce enantiomeric excesses. Supramolecular capsule based on the resorcinarene **127b** delivered up to 62% *ee* in terpene cyclization with nerol as a substrate.

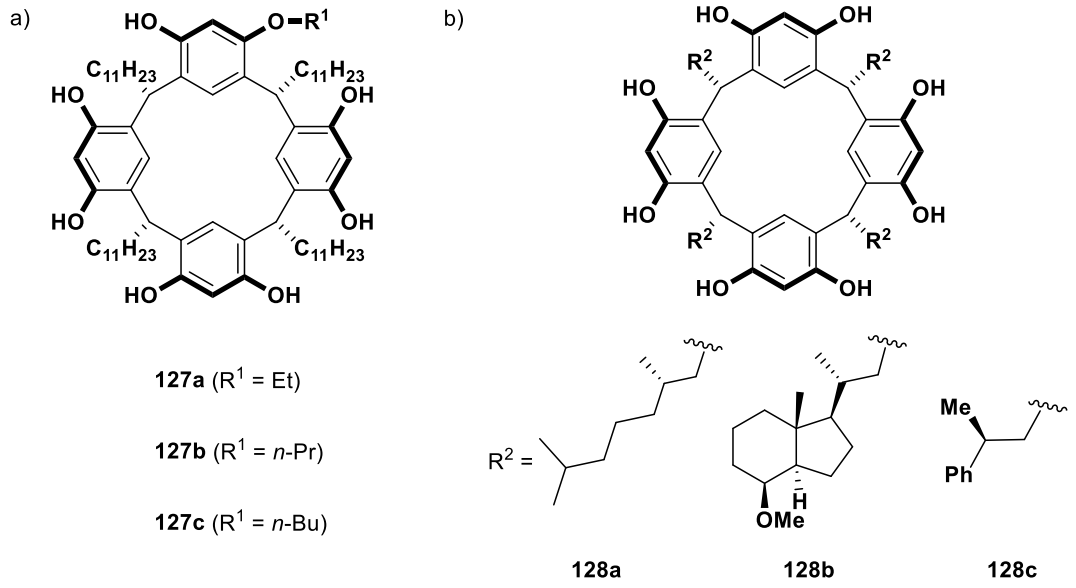


**Figure 11.** Obtained chiral derivatives of resorcin[4]arene with the chiral information a) at the upper rim of the macrocycle; b) at the feet.

The obtained results open up new possibilities to perform enantioselective reactions inside resorcinarene-based capsules. Future studies will involve optimization of the supramolecular catalysts for chirality transfer and expansion of the substrate scope.

# 5. INDEX OF ABBREVIATIONS

| | |
|---|---|
| °C | degree *Celsius* |
| A ⊃ B | B encapsulated within A |
| Å | Ångstrom, $10^{-10}$ m |
| Ar | aryl |
| Bu | butyl |
| CD | circular dichroism |
| δ | chemical shift |
| DCM | dichloromethane |
| DMF | *N*,*N*-dimethylformamide |
| DMSO | dimethyl sulfoxide |
| DOSY | diffusion ordered spectroscopy |
| *ee* | enantiomeric excess |
| eq. | equivalent |
| *e.g.* | lat. *exempli gratia*, for example |
| ESI | electrospray ionisation |
| et al. | lat. *et alia*, and others |
| Et | ethyl |
| FID | flame ionization detector |
| g | gram |
| GC | gas chromatography |
| h | hours |
| h | Planck's constant, $6.626 \cdot 10^{-34}$ J·s |
| HRMS | high-resolution mass spectrometry |
| HPLC | high performance liquid chromatography |
| Hz | hertz |
| IR | infrared spectroscopy |
| $k$ | reaction rate |
| $k_{rel}$ | selectivity of kinetic resolution; $k_{rel} = [(1 - c)(1 - ee)]/[(1 - c)(1 + ee)]$, where $c$ and $ee$ are concentration and enantiomeric excess of the substrate, respectively |
| K | kelvin |
| L | ligand |
| L | liter |

| | |
|---|---|
| m | meter |
| µg | microgram |
| µL | microliter |
| µmol | micromol |
| M | metal |
| M | molarity, mol |
| Me | methyl |
| MS | mass spectrometry |
| min | minutes |
| mL | milliliter |
| mm | millimeter |
| mmol | millimol |
| ν | frequency |
| NOH | nerol |
| NMR | nuclear magnetic resonance |
| pH | lat. *pondus hydrogenii*, negative base 10 logarithm of the activity of the hydrogen ion in a solution |
| Ph | phenyl |
| p$K_a$ | negative base 10 logarithm of the acid dissociation constant ($K_a$) of a solution |
| ppm | parts per million, $10^{-6}$ |
| Pr | propyl |
| r.t. | room temperature |
| THF | tetrahydrofuran |
| TLC | thin-layer chromatography |
| TMS | trimethylsilyl |
| UV | ultraviolet |
| w | water-saturated |

# 6. LITERATURE REFERENCES


[1] D. Voet, J. G. Voet, *Biochemistry 3rd Ed.*, Wiley, New York, **2004**.

[2] S. K. Silverman, *Wiley Encyclopedia of Chemical Biology*, John Wiley & Sons, **2008**.

[3] U. T. Bornscheuer, G. W. Huisman, R. J. Kazlauskas, S. Lutz, J. C. Moore, K. Robins, *Nature* **2012**, *485*, 185–194.

[4] J. H. Schrittwieser, S. Velikogne, M. Hall, W. Kroutil, *Chem. Rev.* **2018**, *118*, 270–348.

[5] R. Breslow, *Acc. Chem. Res.* **1995**, *28*, 146–153.

[6] M. Raynal, P. Ballester, A. Vidal-Ferran, P. W. N. M. van Leeuwen, *Chem. Soc. Rev.* **2014**, *43*, 1734–1787.

[7] Y. Okamoto, T. R. Ward, in *Compr. Supramol. Chem. II* (Ed.: J.L. Atwood), Elsevier, Oxford, **2017**, pp. 459–510.

[8] J.-M. Lehn, *Angew. Chemie* **1990**, *29*, 1304–1319.

[9] J.-M. Lehn, *Proc. Natl. Acad. Sci.* **2002**, *99*, 4763–4768.

[10] F. Biedermann, H. J. Schneider, *Chem. Rev.* **2016**, *116*, 5216–5300.

[11] Cram D. J., *Angew. Chemie* **1988**, *27*, 1009–1020.

[12] J.-M. Lehn, *Angew. Chemie* **1988**, *27*, 89–112.

[13] C. J. Pedersen, *Angew. Chemie* **1988**, *27*, 1021–1027.

[14] C. J. Pedersen, *J. Am. Chem. Soc.* **1967**, *89*, 7017–7036.

[15] B. Dietrich, J.-M. Lehn, J.-P. Sauvage, *Tetrahedron Lett.* **1969**, *10*, 2889–2892.

[16] Cram D. J.; Lein. G.M., *J. Am. Chem. Soc* **1985**, *107*, 3657–3668.

[17] D. J. Chao, Y.; Cram, *J. Am. Chem. Soc* **1976**, *98*, 1015–1017.

[18] B. Dietrich, T. M. Fyles, J.-M. Lehn, L. G. Pease, D. L. Fyles, *J. Chem. Soc. Chem. Commun.* **1978**, 934–936.

[19] J. Zhang, P. X. Ma, *Adv. Drug Deliv. Rev.* **2013**, *65*, 1215–1233.

[20] R. Breslow, *Science* **1982**, *218*, 532–537.

[21] J. K. M. Mackay, L. G.; Wylie, R. S.; Sanders, *J. Am. Chem. Soc.* **1994**, *116*, 3141–3142.

[22] F. Mattei, P.; Diedrich, *Helv. Chim. Acta* **1997**, *80*, 1555–1587.

[23] K. I. Assaf, W. M. Nau, *Chem. Soc. Rev.* **2015**, *44*, 394–418.

[24] N.-Y. Mock, W. L.; Shih, *J. Org. Chem.* **1983**, *48*, 3619–3620.

[25] P. Neri, J. L. Sessler, M. X. Wang, *Calixarenes and Beyond*, Springer, **2016**.

[26] P. Timmerman, W. Verboom, D. N. Reinhoudt, *Tetrahedron* **1996**, *52*, 2663–2704.

[27] M. Chwastek, A. Szumna, *Org. Lett.* **2020**, *22*, 6838–6841.

[28] B. W. Purse, A. Shivanyuk, J. Rebek, *Chem. Commun.* **2002**, *2*, 2612–2613.

[29] M. Luostarinen, A. Åhman, M. Nissinen, K. Rissanen, *Supramol. Chem.* **2004**, *16*, 505–

512.

[30] R. Gutsche, C. D.; Dhawan, B.; No, K. H; Muthukrishman, *J. Am. Chem. Soc.* **1981**, *103*, 3782–3792.

[31] J. A. Gajjar, R. H. Vekariya, H. M. Parekh, *Synth. Commun.* **2020**, *50*, 2545–2571.

[32] Q. He, G. I. Vargas-Zúñiga, S. H. Kim, S. K. Kim, J. L. Sessler, *Chem. Rev.* **2019**, *119*, 9753–9835.

[33] S. J. Nemat, H. Jędrzejewska, A. Prescimone, A. Szumna, K. Tiefenbacher, *Org. Lett.* **2020**, *22*, 5506–5510.

[34] T. Ogoshi, S. Kanai, S. Fujinami, T. Yamagishi, *J. Am. Chem. Soc.* **2008**, *130*, 5022–5023.

[35] J. Pfeuffer-Rooschüz, L. Schmid, A. Prescimone, K. Tiefenbacher, *JACS Au* **n.d.**, *0*, null.

[36] K. Fujita, M.; Oguro, D.; Miyazawa, M.; Oka. H.; Yamaguchi, K.; Ogura, *Nature* **1995**, *378*, 469–471.

[37] M. Kusukawa, T.; Fujita, *Angew. Chemie* **1998**, *37*, 3142–3144.

[38] T. Kusukawa, M. Fujita, *J. Am. Chem. Soc.* **1999**, *121*, 1397–1398.

[39] T. Murase, S. Peschard, S. Horiuchi, Y. Nishioka, M. Fujita, *Supramol. Chem.* **2011**, *23*, 199–208.

[40] H. Takezawa, K. Shitozawa, M. Fujita, *Nat. Chem.* **2020**, *12*, 574–578.

[41] P. Mal, D. Schultz, K. Beyeh, K. Rissanen, J. R. Nitschke, *Angew. Chemie* **2008**, *47*, 8297–8301.

[42] V. F. Slagt, J. N. H. Reek, P. C. J. Kamer, P. W. N. M. Van Leeuwen, *Angew. Chemie* **2001**, *40*, 4271–4274.

[43] V. F. Slagt, P. C. J. Kamer, P. W. N. M. Van Leeuwen, J. N. H. Reek, *J. Am. Chem. Soc.* **2004**, *126*, 1526–1536.

[44] J. H. Jordan, B. C. Gibb, *Chem. Soc. Rev.* **2015**, *44*, 547–585.

[45] C. L. D. Gibb, B. C. Gibb, *J. Am. Chem. Soc.* **2004**, *126*, 11408–11409.

[46] L. S. Kaanumalle, C. L. D. Gibb, B. C. Gibb, V. Ramamurthy, *J. Am. Chem. Soc.* **2004**, *126*, 14366–14367.

[47] M. Yoshizawa, L. Catti, *Acc. Chem. Res.* **2019**, *52*, 2392–2404.

[48] K. Kondo, A. Suzuki, M. Akita, M. Yoshizawa, *Angew. Chemie* **2013**, *125*, 2364–2368.

[49] K. Kondo, M. Akita, T. Nakagawa, Y. Matsuo, M. Yoshizawa, *Chem. Eur. J.* **2015**, *21*, 12741–12746.

[50] K. Kondo, M. Akita, M. Yoshizawa, *Chem. Eur. J.* **2016**, *22*, 1937–1940.

[51] T. Omagari, A. Suzuki, M. Akita, M. Yoshizawa, *J. Am. Chem. Soc.* **2016**, *138*, 499–

502.

[52] C. B. Aakeröy, A. Rajbanshi, P. Metrangolo, G. Resnati, M. F. Parisi, J. Desper, T. Pilati, *CrystEngComm* **2012**, *14*, 6366–6368.

[53] O. Dumele, N. Trapp, F. Diederich, *Angew. Chemie* **2015**, *54*, 12339–12344.

[54] O. Dumele, B. Schreib, U. Warzok, N. Trapp, C. A. Schalley, F. Diederich, *Angew. Chemie* **2017**, *56*, 1152–1157.

[55] N. K. Beyeh, F. Pan, K. Rissanen, *Angew. Chemie* **2015**, *127*, 7411–7415.

[56] L. Turunen, A. Peuronen, S. Forsblom, E. Kalenius, M. Lahtinen, K. Rissanen, *Chem. Eur. J.* **2017**, *23*, 11714–11718.

[57] S. Benz, J. López-Andarias, J. Mareda, N. Sakai, S. Matile, *Angew. Chemie* **2017**, *129*, 830–833.

[58] J. et al. Ho, P., Szydlowski, P., Sinclair, *Nat. Commun.* **2016**, 11299.

[59] L. Chen, J. Xiang, Y. Zhao, Q. Yan, *J. Am. Chem. Soc.* **2018**, *140*, 7079–7082.

[60] T. S. Koblenz, J. Wassenaar, J. N. H. Reek, *Chem. Soc. Rev.* **2008**, *37*, 247–262.

[61] V. Mouarrawis, R. Plessius, J. I. van der Vlugt, J. N. H. Reek, *Front. Chem.* **2018**, *6*, 1–20.

[62] L. Adriaenssens, P. Ballester, *Chem. Soc. Rev.* **2013**, *42*, 3261–3277.

[63] M. Raynal, P. Ballester, A. Vidal-Ferran, P. W. N. M. Van Leeuwen, *Chem. Soc. Rev.* **2014**, *43*, 1734–1787.

[64] L. J. Liu, J. Rebek, in *Hydrog. Bond. Supramol. Struct.* (Eds.: Z.-T. Li, L.-Z. Wu), Springer Berlin Heidelberg, Berlin, Heidelberg, **2015**, pp. 227–248.

[65] L. Avram, Y. Cohen, J. Rebek, *Chem. Commun.* **2011**, *47*, 5368–5375.

[66] J. Meissner, R. S.; Rebek, J. Jr.; Mendoza, *Science* **1995**, *270*, 1485–1488.

[67] J. Kang, J. Santamaria, G. Hilmersson, J. Rebek J., *J. Am. Chem. Soc.* **1998**, *120*, 7389–7390.

[68] J. Chen, J. Rebek, *Org. Lett.* **2002**, *4*, 327–329.

[69] K. Da Zhang, D. Ajami, J. Rebek, *J. Am. Chem. Soc.* **2013**, *135*, 18064–18066.

[70] M. Grajda, M. J. Lewińska, A. Szumna, *Org. Biomol. Chem.* **2017**, *15*, 8513–8517.

[71] L. R. MacGillivray, J. L. Atwood, *Nature* **1997**, *389*, 469–472.

[72] T. Gerkensmeier, W. Iwanek, C. Agena, R. Fröhlich, S. Kotila, C. Näther, J. Mattay, *European J. Org. Chem.* **1999**, 2257–2262.

[73] J. L. Atwood, L. J. Barbour, A. Jerga, *Chem. Commun.* **2001**, *1*, 2376–2377.

[74] A. Shivanyuk, J. Rebek, *Chem. Commun.* **2001**, *1*, 2374–2375.

[75] L. Avram, Y. Cohen, *J. Am. Chem. Soc.* **2002**, *124*, 15148–15149.

[76] A. Shivanyuk, J. Rebek J., *Proc. Natl. Acad. Sci. U. S. A.* **2001**, *98*, 7662–7665.

[77] L. Avram, Y. Cohen, *J. Am. Chem. Soc.* **2003**, *125*, 16180–16181.

[78] S. Slovak, Y. Cohen, *Chem. Eur. J.* **2012**, *18*, 8515–8520.

[79] T. Evan-Salem, I. Baruch, L. Avram, Y. Cohen, L. C. Palmer, J. Rebek, *Proc. Natl. Acad. Sci. U. S. A.* **2006**, *103*, 12296–12300.

[80] S. Horiuchi, H. Tanaka, E. Sakuda, Y. Arikawa, K. Umakoshi, *Chem. Eur. J.* **2016**, *22*, 17533–17537.

[81] E. Mileo, S. Yi, P. Bhattacharya, A. E. Kaifer, *Angew. Chemie* **2009**, *121*, 5441–5444.

[82] Q. Zhang, L. Catti, V. R. I. Kaila, K. Tiefenbacher, *Chem. Sci.* **2017**, *8*, 1653–1657.

[83] S. Yariv-Shoushan, Y. Cohen, *Org. Lett.* **2016**, *18*, 936–939.

[84] A. Cavarzan, A. Scarso, P. Sgarbossa, G. Strukul, J. N. H. Reek, *J. Am. Chem. Soc.* **2011**, *133*, 2848–2851.

[85] G. Bianchini, G. La Sorella, N. Canever, A. Scarso, G. Strukul, *Chem. Commun.* **2013**, *49*, 5322–5324.

[86] Q. Zhang, K. Tiefenbacher, *J. Am. Chem. Soc.* **2013**, *135*, 16213–16219.

[87] J. M. Köster, K. Tiefenbacher, *ChemCatChem* **2018**, *10*, 2941–2944.

[88] L. Catti, K. Tiefenbacher, *Chem. Commun.* **2015**, *51*, 892–894.

[89] L. Catti, A. Pöthig, K. Tiefenbacher, *Adv. Synth. Catal.* **2017**, *359*, 1331–1338.

[90] G. La Sorella, L. Sperni, P. Ballester, G. Strukul, A. Scarso, *Catal. Sci. Technol.* **2016**, *6*, 6031–6036.

[91] T. Caneva, L. Sperni, G. Strukul, A. Scarso, *RSC Adv.* **2016**, *6*, 83505–83509.

[92] Q. Zhang, K. Tiefenbacher, *Nat. Chem.* **2015**, *7*, 197–202.

[93] Q. Zhang, L. Catti, J. Pleiss, K. Tiefenbacher, *J. Am. Chem. Soc.* **2017**, *139*, 11482–11492.

[94] D. J. Quan, M. L.C.; Cram, *J. Am. Chem. Soc.* **1991**, *113*, 2755–2756.

[95] X. Liu, Y. Liu, G. Li, R. Warmuth, *Angew. Chemie* **2006**, *118*, 915–918.

[96] J. Sun, R. Warmuth, *Chem. Commun.* **2011**, *47*, 9351–9353.

[97] M. Mastalerz, *Acc. Chem. Res.* **2018**, *51*, 2411–2422.

[98] M. A. Little, A. I. Cooper, *Adv. Funct. Mater.* **2020**, *30*, 1–30.

[99] M. Brutschy, M. W. Schneider, M. Mastalerz, S. R. Waldvogel, *Adv. Mater.* **2012**, *24*, 6049–6052.

[100] Q. Song, S. Jiang, T. Hasell, M. Liu, S. Sun, A. K. Cheetham, E. Sivaniah, A. I. Cooper, *Adv. Mater.* **2016**, *28*, 2629–2637.

[101] J. H. Zhang, S. M. Xie, L. Chen, B. J. Wang, P. G. He, L. M. Yuan, *Anal. Chem.* **2015**,

*87*, 7817–7824.

[102] A. Kewley, A. Stephenson, L. Chen, M. E. Briggs, T. Hasell, A. I. Cooper, *Chem. Mater.* **2015**, *27*, 3207–3210.

[103] Y. Nishioka, T. Yamaguchi, M. Kawano, M. Fujita, *J. Am. Chem. Soc.* **2008**, *130*, 8160–8161.

[104] A. G. Salles, S. Zarra, R. M. Turner, J. R. Nitschke, *J. Am. Chem. Soc.* **2013**, *135*, 19143–19146.

[105] J. L. Bolliger, A. M. Belenguer, J. R. Nitschke, *Angew. Chemie* **2013**, *52*, 7958–7962.

[106] T. Gadzikwa, R. Bellini, H. L. Dekker, J. N. H. Reek, *J. Am. Chem. Soc.* **2012**, *134*, 2860–2863.

[107] C. Tan, J. Jiao, Z. Li, Y. Liu, X. Han, Y. Cui, *Angew. Chemie* **2018**, *57*, 2085–2090.

[108] D. L. Caulder, R. E. Powers, T. N. Parac, K. N. Raymond, *Angew. Chemie* **1998**, *37*, 1840–1843.

[109] A. V. Davis, D. Fiedler, G. Seeber, A. Zahl, R. Van Eldik, K. N. Raymond, *J. Am. Chem. Soc.* **2006**, *128*, 1324–1333.

[110] A. V. Davis, D. Fiedler, M. Ziegler, A. Terpin, K. N. Raymond, *J. Am. Chem. Soc.* **2007**, *129*, 15354–15363.

[111] C. Zhao, Q.-F. Sun, W. M. Hart-Cooper, A. G. DiPasquale, F. Dean Toste, R. G. Bergman, K. N. Raymond, *J. Am. Chem. Soc.* **2013**, *135*, 18802–18805.

[112] C. J. Brown, R. G. Bergman, K. N. Raymond, *J. Am. Chem. Soc.* **2009**, *131*, 17530–17531.

[113] D. Fiedler, R. G. Bergman, K. N. Raymond, *Angew. Chemie* **2004**, *116*, 6916–6919.

[114] D. Fiedler, H. Van Halbeek, R. G. Bergman, K. N. Raymond, *J. Am. Chem. Soc.* **2006**, *128*, 10240–10252.

[115] W. M. Hart-Cooper, K. N. Clary, F. D. Toste, R. G. Bergman, K. N. Raymond, *J. Am. Chem. Soc.* **2012**, *134*, 17873–17876.

[116] D. Beaudoin, F. Rominger, M. Mastalerz, *Angew. Chemie* **2016**, *55*, 15599–15603.

[117] G. Markiewicz, A. Jenczak, M. Kołodziejski, J. J. Holstein, J. K. M. Sanders, A. R. Stefankiewicz, *Nat. Commun.* **2017**, *8*, 6–13.

[118] H. Jędrzejewska, A. Szumna, *Chem. Rev.* **2017**, *117*, 4863–4899.

[119] H. Jędrzejewska, M. Wierzbicki, P. Cmoch, K. Rissanen, A. Szumna, *Angew. Chemie* **2014**, *53*, 13760–13764.

[120] M. Wierzbicki, A. A. Głowacka, M. P. Szymański, A. Szumna, *Chem. Commun.* **2017**, *53*, 5200–5203.

[121] H. Jędrzejewska, A. Szumna, *Chem. Sci.* **2019**, *10*, 4412–4421.

[122] C. Tan, D. Chu, X. Tang, Y. Liu, W. Xuan, Y. Cui, *Chem. Eur. J.* **2019**, *25*, 662–672.

[123] D. F. Morimoto, M.; Bierschenk, S. M.; Xia, K. T.; Bergman, R. G.; Raymond, K. N.; Toste, *Nat. Catal.* **2020**, *3*, 969–984.

[124] A. Calcaterra, I. D'Acquarica, *J. Pharm. Biomed. Anal.* **2018**, *147*, 323–340.

[125] D. G. I. Kingston, *J. Nat. Prod.* **2000**, *63*, 726–734.

[126] M. A. Jordan, L. Wilson, *Nat. Rev.* **2004**, *4*, 253–265.

[127] D. W. Christianson, *Chem. Rev.* **2006**, *106*, 3412–3442.

[128] J. Degenhardt, T. G. Köllner, J. Gershenzon, *Phytochemistry* **2009**, *70*, 1621–1637.

[129] J. S. Dickschat, *Nat. Prod. Rep.* **2016**, *33*, 87–110.

[130] N. A. Mahizan, S.-K. Yang, C.-L. Moo, A. A.-L. Song, C.-M. Chong, C.-W. Chong, A. Abushelaibi, S.-H. E. Lim, K.-S. Lai, *Molecules* **2019**, *24*.

[131] A. Erkkilä, I. Majander, P. M. Pihko, *Chem. Rev.* **2007**, *107*, 5416–5470.

[132] S. V. Pronin, R. A. Shenvi, *Nat. Chem.* **2012**, *4*, 915–920.

[133] R. Croteau, *Chem. Rev.* **1987**, *87*, 929–954.

[134] R. A. Yoder, J. N. Johnston, *Chem. Rev.* **2005**, *105*, 4730–4756.

[135] D. L. McCormick, J. P.; Barton, *Tetrahedron* **1978**, *34*, 325–330.

[136] C. Tsangarakis, M. Stratakis, *Adv. Synth. Catal.* **2005**, *347*, 1280–1284.

[137] W. Yu, F. Bian, Y. Gao, L. Yang, Z. L. Liu, *Adv. Synth. Catal.* **2006**, *348*, 59–62.

[138] C. Raptis, I. N. Lykakis, C. Tsangarakis, M. Stratakis, *Chem. Eur. J.* **2009**, *15*, 11918–11927.

[139] M. P. Polovinka, D. V. Korchagina, Y. V. Gatilov, I. Y. Bagrianskaya, V. A. Barkhash, V. V. Shcherbukhin, N. S. Zefirov, V. B. Perutskii, N. D. Ungur, P. F. Vlad, *J. Org. Chem.* **1994**, *59*, 1509–1517.

[140] D. A. Kutateladze, D. A. Strassfeld, E. N. Jacobsen, *J. Am. Chem. Soc.* **2020**, *142*, 6951–6956.

[141] R. R. Knowles, S. Lin, E. N. Jacobsen, *J. Am. Chem. Soc.* **2010**, *132*, 5030–5032.

[142] Q. Zhang, J. Rinkel, B. Goldfuss, J. S. Dickschat, K. Tiefenbacher, *Nat. Catal.* **2018**, *1*, 609–615.

[143] Q. Zhang, K. Tiefenbacher, *Angew. Chemie* **2019**, *58*, 12688–12695.

[144] L. D. Syntrivanis, I. Némethová, D. Schmid, S. Levi, A. Prescimone, F. Bissegger, D. T. Major, K. Tiefenbacher, *J. Am. Chem. Soc.* **2020**, *142*, 5894–5900.

[145] S. Merget, L. Catti, G. Piccini, K. Tiefenbacher, *J. Am. Chem. Soc.* **2020**, *142*, 4400–4410.

[146] B. List, R. A. Lerner, C. F. Barbas, *J. Am. Chem. Soc.* **2000**, *122*, 2395–2396.

[147] D. W. C. Ahrendt, K. A.; Borths, C. J.; Macmillan, *J. Am. Chem. Soc.* **2000**, *122*, 4243–4244.

[148] P. Melchiorre, M. Marigo, A. Carlone, G. Bartoli, *Angew. Chemie* **2008**, *47*, 6138–6171.

[149] S. Bertelsen, K. A. Jørgensen, *Chem. Soc. Rev.* **2009**, *38*, 2178–2189.

[150] S. Brandau, A. Landa, J. Franzén, M. Marigo, K. A. Jørgensen, *Angew. Chemie* **2006**, *45*, 4305–4309.

[151] S. G. Ouellet, J. B. Tuttle, D. W. C. MacMillan, *J. Am. Chem. Soc.* **2005**, *127*, 32–33.

[152] M. Marigo, T. Schulte, J. Franzén, K. A. Jørgensen, *J. Am. Chem. Soc.* **2005**, *127*, 15710–15711.

[153] A. Carlone, G. Bartoli, M. Bosco, L. Sambri, P. Melchiorre, *Angew. Chemie* **2007**, *46*, 4504–4506.

[154] D. B. Ramachary, R. Mondal, *Tetrahedron Lett.* **2006**, *47*, 7689–7693.

[155] T. M. Bräuer, Q. Zhang, K. Tiefenbacher, *Angew. Chemie* **2016**, *55*, 7698–7701.

[156] T. M. Bräuer, Q. Zhang, K. Tiefenbacher, *J. Am. Chem. Soc.* **2017**, *139*, 17500–17507.

[157] P. La Manna, M. De Rosa, C. Talotta, C. Gaeta, A. Soriente, G. Floresta, A. Rescifina, P. Neri, *Org. Chem. Front.* **2018**, *5*, 827–837.

[158] D. Sokolova, K. Tiefenbacher, *RSC Adv.* **2021**, *11*, 24607–24612.

# 7. REPRINTS AND REPRINT PERMISSION

## Royal Society of Chemistry

The manuscript published in *RSC Advances* (Open Access), figures 7-10, and tables 1-2 were reproduced from Ref. [158] with permission from the Royal Society of Chemistry. A summary of the manuscript can be found in chapter 3.1.

***Bibliographic data of the publication:***

**Optimized iminium-catalyzed 1,4-reductions inside the resorcinarene capsule: achieving >90% ee with proline as catalyst**

Daria Sokolova[a], Konrad Tiefenbacher*[a,b]

[a] Department of Chemistry, University of Basel, Mattenstrasse 24a, CH-4058 Basel, Switzerland

[b] Department of Biosystems Science and Engineering, ETH Zürich, Mattenstrasse 26, CH-4058 Basel, Switzerland

*Corresponding Author: konrad.tiefenbacher@unibas.ch; tkonrad@ethz.ch

Originally published in *RSC Adv.*, **2021**, 11, 24607-24612.

DOI: 10.1039/d1ra04333a

URL: https://pubs.rsc.org/en/content/articlelanding/2021/ra/d1ra04333a

RSC Advances

PAPER

View Article Online
View Journal | View Issue



Check for updates

Cite this: *RSC Adv.*, 2021, **11**, 24607

# Optimized iminium-catalysed 1,4-reductions inside the resorcinarene capsule: achieving >90% ee with proline as catalyst†

Daria Sokolova [a] and Konrad Tiefenbacher *[ab]

In previous work, we demonstrated that iminium-catalysed 1,4-reductions inside the supramolecular resorcinarene capsule display increased enantioselectivities as compared to their regular solution counterparts. Utilizing proline as the chiral catalyst, enantioselectivities remained below 80% ee. In this study, the reaction conditions were optimized by determining the optimal capsule loading and HCl content. Additionally, it was found that alcohol additives increase the enantioselectivity of the capsule-catalysed reaction. As a result, we report enantioselectivities of up to 92% ee for iminium-catalysed 1,4-reductions relying on proline as the sole chiral source. This is of high interest, as proline is unable to deliver high enantioselectivities for 1,4-reductions in a regular solution setting. Investigations into the role of the alcohol additive revealed a dual role: it not only slowed down the background reaction but also increased the capsule-catalysed reaction rate.

Received 4th June 2021
Accepted 5th July 2021

DOI: 10.1039/d1ra04333a

rsc.li/rsc-advances

## Introduction

The self-assembled resorcinarene hexamer **I** (Fig. 1a), first reported by Atwood[1] in the solid state in 1997, comprises one of the easiest to access molecular containers based on hydrogen bonds. It assembles from six resorcinarene units **1**, readily accessible in one step on a large scale, and eight water molecules.[1–3] Due to its dynamic nature, it can entrap guest molecules temporarily inside its cavity.[2,4–9] The properties of **I** in solution were studied in detail, mainly by the groups of Rebek and Cohen.[2–7,9–15] More recently, this container has started being explored as a container for other catalysts[16] or as a catalyst itself.[17,18] The field has been reviewed,[19–23] and novel applications have been found very recently.[24–27] In 2016, our group reported that iminium-catalysis can be performed inside capsule **I** (Fig. 1b).[28,29] Later work by the Neri group extended iminium catalysis inside **I** to cycloadditions.[30] The α,β-unsaturated aldehyde first forms an iminium species with the chiral amine catalyst L-proline (**3a**). This iminium species is encapsulated due to the high affinity of the capsule **I** for cationic species. The subsequent reduction with Hantzsch ester **2**, therefore, has to take place inside the confined environment of the capsule, delivering much higher enantioselectivities than in the absence of container **I**.[28,29]

Our understanding of capsule **I**-catalysis improved substantially over the last years. For instance, the importance of HCl as a co-catalyst for a selection of reactions inside **I** was elucidated.[31] However, the influence of HCl on iminium-catalysed reactions inside **I** remains unknown. This work aimed at (1) elucidating the role of HCl for the iminium catalysis inside **I**; (2) reducing the amount of capsule catalyst required, as originally 26 mol% were utilized; (3) optimizing the reaction conditions to improve the enantioselectivity. We

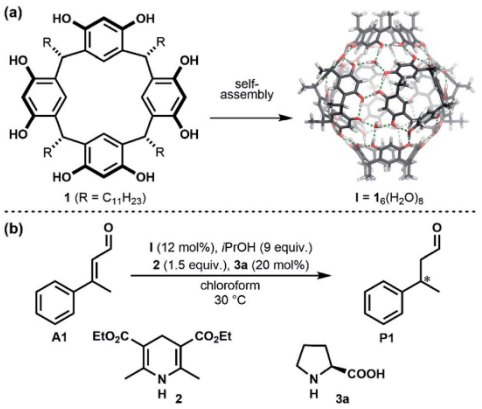


Fig. 1 (a) Self-assembly of monomer **1** into hexameric capsule **I**. (b) General scheme of iminium catalysed 1,4-reduction inside capsule **I**.

[a]*Department of Chemistry, University of Basel, 4058 Basel, Switzerland. E-mail: konrad.tiefenbacher@unibas.ch*

[b]*Department of Biosystems Science and Engineering, ETH Zürich, 4058 Basel, Switzerland. E-mail: tkonrad@ethz.ch*

† Electronic supplementary information (ESI) available: Experimental details, and copies of GC spectra. See DOI: 10.1039/d1ra04333a

here report the results of this effort. As a highlight of these studies, unprecedented enantioselectivities of up to 92% were achieved for the 1,4-reduction of α,β-unsaturated aldehydes[32–34] inside capsule **I** using simple proline as the sole source of chiral information. This is of high interest as proline in a regular solution setting is unable to deliver high enantioselectivities for 1,4-reductions.[34]

## Results and discussion

As a first step, we aimed at reducing the unusually high capsule loading (26 mol%). This loading was initially selected[28] to ensure complete uptake of proline (20 mol%) and its iminium species. Utilizing the standard reaction conditions with substrate **A1** (1 equiv. of **A1**, *c*(**A1**) = 0.15 M in chloroform, 1.5 equiv. of reducing agent **2**, 0.2 equiv. of amine catalyst **3a**; Section 3.2 in ESI†), the influence of the capsule loading (8–26 mol%) was explored (Fig. 2a). Interestingly, a peak selectivity (80% ee) was found at 12 mol%, which deteriorated both for increasing and decreasing loadings. This surprising finding may be a result of two opposing effects: (1) at low capsule loadings, the iminium reaction outside of the capsule exerts a detrimental effect on the ee (background iminium reaction, <12 mol%, entries 1 and 2 of Table S1†); (2) at higher capsule loadings, the racemic background reaction catalysed by capsule **I** itself starts dominating (>12 mol%, entries 4–10 of Table S1†). This background reaction is caused by the activation of the aldehyde substrate by the capsule itself (without proline) and leads to a racemic product as described in our previous work.[28] Therefore, 12 mol% **I** was selected for further studies.

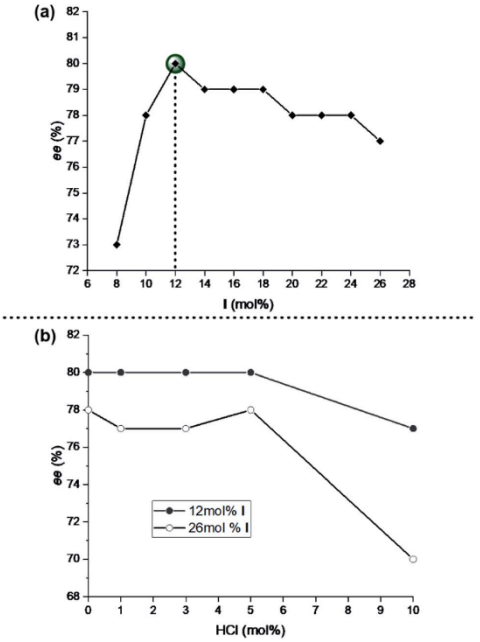


Fig. 2 (a) Optimization of the capsule I loading (8–26 mol%) under the standard reaction conditions using aldehyde **A1**: 1 equiv. **A1**, *c*(**A1**) = 0.15 M in chloroform, 1.5 equiv. **2**, 0.2 equiv. **3a**. The optimal amount of I (12 mol%) is highlighted. (b) Influence of the HCl content on the standard reaction utilizing either 12 or 26 mol% of capsule I. Enantiomeric excesses were determined with chiral GC measurements. The values reported refer to measurements after 72 h of reaction time.

In the previous work of our group, it was already demonstrated that Hantzsch ester **2** and L-proline (**3a**) are the most suitable hydride source and chiral catalyst, respectively.[28,29] In this study, different L-proline loadings were evaluated with the newly optimized capsule **I** loading of 12 mol%. As can be seen in Table S2,† the optimum was found at 20 mol% of L-proline.

Next, the influence of HCl on the enantioselectivity of the standard reaction was explored. It was studied for two different capsule loadings: the optimized 12 mol% and the previously utilized 26 mol%.[28,29] As can be seen in Fig. 2b, the enantioselectivity of the reaction does not benefit from HCl traces. Contrarily, larger HCl loadings (>5 mol%) even lead to a drop in enantioselectivity, presumably *via* an acid-catalysed racemic background reaction (Table S3†). A similar trend is observed for reactions with 26 mol% of **I**. Hence, the addition of HCl is not required for the iminium-catalysed 1,4-reductions inside capsule **I**. This finding is in line with our previous report that not all reactions inside **I** depend on an acid co-catalyst.[31]

After having established the optimal capsule (12 mol%) and proline (20 mol%) loadings, and HCl content (none), further additives were investigated. Of particular interest were alcohol additives, as their interactions with the resorcinarene capsule are well documented.[15,35–37] The Cohen group investigated the incorporation of different alcohols into the resorcinarene capsule in solution and demonstrated that they can replace water molecules of the hydrogen bond network.[15,36] Additionally, in the solid state it was reported that the incorporation of nPrOH into the hydrogen network of the resorcinarene hexamer results in 25% larger assemblies.[38] These reports prompted us to investigate the influence of different alcohol additives on the iminium catalysis inside **I**. Indeed, initial

Table 1 Optimization of the alcohol additive under the standard reaction conditions: 1 equiv. **A1**, *c*(**A1**) = 0.15 M, 12 mol% of I, 1.5 equiv. **2**, 0.2 equiv. **3a**[a]

| Entry | Alcohol | Yield (%) | Conversion (%) | ee (%) |
|---|---|---|---|---|
| 1 | — | 89 ± 1 | 93 ± 1 | 77 ± 1 (*S*) |
| 2 | MeOH | 89 ± 1 | 93 ± 1 | 80 ± 2 (*S*) |
| 3 | EtOH | 89 ± 3 | 94 ± 2 | 80 ± 2 (*S*) |
| 4 | nPrOH | 90 ± 1 | 94 ± 2 | 80 ± 2 (*S*) |
| 5 | iPrOH | 91 ± 1 | 94 ± 2 | 83 ± 2 (*S*) |
| 6 | nBuOH | 89 ± 2 | 94 ± 2 | 80 ± 2 (*S*) |

[a] Conversions, yields, and enantiomeric excesses were determined with achiral and chiral GC measurements. The values reported refer to measurements after 72 h of reaction time. Reactions were performed in triplicate and standard deviations were determined

tests revealed that alcohol additives increased the enantioselectivity of the standard reaction. An initial screening indicated that the best results were obtained with 9 equiv. of alcohol per capsule (Table S4†). Subsequently, several alcohol additives were screened (Table 1). As shown in Table 1 addition of each of the tested alcohols led to a slight increase of the ee, with iPrOH performing slightly better than the alternatives concerning yield and ee. Although the change in ee was not very big (6% ee, see entries 1 and 5 in Table 1), it was fully reproducible. The effect of the iPrOH additive was studied with a series of substrates (Table 2). In all cases, the combination of capsule **I** and iPrOH resulted in higher enantioselectivities. As reported in our previous work on the substrate scope,[29] the effect of the capsule on substrate **A5** was lower than in the other four cases; most likely due to the lack of an aromatic moiety that facilitates π–π interactions with the capsule walls. Most interestingly, for two substrates (**A2** and **A3**), enantioselectivities >90% ee were achieved. This is remarkable, as proline is unable to deliver high enantioselectivities for 1,4-reductions in a regular solution setting.[34] Only in combination with the capsule catalyst and iPrOH, these high selectivities are observed.

How does iPrOH influence the enantioselectivity of the capsule-catalysed reaction? Initially, we investigated the influence of iPrOH on the capsule structure and size, as it was reported that alcohol incorporation can increase the size of the

Table 2 Results of reactions with different substrates under optimized conditions: 1 equiv. A, *c*(A) = 0.15 M in chloroform, 12 mol% I, 1.5 equiv. **2**, 0.2 equiv. **3a**, 9 equiv. iPrOH, (bright-green). Comparison to reactions in the presence of 12 mol% of capsule I, but the absence of iPrOH (dark-green); reactions in the absence of capsule I, and the presence of 9 equiv. of iPrOH (dark-grey); reactions in the absence of both capsule I and iPrOH (light-grey)[a]

| Entry | Aldehyde | I | *i*PrOH | Yield (%) | *ee* (%) |
|---|---|---|---|---|---|
| 1 | 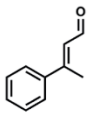 A1 | yes | yes | 91±1 | 83±2 (*S*) |
| | | yes | no | 89±1 | 77±1 (*S*) |
| | | no | yes | 45±7 | 1±2 (*S*) |
| | | no | no | 50±13 | 3±2 (*S*) |
| 2 | 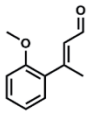 A2 | yes | yes | 89±7 | 92±0 (*S*) |
| | | yes | no | 76±4 | 83±1 (*S*) |
| | | no | yes | 5±0 | 5±2 (*S*) |
| | | no | no | 5±0 | 6±1 (*S*) |
| 3 | 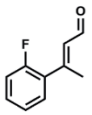 A3 | yes | yes | 97±0 | 92±0 (*S*) |
| | | yes | no | 95±2 | 88±0 (*S*) |
| | | no | yes | 16±2 | 6±0 (*S*) |
| | | no | no | 15±0 | 3±1 (*S*) |
| 4 | 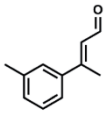 A4 | yes | yes | 67±2 | 57±0 (*S*) |
| | | yes | no | 65±1 | 55±1 (*S*) |
| | | no | yes | 16±1 | 3±5 (*S*) |
| | | no | no | 18±2 | 3±1 (*S*) |
| 5 | 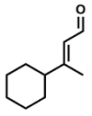 A5 | yes | yes | 72±1 | 58±1 (*S*) |
| | | yes | no | 66±9 | 55±1 (*S*) |
| | | no | yes | 60±0 | 30±1 (*S*) |
| | | no | no | 61±2 | 35±0 (*S*) |

[a] Conversions, yields, and enantiomeric excesses were determined by GC measurements. The values reported refer to measurements after 72 h of reaction time. Reactions were performed in triplicate and standard deviations were determined

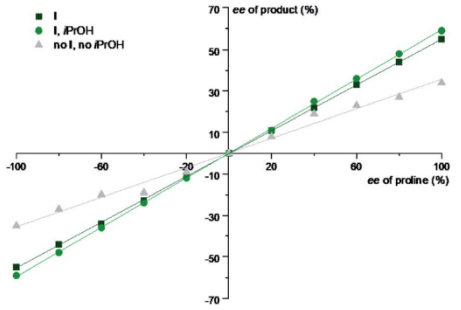


Fig. 3 Non-linear effects study of iminium catalysed 1,4-reduction under optimized conditions using aldehyde **A5**: 1 equiv. **A5**, *c*(**A5**) = 0.15 M in chloroform, 1.5 equiv. **2**, 0.2 equiv. of proline (mixtures of L- and D-proline of different ratios). Different reaction conditions (absence/presence of I and/or iPrOH) were explored. Enantiomeric excesses were determined by chiral GC measurements. For more details, see Section 3.7 of the ESI.†

capsule by 25%, at least in the solid state.[38] However, DOSY-NMR data indicates that the size of the capsule does not change upon the addition of iPrOH (see Section 5 of the ESI† for diffusion coefficients). This is in line with observations in solution from the Cohen group, who reported the replacement of water molecules in the hydrogen bond network by iPrOH without a significant change in the assembly size.[36]

Another hypothesis centered on the idea that the alcohol additive might influence proline–proline interactions in the capsule.

If such interactions play a role, non-linear effects (NLE) should be observable. Therefore, a NLE study was performed. Substrate **A5** was chosen since it yields the highest ee in the absence of the capsule (Table 2) and thus facilitates the observation of changes. In all the cases, linear graphs were obtained (Fig. 3). Accordingly, we can exclude iPrOH-effected changes in the proline–proline interactions as the source of the increased enantioselectivity.

Subsequently, we decided to investigate the initial rates and initial ee of the reaction, in order to elucidate the role of the iPrOH additive. Substrate **A2** was chosen for this study as it displays the fastest kinetics. Four reactions (presence/absence of capsule **I**; presence/absence of alcohol additive) were studied in parallel. The capsule-free reactions turned out to be faster than the capsule-mediated ones, although they plateaued at approx. 40–50% conversion (Fig. 4a). Slowed down kinetics for iminium catalysis inside the capsule is to be expected as the Hantzsch ester and the iminium species have to be co-encapsulated for conversion. More interestingly, the alcohol additive suppressed the reaction rate in the absence of capsule; however, it increased the rate in the presence of capsule **I**. A different trend was observed when following the initial enantioselectivity of the reaction (Fig. 4b). While the influence of alcohol additive was negligible for the reactions without capsule, the capsule-mediated reaction benefited from the additive (92% ee *vs.* 84% ee).

We interpret the results the following way: the increased enantioselectivity in the presence of alcohol additive and

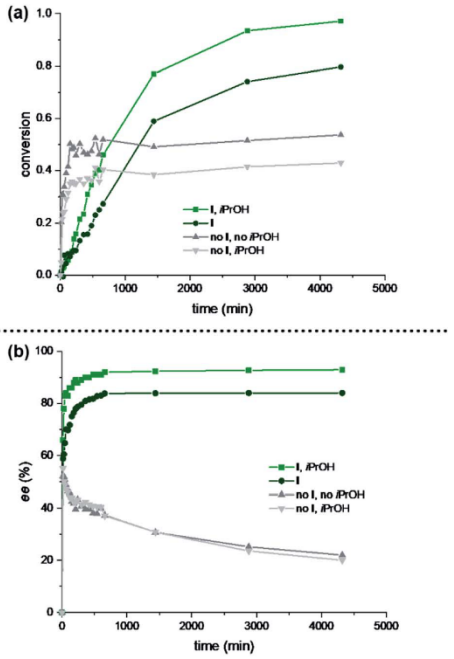


Fig. 4 Influence of iPrOH on the initial rates and enantiomeric excesses of the reaction under optimized conditions using aldehyde **A2**: 1 equiv. **A2**, *c*(**A2**) = 0.15 M in chloroform, 1.5 equiv. **2**, 0.2 equiv. **3a**. Conversions and ees were determined with achiral and chiral GC measurements, respectively. (a) Conversions of reactions in the presence/absence of capsule I (12 mol% if present); the presence/absence of alcohol additive (9 equiv. if present). (b) Enantiomeric excesses of reactions in the presence/absence of capsule I (12 mol% if present); the presence/absence of alcohol additive (9 equiv. if present). For more details, see Section 3.8 of the ESI.†

capsule is likely a consequence of two effects. (1) The reduced background reaction of the free iminium species (compare grey lines in Fig. 4a) that yields low ees. (2) The increased reaction rate in the capsule (compare green lines in Fig. 4a). The acceleration of the reaction in the presence of alcohol additive and capsule (light-green line in Fig. 4a) likely stems from faster exchange kinetics of the reagents in/out of the capsule, as it is known that polar additives destabilize the hydrogen-bonding network.[2] These results indicate that the proline-catalysed reaction inside capsule **I** is highly enantioselective, and is only reduced to some extent by the background reaction outside of the capsule that delivers basically racemic product.

## Conclusions

We present optimized reaction conditions for the iminium-catalysed 1,4-reduction of α,β-unsaturated aldehyde inside the supramolecular capsule **I**. The capsule loading was successfully

 

reduced from 26 to 12 mol%. Furthermore, it was established that HCl is not required as a co-catalyst. Most interestingly, it was found that alcohol additives have a beneficial role concerning the enantioselectivities observed. In two cases, products with 92% ee were formed. To our knowledge, this is the first time that such high enantioselectivities were observed for iminium-catalysed 1,4-reductions utilizing proline as the sole chiral source. While proline performs poorly in solution, the increased interactions inside the confined space of I lead to a dramatic increase in enantioselectivity. According to our initial hypothesis,[28,29] this ee-increase stems from a selective shielding of one side of the iminium species by the inner wall of capsule I. This study demonstrates that this enantioselectivity can be further increased by alcohol additives that not only decrease the background reaction but also accelerate the capsule-catalysed process. We are convinced that these results not only strengthen our understanding of confinement catalysis but will also be transferable to other reaction classes.

## Author contributions

K. T. conceived the original idea and supervised the project. D. S. carried out and analysed the experiments. D. S. and K. T. compiled the manuscript.

## Conflicts of interest

There are no conflicts to declare.

## Acknowledgements

This work was supported by funding from the European Research Council Horizon 2020 Programme [ERC Starting Grant 714620-TERPENECAT]. We also thank Suren Nemat for helpful discussions.

## Notes and references

1 L. R. MacGillivray and J. L. Atwood, A chiral spherical molecular assembly held together by 60 hydrogen bonds, *Nature*, 1997, **389**, 469–472.
2 L. Avram and Y. Cohen, Spontaneous formation of hexameric resorcinarene capsule in chloroform solution as detected by diffusion NMR, *J. Am. Chem. Soc.*, 2002, **124**, 15148–15149.
3 L. Avram, Y. Cohen and J. Rebek, Recent advances in hydrogen-bonded hexameric encapsulation complexes, *Chem. Commun.*, 2011, **47**, 5368–5375.
4 A. Shivanyuk and J. Rebek, Reversible encapsulation by self-assembling resorcinarene subunits, *Proc. Natl. Acad. Sci. U. S. A.*, 2001, **98**, 7662–7665.
5 L. Avram and Y. Cohen, Discrimination of guests encapsulation in large hexameric molecular capsules in solution: pyrogallol[4]arene *versus* resorcin[4]arene capsules, *J. Am. Chem. Soc.*, 2003, **125**, 16180–16181.
6 L. Avram and Y. Cohen, Effect of a cationic guest on the characteristics of the molecular capsule of resorcinarene: a diffusion NMR study, *Org. Lett.*, 2003, **5**, 1099–1102.
7 M. Yamanaka, A. Shivanyuk and J. Rebek, Kinetics and thermodynamics of hexameric capsule formation, *J. Am. Chem. Soc.*, 2004, **126**, 2939–2943.
8 L. Avram and Y. Cohen, Self-recognition, structure, stability, and guest affinity of pyrogallol[4]arene and resorcin[4]arene capsules in solution, *J. Am. Chem. Soc.*, 2004, **126**, 11556–11563.
9 L. Avram and Y. Cohen, Self-assembly of resorcin[4]arene in the presence of small alkylammonium guests in solution, *Org. Lett.*, 2008, **10**, 1505–1508.
10 A. Shivanyuk and J. Rebek, Assembly of resorcinarene capsules in wet solvents, *J. Am. Chem. Soc.*, 2003, **125**, 3432–3433.
11 T. Evan-Salem, I. Baruch, L. Avram, Y. Cohen, L. C. Palmer and J. Rebek, Resorcinarenes are hexameric capsules in solution, *Proc. Natl. Acad. Sci. U. S. A.*, 2006, **103**, 12296–12300.
12 E. S. Barrett, T. J. Dale and J. Rebek, Assembly and exchange of resorcinarene capsules monitored by fluorescence resonance energy transfer, *J. Am. Chem. Soc.*, 2007, **129**, 3818–3819.
13 E. S. Barrett, T. J. Dale and J. Rebek, Stability, dynamics, and selectivity in the assembly of hydrogen-bonded hexameric capsules, *J. Am. Chem. Soc.*, 2008, **130**, 2344–2350.
14 S. Slovak and Y. Cohen, In-out interactions of different guests with the hexameric capsule of resorcin[4]arene, *Supramol. Chem.*, 2010, **22**, 803–807.
15 S. Slovak, L. Avram and Y. Cohen, Encapsulated or not encapsulated? mapping alcohol sites in hexameric capsules of resorcin[4]arenes in solution by diffusion NMR spectroscopy, *Angew. Chem., Int. Ed.*, 2010, **49**, 428–431.
16 A. Cavarzan, A. Scarso, P. Sgarbossa, G. Strukul and J. N. H. Reek, Supramolecular control on chemo- and regioselectivity via encapsulation of (NHC)-Au catalyst within a hexameric self-assembled host, *J. Am. Chem. Soc.*, 2011, **133**, 2848–2851.
17 G. Bianchini, G. La Sorella, N. Canever, A. Scarso and G. Strukul, Efficient isonitrile hydration through encapsulation within a hexameric self-assembled capsule and selective inhibition by a photo-controllable competitive guest, *Chem. Commun.*, 2013, **49**, 5322–5324.
18 Q. Zhang and K. Tiefenbacher, Hexameric resorcinarene capsule is a Brønsted acid: investigation and application to synthesis and catalysis, *J. Am. Chem. Soc.*, 2013, **135**, 16213–16219.
19 Q. Zhang, L. Catti, L. D. Syntrivanis and K. Tiefenbacher, En route to terpene natural products utilizing supramolecular cyclase mimetics, *Nat. Prod. Rep.*, 2019, **36**, 1619–1627.
20 S. Gambaro, M. De Rosa, A. Soriente, C. Talotta, G. Floresta, A. Rescifina, C. Gaeta and P. Neri, A hexameric resorcinarene capsule as a hydrogen bonding catalyst in the conjugate addition of pyrroles and indoles to nitroalkenes, *Org. Chem. Front.*, 2019, **6**, 2339–2347.

21 Y. Zhu, J. Rebek and Y. Yu, Cyclizations catalyzed inside a hexameric resorcinarene capsule, *Chem. Commun.*, 2019, **55**, 3573–3577.
22 I. Némethová, L. D. Syntrivanis and K. Tiefenbacher, Molecular capsule catalysis: ready to address current challenges in synthetic organic chemistry?, *Chimia*, 2020, **74**, 561–568.
23 C. Gaeta, P. La Manna, M. De Rosa, A. Soriente, C. Talotta and P. Neri, Supramolecular catalysis with self-assembled capsules and cages: what happens in confined spaces, *ChemCatChem*, 2021, **13**, 1638–1658.
24 S. Merget, L. Catti, G. Piccini and K. Tiefenbacher, Requirements for terpene cyclizations inside the supramolecular resorcinarene capsule: bound water and its protonation determine the catalytic activity, *J. Am. Chem. Soc.*, 2020, **142**(9), 4400–4410.
25 L. D. Syntrivanis, I. Némethová, D. Schmid, S. Levi, A. Prescimone, F. Bissegger, D. T. Major and K. Tiefenbacher, Four-step access to the sesquiterpene natural product presilphiperfolan-1β-ol and unnatural derivatives *via* supramolecular catalysis, *J. Am. Chem. Soc.*, 2020, **142**, 5894–5900.
26 P. La Manna, C. Talotta, M. De Rosa, A. Soriente, C. Gaeta and P. Neri, An atom-economical method for the formation of amidopyrroles exploiting the self-assembled resorcinarene capsule, *Org. Lett.*, 2020, **22**, 2590–2594.
27 S. Gambaro, C. Talotta, P. Della Sala, A. Soriente, M. De Rosa, C. Gaeta and P. Neri, Kinetic and thermodynamic modulation of dynamic imine libraries driven by the hexameric resorcinarene capsule, *J. Am. Chem. Soc.*, 2020, **142**, 14914–14923.
28 T. M. Bräuer, Q. Zhang and K. Tiefenbacher, Iminium catalysis inside a self-assembled supramolecular capsule: modulation of enantiomeric excess, *Angew. Chem., Int. Ed.*, 2016, **55**, 7698–7701.
29 T. M. Bräuer, Q. Zhang and K. Tiefenbacher, Iminium catalysis inside a self-assembled supramolecular capsule: scope and mechanistic studies, *J. Am. Chem. Soc.*, 2017, **139**, 17500–17507.
30 P. La Manna, M. De Rosa, C. Talotta, C. Gaeta, A. Soriente, G. Floresta, A. Rescifina and P. Neri, The hexameric resorcinarene capsule as an artificial enzyme: Ruling the regio and stereochemistry of a 1,3-dipolar cycloaddition between nitrones and unsaturated aldehydes, *Org. Chem. Front.*, 2018, **5**, 827–837.
31 J. M. Köster and K. Tiefenbacher, Elucidating the importance of hydrochloric acid as a cocatalyst for resorcinarene-capsule-catalyzed reactions, *ChemCatChem*, 2018, **10**, 2941–2944.
32 W. Y. Jung, M. T. Hechavarria Fonseca, N. Vignola and B. List, Metal-free, organocatalytic asymmetric transfer hydrogenation of α,β-unsaturated aldehydes, *Angew. Chem., Int. Ed.*, 2004, **44**, 108–110.
33 J. W. Yang, M. T. Hechavarria Fonseca and B. List, A metal-free transfer hydrogenation: organocatalytic conjugate reduction of α,β-unsaturated aldehydes, *Angew. Chem., Int. Ed.*, 2004, **43**, 6660–6662.
34 S. G. Ouellet, J. B. Tuttle and D. W. C. MacMillan, Enantioselective organocatalytic hydride reduction, *J. Am. Chem. Soc.*, 2005, **127**, 32–33.
35 B. Schnatwinkel, I. Stoll, A. Mix, M. V. Rekharsky, V. V. Borovkov, Y. Inoue and J. Mattay, Monomeric, dimeric and hexameric resorcin[4]arene assemblies with alcohols in apolar solventswzy, *Chem. Commun.*, 2008, 3873–3875.
36 S. Slovak and Y. Cohen, The effect of alcohol structures on the interaction mode with the hexameric capsule of resorcin[4]arene, *Chem.–Eur. J.*, 2012, **18**, 8515–8520.
37 O. Ugono and K. T. Holman, An achiral form of the hexameric resorcin[4]arene capsule sustained by hydrogen bonding with alcohols, *Chem. Commun.*, 2006, 2144–2146.
38 R. M. Payne and C. L. Oliver, A propanol-seamed: C-methylcalix[4]resorcinarene hexamer accessible *via* solution crystallization, liquid-assisted grinding and vapour sorption, *CrystEngComm*, 2018, **20**, 1919–1922.